The Role of CDK2 and CDK9 in the Radiation Response of human HNSCC Cancer Cells

DISSERTATION

zur Erlangung des akademischen Grades

**Doctor rerum naturalium
(Dr. rer. nat.)**

vorgelegt

der Fakultät Mathematik und Naturwissenschaften
der Technischen Universität Dresden

von

Ahmed Soffar (M.Sc.)

geboren am 18.08.1980 in Beheira/Ägypten.

Gutachter: Prof. Dr. Nils Cordes
               Prof. Dr. Herwig O. Gutzeit

eingereicht am: 07.05.2013
verteidigt am: 11.07.2013

The Role of CDK2 and CDK9 in the Radiation Response of human HNSCC Cancer Cells

THESIS

to obtain the academic degree

Doctor rerum naturalium
(Dr. rer. nat.)

submitted to

The Faculty of Mathematic and Natural Sciences
Dresden University of Technology

by

Ahmed Soffar (M.Sc.)

born on 18.08.1980 in Beheira/Egypt.

Reviewers: Prof. Dr. Nils Cordes
                      Prof. Dr. Herwig O. Gutzeit

Submission: 07.05.2013
Defence: 11.07.2013

To my family

"Time is shorter than you"

Table of Contents

List of Abbreviations

2D	Two dimensional
3D	Three dimensional
53BP1	p53 binding protein 1
γH2AX	Phosphorylated H2AX at serine 139
APS	Ammonium persulphate
ATM	Ataxia telangiectasia mutated protein
ATP	Adenosine triphosphate
ATR	ATM and Rad3-related protein
ATRIP	Ataxia telangiectasia and Rad3-related interacting protein
BER	Base excision repair
BCA	Bicinchoninic acid
BrdU	5-Bromo-2´-deoxyuridine
BSA	Bovine serum albumin
C	Carboxyl
CAK	CDK activating kinase
Cdc25	Cell division cycle 25
Cdc7	Cell division cycle 7
CDK	Cyclin-dependent kinase
CDK2$^{-/-}$ MEF	CDK2 knockout mouse embryonic fibroblast
CHK1	Checkpoint kinase 1
CHK2	Checkpoint kinase 2
CMV	Cytomegalovirus
CO_2	Carbon dioxide
Co siRNA	Non-specific siRNA
CTD	Carboxyl terminal domain
DAPI	4',6-diamidino-2-phenylindole
ddH$_2$O	Double distilled water
DMEM	Dulbecco's modified Eagle's medium
DNA	Deoxyribonucleic acid
DNA-PK	DNA-dependent protein kinase
DNA-PKcs	Catalytic subunit of DNA-PK

dNTP	Deoxyribonucleotide triphosphates
DSB	double strand break
e.g.	For example
EDTA	Ethylenediaminetetraacetic acid
FBS	Fetal bovine serum
FL	Fluorescence intensity
FITC	Fluorescein isothiocyanate
FSC	Forward scatter
G418	Geneticin®
Gy	Gray
hCDK9	Human CDK9
HCl	Hydrochloric acid
HNSCC	Head and neck squamous cell carcinoma
HR	Homologous recombination
HRP	horseradish peroxidase
IgG	Immunoglobulin G
kb	Kilo base pair
LB medium	Lysogeny broth medium
LigIV	DNA ligase IV
lrECM	Laminin-rich extracellular matrix
LSM	Laser scanning microscope
Mre11	Meiotic recombination 11 homologue
MRN	Protein complex of Mre11, Rad50 and NBS1
N	Amino
NBS1	Nijmegen breakage syndrome 1
NEAA	Non-essential amino acid
NHEJ	Non-homologous end-joining
PBS	Phosphate-buffered saline
PBSA	1% BSA in 1xPBS
PBST	PBS(1x)/0.05% Tween 20
PCNA	Proliferating-Cell-Nuclear-Antigen
PCR	Polymerase chain reaction
PE	Plating efficiency
PI	Propidium iodide
pTEFb	Positive transcription elongation factor b
Rb	Retinoblastoma protein

List of Abbreviations

rcf	Relative centrifugal force
RIPA	Radioimmunoprecipitation Assay
RNA	Ribonucleic acid
RNase	Ribonuclease
RNAPII	RNA polymerase II
Rpb1-CTD	CTD of the large subunit of RNAPII
rpm	Round per minute
RT	Room temperature
S	Serine
SDS	Sodium dodecyl sulphate
SDS-PAGE	SDS-polyacrylamide gel electrophoresis
SF	Surviving fraction
SOC medium	Super Optimal broth with Catabolite repression medium
SSC	Side scatter
siRNA	Small interfering ribonucleic acid
SSB	Single strand break
T	Threonine
TBE buffer	Tris/Borate/EDTA buffer
UV	Ultraviolet
WT MEF	Wild type mouse embryonic fibroblast
Y	Tyrosine

Otherwise, symbols of the international system of units were used

1   Introduction

Cancer is a key public health concern accounting for more than seven million deaths worldwide in 2008 (Ferlay et al., 2010; IARC, 2008; Thun et al., 2009). It arises from a single cell after a transformation process, which results from genetic mutations in protooncogenes or tumour suppressor genes that lead to uncontrolled cell proliferation (Baumann et al., 2008; Burkhart & Sage, 2008; Finlay et al., 1989; Hahn & Weinberg, 2002; Hanahan & Weinberg, 2000; Hanahan & Weinberg, 2011; Jacks & Weinberg, 2002; Karnoub & Weinberg, 2008; Lodish et al., 2000b; Lu et al., 2012; Vogelstein & Kinzler, 2004).

Head and neck squamous cell carcinoma (HNSCC) is the sixth most common type of cancer worldwide with an incidence of more than half a million new cases annually (Parkin et al., 2005; Vokes et al., 1993; Wilken et al., 2011). Early stages of HNSCC (stage I and stage II) have high cure rates. However, at advanced stages (stage III and IV), the local tumour control and survival rates decrease dramatically (Parker et al., 1997). Due to their inconspicuous location, many cases of HNSCC are discovered at a later stage (Wilken et al., 2011). Despite continuing research and advances in conventional therapies the overall survival rates for HNSCC had only marginal improvement in the last several decades with an overall five year survival rate of as low as 50% (Arbes et al., 1999; Argiris et al., 2004; Forastiere et al., 2001; Stell, 1989; Vokes et al., 1993; Wilken et al., 2011). As a result, there is a significant interest in developing potential alternative and less toxic therapies for head and neck cancer to reduce the side effects and toxicity and to achieve better clinical outcome (Wilken et al., 2011).

The classical cancer treatment regimes include surgery, radiotherapy and chemotherapy. Radiotherapeutic treatment uses photons and electrons to cure patients or control tumour growth (Lawrence et al., 2008). It is estimated that 50% of cancer patients receive radiotherapy that contributes to 40% of curative treatment (Deutsche Krebshilfe; Baskar et al., 2012; Eke et al., 2010). The functional consequences of irradiation include cell killing, deoxyribonucleic acid (DNA) damage and repair, cell cycle alterations, altered gene transcription and genomic instability (Baumann et al., 2008). Among these consequences, induction of cancer cell death is the main goal of radiotherapy (Baskar et al., 2012; Baumann et al., 2008). Several ways, such as mitotic catastrophe, apoptosis, necrosis, senescence and autophagy, contribute to the elimination of cancer cells after irradiation (Baumann et al., 2008; Chary & Jain, 1989; de Bruin & Medema, 2008; Dewey

et al., 1995; Padera et al., 2004; Roninson et al., 2001; Vakifahmetoglu et al., 2008). Cell death via mitotic catastrophe is the most important effect of ionising radiation in solid tumours (Baumann et al., 2008; Dewey et al., 1995; Hedman, 2012).

The combination of radiotherapy with cytotoxic chemotherapeutic agents is widely used to improve the curative rates of radiotherapy (McGinn et al., 1996; Stratford, 1992). As chemotherapeutic agents do not differentiate between tumour tissues and normal tissues, the improvement of curative rates using the combined radio-chemotherapeutic regime is limited by the cytotoxicity of the chemotherapeutic agents to normal tissues (Wachsberger et al., 2003). Therefore, identification of suitable targets to specifically treat cancer cells is necessary to minimise the normal tissue damage and to improve the therapeutic outcome.

Interestingly, the radiosensitivity of cells varies according to the cell cycle phases (Choy et al., 2008; Sinclair, 1968; Sinclair & Morton, 1963; Terasima & Tolmach, 1963; Watanabe & Horikawa, 1980). Radiation-induced DNA damage activates cell cycle checkpoints to arrest cell cycle progression (Harrison & Haber, 2006; Melo & Toczyski, 2002; Sancar et al., 2004; Weitzman et al., 2013). This provides enough time for DNA damage repair and prevents replication and segregation of the damaged genome (Weinert et al., 1994; Weitzman et al., 2013; Yata & Esashi, 2009). Therefore, manipulating the cell cycle by targeting cell cycle regulators, such as cyclin-dependent kinases (CDKs), might assist cancer treatment optimisation (Canavese et al., 2012; Diaz-Padilla et al., 2009; Malumbres et al., 2008).

CDKs are a group of serine/threonine protein kinases and are involved in regulating cell cycle progression, DNA damage response and transcription (Aleem & Kaldis, 2006; Wohlbold & Fisher, 2009). The critical role for CDKs in several cellular functions and frequent aberrations of their activity in cancer encouraged an intensive screening for small-molecule CDK pharmacological inhibitors to block the CDK activity (Canavese et al., 2012; Diaz-Padilla et al., 2009; Malumbres et al., 2008). Despite intensive research on CDKs as potential anticancer targets, studies evaluating targeting of CDKs in combination with irradiation are rare and the specific contribution of CDKs as adjuvant targets for radiotherapy remains poorly understood. A key question to be answered is which CDK or group of CDKs is a suitable target to attenuate the cellular radiosensitivity of cancer cells.

This study evaluated the role of CDK2 and CDK9 as targets to disturb the response of HNSCC cells to ionising radiation. The choice of CDK2 as a target is based on its vital role in cell cycling and DNA damage repair (Satyanarayana & Kaldis, 2009a) as well as unpublished preliminary data generated by Prof. Cordes and Prof. Aleem (Alexandria University, Egypt) show that mouse embryonic fibroblasts knockout for CDK2

(CDK2$^{-/-}$ MEFs) are more sensitive to ionising radiation as compared to wild type mouse embryonic fibroblasts (WT MEFs). CDK9 was chosen as recent reports suggested that it is involved in maintaining the genomic integrity (Yu & Cortez, 2011; Yu et al., 2010).

The hypothesis of this work was that human HNSCC cells are radiosensitised by inhibition of CDK2 or CDK9. We were able to confirm this hypothesis by taken into account cell line- as well as growth condition-dependent differences.

Hence, the results of this study are of considerable importance in understanding the molecular mechanisms of the radiation-induced cell cycle response and the possible role of CDK2 and CDK9 in this process. This knowledge might assist the improvement of a targeted therapy for treating HNSCC.

2 Background

2.1 Cell Cycle as a Target for Radiotherapy

In contrast to normal cells that proliferate only in response to developmental or mitogenic signals, cancer cells undergo limitless replicative cycles (Hanahan & Weinberg, 2000; Lapenna & Giordano, 2009). This does not mean that the cell cycle of cancer cells is basically different from normal cells; instead cancer cells proliferate because they are no longer subject to signals that govern normal cell proliferation and homeostasis (Deshpande et al., 2005; Hanahan & Weinberg, 2000). The cell cycle regulatory shunt in cancer cells mainly occurs via the acquisition of special capabilities such as growth signal autonomy, insensitivity to antigrowth signals and resistance to apoptosis (Deshpande et al., 2005; Hanahan & Weinberg, 2000).

Similar to normal cells, cancer cells pass through the well-known phases of the cell cycle: Gap1 (G1), Synthetic phase (S phase), Gap2 (G2) and Mitosis (M phase) (Pines, 1995; Sanchez & Dynlacht, 2005; Sherr, 1996). The progression of these different cell cycle phases is regulated by a family of protein kinases known as CDKs (Sanchez & Dynlacht, 2005; Sherr, 1996). CDKs, together with their regulatory proteins "Cyclins", are considered as the molecular engine of the cell cycle machinery (Dickson & Schwartz, 2009; Esposito et al., 2013; Halperin et al., 2008).

Cell cycle kinetic plays a crucial role in the response of cells to ionising radiation. In general, proliferative cells are more susceptible to ionising radiation than non-proliferative cells (Choy et al., 2008). The cytotoxic effect of radiotherapy depends on the position of the cell in the cell cycle. The cell cycle phase dependency of radiosensitivity of cells was first reported in HeLa cells by Terasima and Tolmach (Terasima & Tolmach, 1963). In response to irradiation, cells in G2 and M phases of the cell cycle are the most radiosensitive, S phase cells are the most radioresistant and G1 cells show moderate radiosensitivity (Burki, 1980; Choy et al., 2008; Chuang & Liber, 1996; Dewey et al., 1970; Jostes et al., 1980; Leonhardt et al., 1997; Sinclair, 1968; Sinclair & Morton, 1963; Terasima & Tolmach, 1963; Watanabe & Horikawa, 1980). Therefore, the ability to manipulate the cell cycle regulation seems likely to have an important therapeutic impact on cancer treatment. For example, modulation of checkpoint response to DNA damage or elimination of the radioresistant S phase cell population may enhance the radiation response of cells to radiotherapy (Choy et al., 2008; Moretti et al., 2010).

2.2   Cell Cycle Checkpoints and DNA Damage Repair

Several studies have reported that DNA is the main subcellular target for ionising radiation (Hallahan et al., 1993; Valentin, 2005). Among ionising radiation-induced DNA lesions are DNA base damage, single strand break (SSB) and double strand break (DSB) (Han & Yu, 2010). DNA base damages play a minor role in radiation mutagenesis and can be repaired via the base excision repair (BER) pathway (Han & Yu, 2010). Most of the SSBs are repaired through DNA ligation (Han & Yu, 2010; von Sonntag, 1987). On the contrary, DSBs are much more difficult to repair and persist as damaged DNA sites of about 15 to 20 nucleotides in size (Stewart, 2001; Ward, 1981). Inefficient repair of DSBs may lead to micronuclei formation, chromosome aberrations and deprivation of the proliferative integrity of the cell's genome (Baskar et al., 2012; Brock & Williams, 1985; Deschner & Gray, 1959; Difilippantonio et al., 2002; Goodhead, 1994; Hall, 1972; Helleday et al., 2007; Hoeijmakers, 2001; Lea, 1955; McBride & Withers, 2008; Vidal et al., 2001; Ward, 1988; Ward, 1995; Zhu et al., 2002).

The initiation of each of the four successive cell cycle phases depends on the completion of the previous phase. Cell cycle checkpoints are the mechanisms that control this ordered dependency (Deckbar et al., 2011; Fleck & Nielsen, 2004; Lodish et al., 2000a). In response to genotoxic stress, cells activate the DNA damage checkpoint pathways and arrest progression of the cells cycle (Su, 2006; Weitzman et al., 2013; Wohlbold & Fisher, 2009). The rationale behind the cell cycle arrest is to provide adequate time for DNA damage repair (Deckbar et al., 2011; Fleck & Nielsen, 2004; Weinert et al., 1994; Weitzman et al., 2013; Yata & Esashi, 2009). After efficient DNA damage repair, cells are released from the cell cycle arrest and continue to divide (Soule et al., 2010). Loss or attenuation of cell cycle control may compromise the genome fidelity due to insufficient time to repair the DNA damage (Xing et al., 2007).

There are two main DNA damage checkpoints: the G1/S checkpoint and the G2/M checkpoint (Bakkenist & Kastan, 2003; Latif et al., 2001; Sancar et al., 2004; Zhao et al., 2002). The G1/S checkpoint occurs at the end of the G1 phase and functions to check the integrity of the genome before DNA replication (Figure 2.1) (d'Adda di Fagagna et al., 2003). The G2/M checkpoint occurs at the end of the G2 phase and prevents cells with DNA lesions from entering mitosis (Deckbar et al., 2011; Fleck & Nielsen, 2004).

The checkpoint responses are primarily induced via two protein kinases: Ataxia telangiectasia mutated protein (ATM) and ataxia telangiectasia and Rad3-related protein (ATR) (Abraham, 2001; Durocher & Jackson, 2001; Harper & Elledge, 2007). ATM is primary activated in response to DSBs. First, the trimeric MRN complex, which consists of Mre11 (Meiotic recombination 11 homologue), Rad50 (a structural maintenance of

chromosome protein) and NBS1 (Nijmegen breakage syndrome 1), recognises the sites of DSBs. ATM is then recruited to the DNA damage site by direct interaction with the MRN complex and is activated by phosphorylation at residue serine (S) 1981 (Bakkenist & Kastan, 2003; Berkovich et al., 2007). Active ATM phosphorylates the histone variant 2AX at S139 (γH2AX) around the site of the DNA damage leading to further accumulation of MRN complexes and amplification of the checkpoint signal (Bristow & Hill, 2008; Yata & Esashi, 2009).
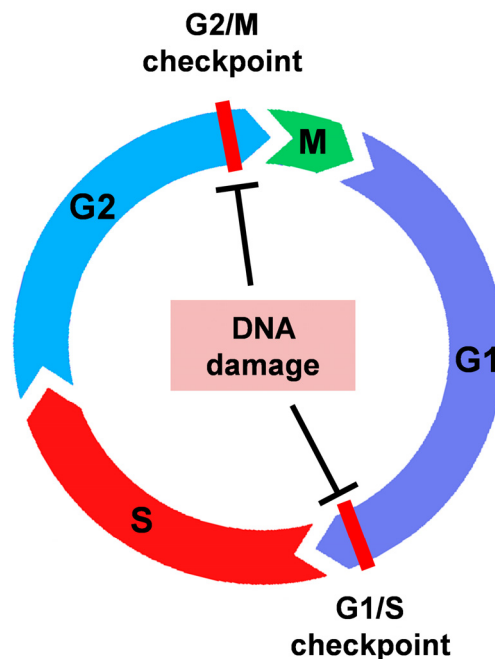
Figure 2.1. DNA damage checkpoints. G1/S and G2/M checkpoints are located at the end of the G1 and G2 phases, respectively.

ATR, on the other hand, is mainly involved in the response to SSBs and stalled replication forks (Bartek & Lukas, 2007; Bohgaki et al., 2010; Jazayeri et al., 2006; Shiloh, 2003). It is activated by the presence of single-strand DNA (ssDNA). Thereby, the ATR/ATR interacting protein (ATRIP) complex is recruited to the ssDNA region where it becomes fully activated (Jazayeri et al., 2006; Mordes et al., 2008).

Activated ATM or ATR then phosphorylates and activates their downstream substrates such as checkpoint kinase 1 (CHK1), checkpoint kinase 2 (CHK2) and p53 (Banin et al., 1998; Canman et al., 1998; Niida & Nakanishi, 2006). Via these downstream substrates, signalling from the components of the DNA damage response culminates in a checkpoint arrest (Latif et al., 2001).

The activation of p53 plays a central role in G1 arrest in response to genotoxic stress. Upon DNA damage, p53 is phosphorylated by ATM or ATR at several phosphorylation sites on its transactivation domain (Banin et al., 1998; Chehab et al.,

6

1999; Lim et al., 2000). The phosphorylation of p53 leads to the synthesis of CDK inhibitor 1A (p21$^{Cip1/Waf1/Sdi1}$) which binds to and inhibits the kinase activity of CDK2 and CDK4 (Banin et al., 1998; Canman et al., 1998; Sancar et al., 2004; Tibbetts et al., 1999). This leads to p21-mediated G1 arrest (Figure 2.2) (Harper et al., 1993; Li et al., 1994). Several studies have demonstrated that the G1 checkpoint activation is a slow process. It takes up to 6 h to abolish the S phase entry (Deckbar et al., 2010; Gadbois & Lehnert, 1997; Linke et al., 1997).
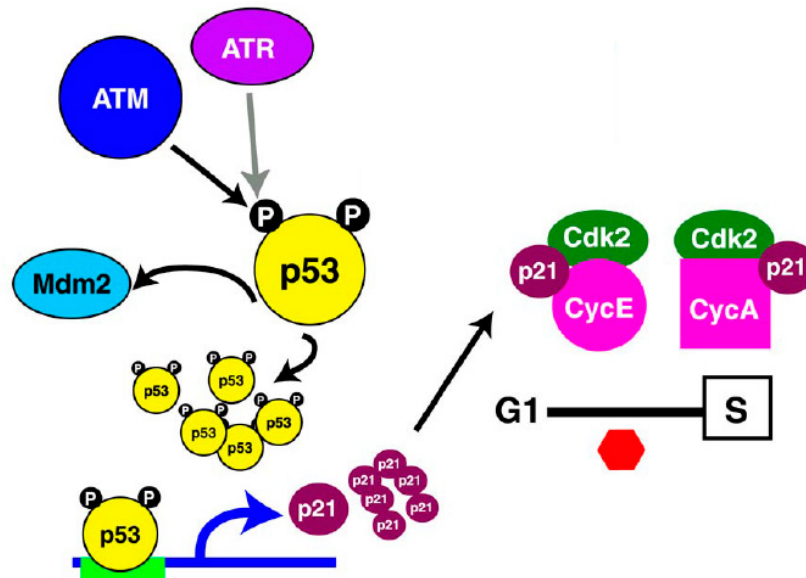
Figure 2.2. p53 activation mediates cell cycle arrest. The phosphorylation of p53 by ATM or ATR leads to the expression of p21 that inhibits the activity of CDKs (modified after Latif et al., 2001).

In the G2/M checkpoint, the activated CHK1 or CHK2 phosphorylates and inhibits the cell division cycle 25 (Cdc25) phosphatase activity (Deckbar et al., 2010; Zhao et al., 2002). As the phosphatase activity of Cdc25 is required for removal of the inhibitory phosphates from CDKs, the inhibition of Cdc25 delays the activation of CDK1 and leads to G2 cell cycle arrest (Figure 2.3) (Mailand et al., 2000; Mailand et al., 2002). Another p53-dependent pathway that induces a cell cycle G2/M arrest via transactivation of p21 has been described. However, the exact function of this pathway is not understood (Bruno et al., 2006; Chan et al., 2000; Lukas et al., 2004; Taylor & Stark, 2001).

During the cell cycle arrest, there are two main mechanisms to repair DSBs in eukaryotic cells: non-homologous end-joining (NHEJ) and homologous recombination (HR) (Helleday et al., 2007; Sancar et al., 2004). NHEJ is an error-prone repair mechanism and usually results in deletions or insertions at the site of DNA damage. NHEJ is active during all cell cycle phases but the favoured DNA damage repair mechanism during the G1 and early S phases (Figure 2.4). On the other hand, HR is preferred during

late S and G2 phases and results in high-fidelity error-free repair (Couedel et al., 2004; Han & Yu, 2010; Mills et al., 2004; Rothkamm et al., 2003; Saintigny et al., 2001; Saleh-Gohari & Helleday, 2004; Takata et al., 1998).
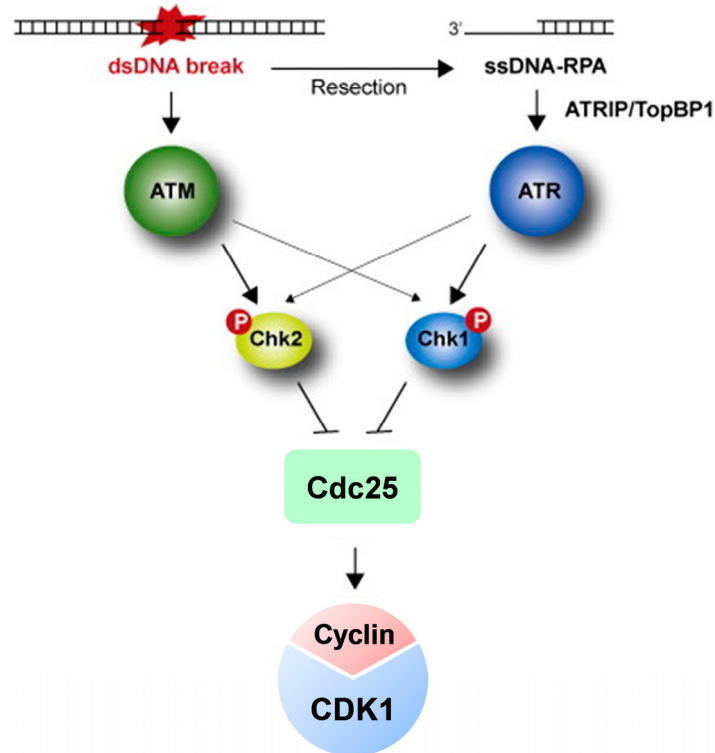
Figure 2.3. ATM or ATR checkpoint signalling inhibits the activity of CDK/Cyclin complexes. In response to DNA damage, activated ATM or ATR phosphorylates and activates CHK1 and CHK2 that inhibit the Cdc25 phosphatase activity and prevent the activation of CDK/Cyclin complexes (modified after Yata & Esashi, 2009).
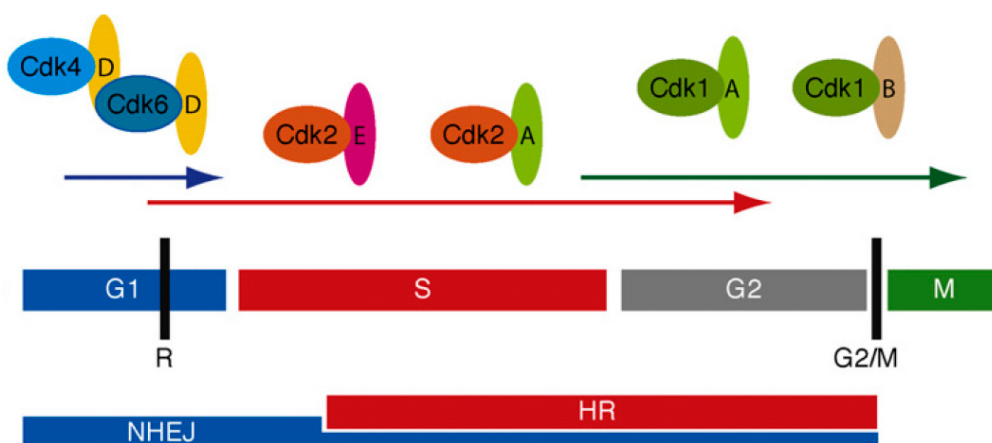
Figure 2.4. NHEJ and HR are regulated differentially through the cell cycle. NHEJ is the dominant repair pathway in the G1 and early S phases but stays active throughout the cell cycle while HR is active only during late S and G2 (modified after Wohlbold & Fisher, 2009).

NHEJ ligates the two ends of a DSB without sequence homology (Han & Yu, 2010). The first step in this process is the binding of Ku70/Ku80 heterodimer to the DNA ends (Fleck & Nielsen, 2004). The Ku heterodimer then recruits the catalytic subunit of DNA-PK (DNA-PKcs) to form the DNA-dependent protein kinase (DNA-PK) holoenzyme (Gottlieb & Jackson, 1993; Smith et al., 1999; Smith & Jackson, 1999; Yata & Esashi, 2009). DNA-PKcs is activated by autophosphorylation and displays serine/threonine kinase activity (Han & Yu, 2010). Activated DNA-PKcs phosphorylates and activates additional repair proteins including the ARTEMIS nuclease. ARTEMIS or the MRN complex processes the DNA ends (Lans et al., 2012) that are then ligated by the XLF/XRCC4/DNA ligase IV complex (Figure 2.5) (Ahnesorg et al., 2006; Drouet et al., 2005; Drouet et al., 2006; Fleck & Nielsen, 2004; Goodarzi et al., 2006; Yata & Esashi, 2009).
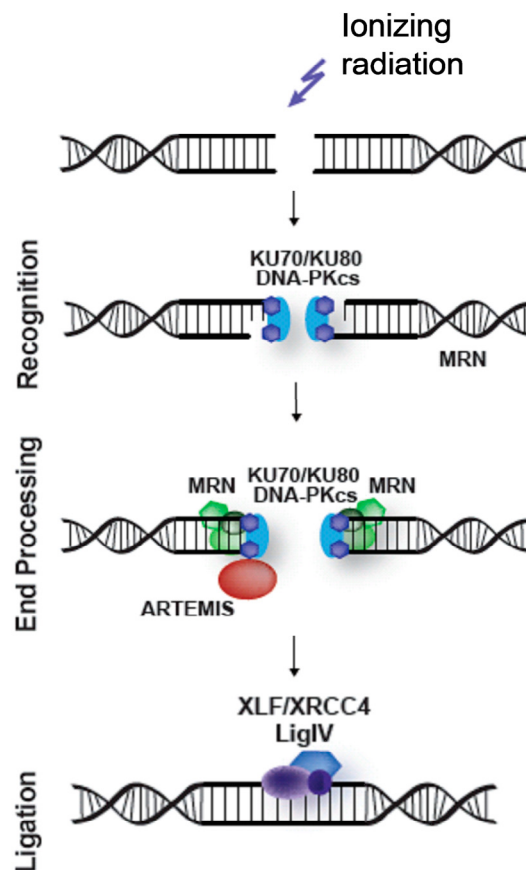
Figure 2.5. Schematic of the NHEJ pathway. Binding of Ku70/Ku80 heterodimer binds to DSB ends and recruits the catalytic subunit of DNA-PK (DNA-PKcs). The activated DNA-PKcs phosphorylates ARTEMIS which process the DSB ends. The MRN complex may also process the DSB ends. The XLF/XRCC4/DNA ligase IV (LigIV) complex joins the two broken DNA ends (modified after Lans et al., 2012).

HR repair, on the other hand, uses an undamaged sister chromatid or a homologous chromosome as a template for repair. The repair process starts with a nucleolytic resection of the DSB by the MRN complex in the 5'-3' direction to generate 3' ssDNA ends, which are bound by RPA. RAD52 binds to RPA and stimulates the binding of RAD51 to the 3' ssDNA ends. Subsequently, RAD54 stimulates the RAD51-associated ssDNA to invade into the homologous duplex DNA. After repair synthesis and ligation, two Holliday junctions are formed and branch migration can occur. Finally, the holliday junctions are resolved (Figure 2.6) (Fleck & Nielsen, 2004; Han & Yu, 2010; West, 2003; Wyman & Kanaar, 2004).
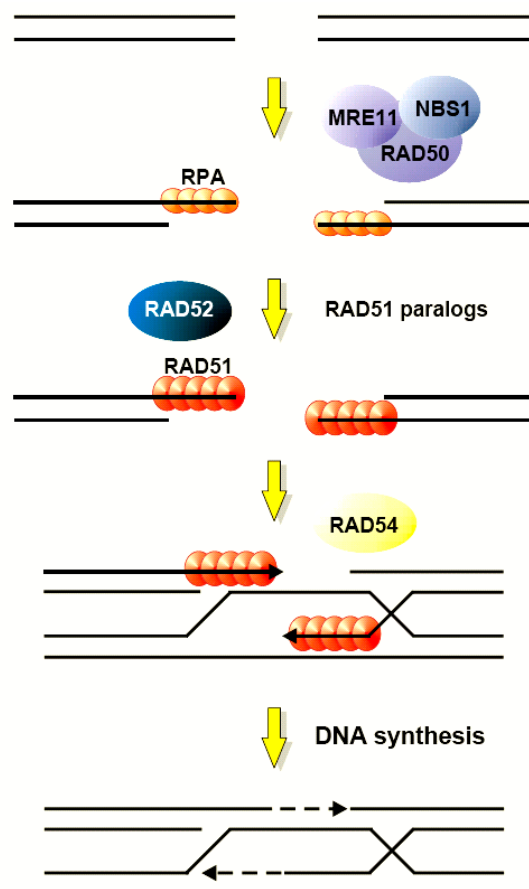
Figure 2.6. Schematic representation of the HR repair pathway. HR is initiated by DNA end-resection generating ssDNA ends. The generated ssDNA ends are bound by RPA, which is subsequently replaced by RAD51. RAD54 stimulates the invasion of the RAD51 flanked-ssDNA ends to a homologous DNA template and promotes DNA synthesis and repair (modified after Fleck & Nielsen, 2004)

2.3 Cyclin-Dependent Kinases

CDKs are a group of serine/threonine protein kinases firstly discovered for their role in regulating the cell cycle (Malumbres & Barbacid, 2005; Nigg, 1995; Norbury & Nurse, 1992; Nurse, 1994; Orend et al., 2003; Pines, 1995; Schafer, 1998). Also, they are

implicated in many other cellular functions such as transcription regulation (transcriptional CDKs), mRNA processing and nerve cell differentiation (Bartkowiak et al., 2010; Blazek et al., 2011; Bres et al., 2008; Cruz & Tsai, 2004; Kohoutek & Blazek, 2012; Pirngruber et al., 2009; Romano & Giordano, 2008). The activity of CDKs is regulated either positively by Cyclins or negatively by CDK inhibitors. In addition, sequential phosphorylation and dephosphorylation events at certain threonine or tyrosine residues of CDKs control their activity (Obaya & Sedivy, 2002; Orend et al., 2003). Up to date, 13 CDK candidates (CDK1-CDK13) were indentified. At least four CDKs (CDK1, CDK2, CDK4 and CDK6) are directly involved in cell cycle regulation (cell cycle CDKs).

Cell cycle CDKs act as on/off switches for the cell cycle of human cells and form, together with Cyclins, a panel of heterodimeric complexes that precisely regulate the progression of each cell cycle phase as well as the transition through the cell cycle phases (Figure 2.7) (Pavletich, 1999; Shapiro, 2006).
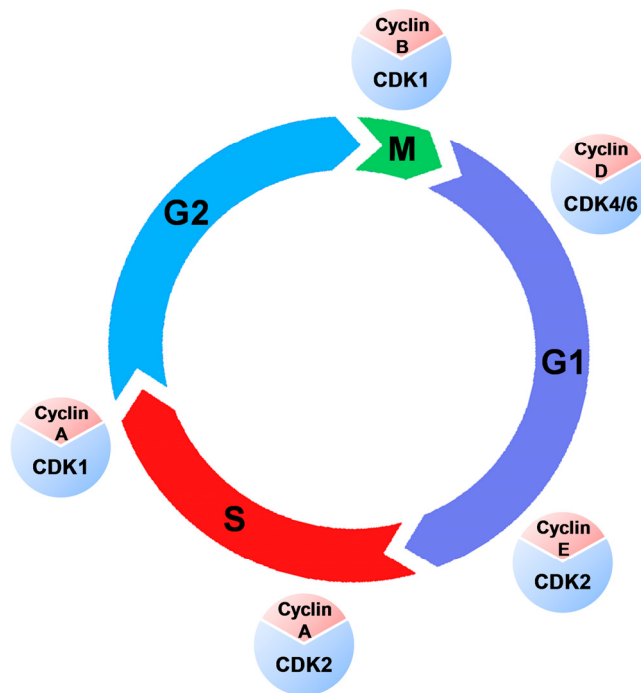
Figure 2.7. The phases of the cell cycle (G1, S, G2 and M) and their regulatory CDK/Cyclin complexes.

During the cell cycle, complexes of CDK4 or CDK6 with Cyclin D are activated in early G1 phase and phosphorylate the retinoblastoma protein (Rb) family members (Rb, p107 and p130) (Sherr, 1995; Sherr & Roberts, 2004). This leads to the release of the E2F transcription factor that initiates cell-cycle gene transcription and subsequently promotes cell cycle progression (Cobrinik, 2005; Dyson, 1998; Weinberg, 1995). Early E2F responsive genes include Cyclin E and Cyclin A (Boonstra & Post, 2004; Lundberg &

Weinberg, 1998; Malumbres & Barbacid, 2005; Sherr & Roberts, 1999). In the late G1 phase, CDK2/Cyclin E activity completes the phosphorylation of Rb leading to G1/S phase transition and S phase initiation (Figure 2.8) (Boonstra & Post, 2004; Lundberg & Weinberg, 1998; Ohtsubo et al., 1995; Sherr & Roberts, 1999; Sherr & Roberts, 2004; Trimarchi & Lees, 2002).

Later, CDK2/Cyclin A activity is required for the progression of the S phase and DNA duplication (Malumbres & Barbacid, 2005). At the end of the S phase, Cyclin A associates with CDK1. Both CDK2/Cyclin A and CDK1/Cyclin A complexes target several common substrates that are involved in the DNA replication (e.g. Cdc7) and the control of cell-cycle progression (e.g. Rb, p53 and BRCA2). During G2 phase, Cyclin A is degraded whereas Cyclin B is actively synthesised. The formation of CDK1/Cyclin B is believed to be essential for the initiation and progression of mitosis (Malumbres & Barbacid, 2005; Malumbres & Barbacid, 2009; Nigg, 2001; Riabowol et al., 1989). Finally, Cyclin B destruction is necessary for exit from mitosis (Murray, 1995; Sullivan & Morgan, 2007).
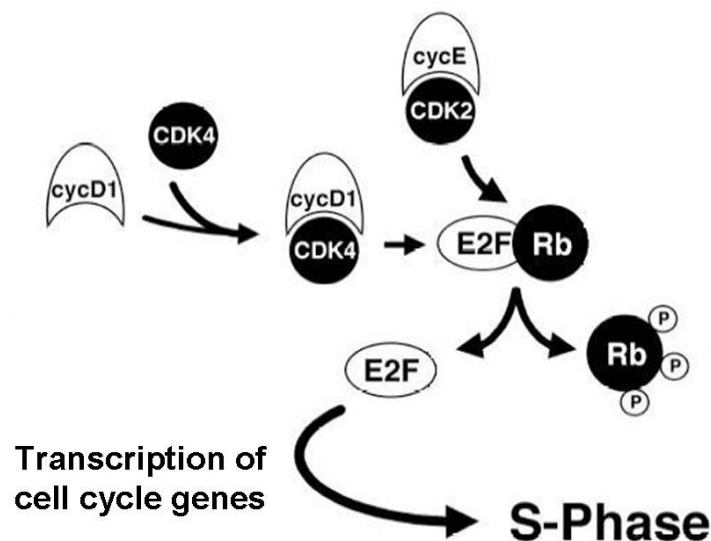
Figure 2.8. The mechanism of the inhibitory phosphorylation of Rb. CDK4/Cyclin D and CDK2/Cyclin E complexes during the G1 phase release the E2F transcription factor. The E2F transcription factor starts transcription of a set of cell cycle genes leading to G1 phase progression and G1/S phase transition (modified after Daniel, 2002).

CDK3/Cyclin C complexes are involved in re-entrance from G0 to G1 phase (Ren & Rollins, 2004) and CDK5 kinase activity regulates neuronal functions (Cruz & Tsai, 2004).

CDK7 together with Cyclin H and Mat1 form a trimeric multifunctional complex. This complex is able to regulate the cell cycle as CDK activating kinase (CAK) and the transcription via phosphorylating the carboxyl terminal domain (CTD) of RNA polymerase II (RNAP II) (Wallenfang & Seydoux, 2002).

CDK8-CDK13 (also known as transcriptional CDKs) are mainly involved in transcription regulation (Akoulitchev et al., 2000; Bartkowiak et al., 2010; Blazek et al., 2011; Chen et al., 2006; Chen et al., 2007; Garriga & Grana, 2004; Hu et al., 2007; Kasten & Giordano, 2001; Kohoutek & Blazek, 2012). Recently, it was reported that CDK9 functions to maintain the genomic integrity (Yu & Cortez, 2011; Yu et al., 2010).

The activities of CDK/Cyclin complexes are regulated by two families of CDK inhibitors (INK4 family and Cip/Kip family). The INK4 family (p16^{INK4a}, p15^{INK4b}, p18^{INK4c}, p19^{INK4d}) specifically inhibits CDK4 and CDK6 activities while the Cip/Kip family (p21$^{Cip1/Waf1/Sdi1}$, p27^{Kip1}, p57^{Kip2}) is able to inactivate all G1 CDK/Cyclin complexes and, to a lesser extent, CDK1/Cyclin B complexes (Aprelikova et al., 1995; Harper et al., 1995; Hengst & Reed, 1998; Lee et al., 1995; O'Connor, 1997; Polyak et al., 1994; Roussel, 1999; Satyanarayana & Kaldis, 2009b; Soffar et al., 2013; Toyoshima & Hunter, 1994).

2.4   Targeting of CDKs in Cancer Therapy

Deregulation of the activity of cell cycle protein kinases is a hallmark of cancer (Esposito et al., 2013; Lapenna & Giordano, 2009; Malumbres & Barbacid, 2009; Rizzolio et al., 2010; Santamaria et al., 2007). Mutations resulting in overexpression or hyperactivation of CDKs in cancers have been reported in several studies (Easton et al., 1998; Kim et al., 1999; Malumbres & Barbacid, 2009; McDonald & El-Deiry, 2000; Nevins, 2001; Ortega et al., 2002; Tsihlias et al., 1999; Vermeulen et al., 2003; Wolfel et al., 1995; Yamamoto et al., 1998). Therefore, CDKs are regarded as promising targets for cancer therapy (Esposito et al., 2013; Graf et al., 2011; Rizzolio et al., 2010).

The intensive research for small molecule pharmacological inhibitors targeting CDKs resulted in the identification of various candidates that are able to inhibit CDK activity and cease proliferation (Canavese et al., 2012; Diaz-Padilla et al., 2009; Lapenna & Giordano, 2009; Malumbres et al., 2008). The major CDK targets of these inhibitors are CDK1, CDK2, CDK4, CDK6, CDK7 and CDK9 (Graf et al., 2011). First-generation CDK pharmacological inhibitors (e.g. Flavopiridol and *R*-Roscovitine) are now in late-stage clinical trials (Canavese et al., 2012; Colevas et al., 2002; Kelland, 2000). However, these pharmacological inhibitors have shown only modest activity (Byrd et al., 2007; Malumbres et al., 2008). A second generation of CDK pharmacological inhibitors (e.g. ZK 304709) are now under investigation in advanced preclinical or clinical studies (Malumbres et al., 2008; Siemeister et al., 2006). Nevertheless, none of these molecules has already been approved as a drug for cancer therapy (Galons et al., 2010; Graf et al., 2011).

Despite their critical role on several cellular functions and the intensive investigation of these proteins as potential cancer targets, studies evaluating the role of CDKs as molecular targets to enhance cancer response to ionising radiation are rare.

In this work, we investigated two candidates of the CDK family, CDK2 and CDK9, as potential molecular targets to enhance the cancer cell response to ionising radiation.

2.4.1   CDK2

Structurally, CDK2 exhibits a large protein kinase domain which contains three important phosphorylation sites (Endicott et al., 1999; Johnson & Lewis, 2001). The two deactivating phosphorylation sites are threonine (T) 14 and tyrosine (Y) 15 and the activating phosphorylation site is T160 (Figure 2.9A). X-ray crystallography revealed that CDK2 is composed of a small N-terminal lobe and a large C-terminal lobe (Figure 2.9B) (De Bondt et al., 1993). The amino (N)-terminal lobe comprises of a highly conserved beta-sheet (Baumli et al., 2008), while the carboxyl (C)-terminal lobe is composed of six alpha-helices and one beta-sheet. This two-lobed structure forms an adenosine triphosphate (ATP)-binding cleft constituting the active site (Hanks & Hunter, 1995; Hu et al., 1994; Ubersax & Ferrell, 2007). Activation of CDK2 requires binding of a regulatory cyclin unit such as Cyclin E or Cyclin A, phosphorylation of T160 by a CAK and dephosphorylation on T14/Y15 by Cdc25 for complete kinase activation (Bartova et al., 2004; Lunn et al., 2010).

CDK2 as a target for cancer therapy attracted increasing attention as it contributes to vital cell cycle regulatory pathways such as G1 phase progression, cell cycle transitions (G1/S as well as G2/M phase transitions) and G2/M checkpoint activation (Aleem et al., 2004; Kaldis & Aleem, 2005; Sherr & Roberts, 2004). Furthermore, CDK2 targets a set of substrates that regulate G1/S checkpoint and DNA damage repair response (Esashi et al., 2005; Muller-Tidow et al., 2004; Myers et al., 2007; Neganova et al., 2011; Ruffner et al., 1999; Satyanarayana & Kaldis, 2009b). Several studies reported that CDK2/Cyclin A complex regulates substrates that are involved in NHEJ (e.g. Ku70) (Lee & Desiderio, 1999; Lin & Desiderio, 1994; Muller-Tidow et al., 2004). Moreover, DNA Polymerase λ, a protein involved in regulating NHEJ as well as BER, is also a substrate of CDK2 (Frouin et al., 2005; Wimmer et al., 2008; Wohlbold & Fisher, 2009). CDK2 also regulates ATRIP phosphorylation on S224 and modulates the ability of ATR/ATRIP complex to promote cell cycle arrest in response to DNA damage (Myers et al., 2007).

In this work, the investigation of CDK2 as a target to modulate the cellular radiation response of HNSCC is based on its role cell cycling and DNA damage repair (Esashi et al., 2005; Muller-Tidow et al., 2004; Myers et al., 2007; Neganova et al., 2011; Ruffner et al., 1999; Satyanarayana et al., 2008; Satyanarayana & Kaldis, 2009b) as well as on unpublished data generated by Prof. Cordes and Prof. Aleem (Alexandria University, Egypt) show that CDK2$^{-/-}$ MEFs are more radiosensitive than WT MEFs.

A

B
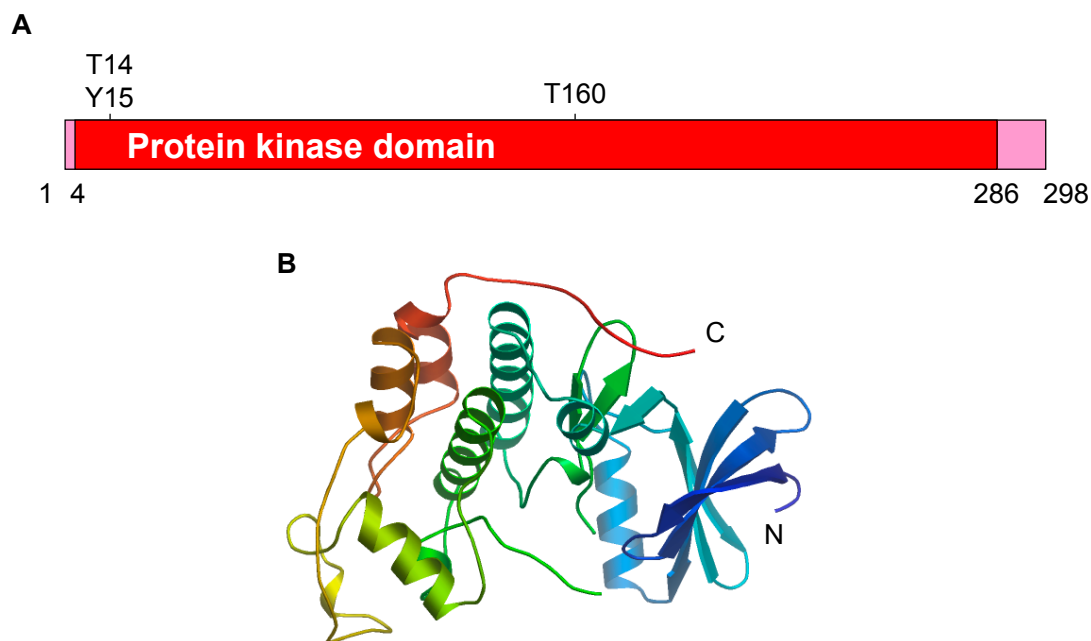
Figure 2.9. Structure of human CDK2. (A) Schematic of CDK2 showing the protein kinase domain (red), the inhibitory phosphorylation sites T14 and Y15 and the activating phosphorylation site T160. **(B)** Crystal structure of human CDK2 (http://www.phosphosite.org (CDK2-human-1AQ1)). CDK2 is composed of a small N-terminal lobe (right) and a large C-terminal lobe (left). Protein substrates bind to the active CDK2/Cyclin complex in the wide cleft between the small and large lobes (De Bondt et al., 1993).

2.4.2   CDK9

The structure of CDK9 is similar to CDK2 (Baumli et al., 2008). It contains a conserved protein kinase domain with an activating phosphorylation site (T186) (Figure 2.10A) (Baumli et al., 2008). CDK9 has a C-terminal tail with a largely non-conserved sequence (Baumli et al., 2012). This C-terminal tail is necessary for the nuclear import of the CDK9/Cyclin complex (Napolitano et al., 2003). CDK9 is composed of two lobes (Figure 2.10B). The N-terminal lobe is mainly comprised of beta-sheet and the C-terminal lobe is mainly consisted of alpha-helices (Baumli et al., 2008).

CDK9 is activated by forming heterodimeric complexes with either Cyclin T or Cyclin K families (Garriga et al., 2003; Peng et al., 1998; Yu & Cortez, 2011; Zhu et al., 1997). The activity of CDK9 is inhibited by both 7SK and HEXIM1 proteins (Michels et al., 2004).

CDK9 together with Cyclin T or Cyclin K form a complex known as positive transcription elongation factor b (pTEFb). This complex promotes transcription elongation by phosphorylating the CTD of the large subunit of RNAPII (Rpb1-CTD) on the S2 residue (Yu & Cortez, 2011). CDK9 also phosphorylates Rpb1-CTD on S5 (Ramanathan et al., 2001; Zhou et al., 2000). pTEFb modulates other cellular functions such as co-transcriptional histone modification, mRNA processing and mRNA export (Bres et al.,

2008; Pirngruber et al., 2009; Romano & Giordano, 2008). A recent study showed that CDK9 together with Cyclin K but not cyclin T are involved in maintaining the genome integrity after replication stress (Yu et al., 2010).

A

B
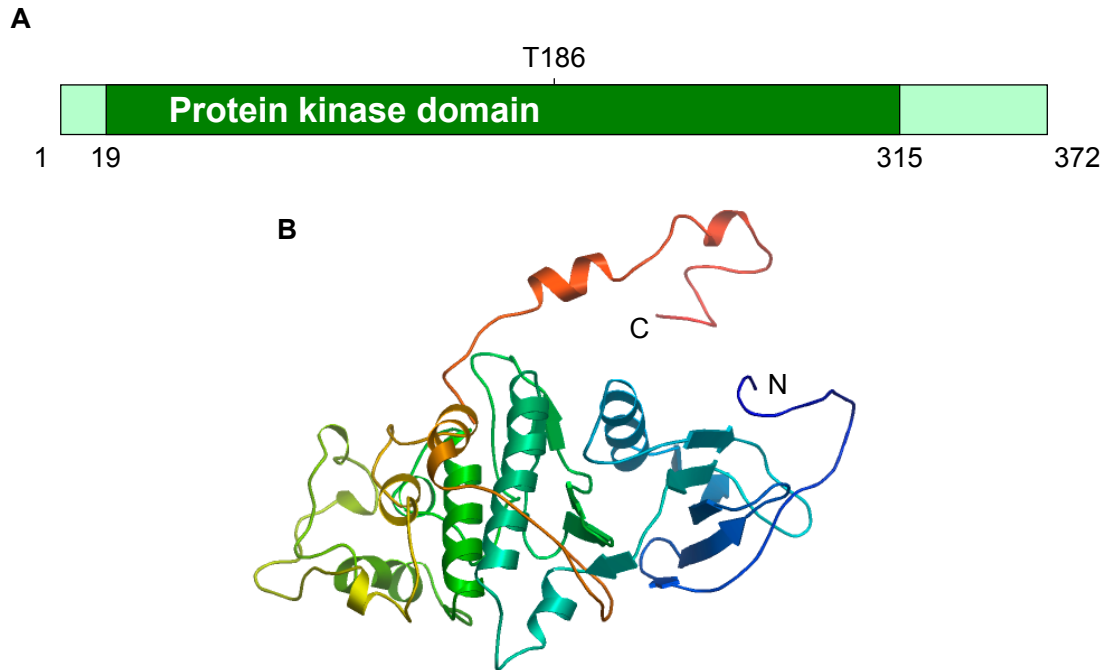
Figure 2.10. Structure of human CDK9. (A) Schematic of CDK9 showing the protein kinase domain (green) and the activating phosphorylation site T186. **(B)** Crystallographic structure of human CDK9 (http://www.phosphosite.org (CDK9-human-1PF6)).

Recently, CDK9 was reported to impact the cell cycle recovery after a transient pulse of Hydroxyurea or Aphidicolin and stimulates γH2AX phosphorylation in the absence of exogenous damage (Liu & Herrmann, 2005; Yu et al., 2010). In addition, co-immunoprecipitation studies showed that the CDK9/Cyclin K complex interacts with ATR, ATRIP and other DNA repair and checkpoint signalling proteins suggesting that CDK9/Cyclin K plays a role in maintaining genome integrity (Yu et al., 2010).

Based on its recently described role in DNA damage repair response, we investigated CDK9 as a target to improve cancer cell response to radiotherapy.

3   Aim of Work

The radiosensitivity of tumour cells depends mainly on their capacity to maintain genomic integrity. This requires efficient repair of radiation-induced DNA DSBs (Dikomey & Brammer, 2000; Hanahan & Weinberg, 2000; Jeggo & Lobrich, 2006a; Karnoub & Weinberg, 2008), a process governed by the cell cycle. Particularly, the action of integrating the molecular mechanisms of radiation-induced damage and cell cycling is still not well understood (Dikomey & Brammer, 2000; Iliakis et al., 2003; Jeggo & Lobrich, 2006b).

The crucial role of CDKs in cell cycling and DNA damage repair and the frequent aberrations of their activities in cancer encouraged an intensive screening for small-molecule CDK pharmacological inhibitors that block the CDK activity (Canavese et al., 2012; Diaz-Padilla et al., 2009; Malumbres et al., 2008). Despite the intensive research regarding CDKs as target for cancer therapy, studies evaluating their role in response of cancer cells to irradiation are rare.

Therefore, the aim of this work is to identify the molecular role of CDK2 and CDK9 in cellular response of human HNSCC cancer cells to ionising radiation. To achieve this goal, we analysed several parameters such as clonogenic cell survival, DNA repair, cell cycle progression, apoptosis induction and expression and phosphorylation of various cell cycle and DNA repair proteins. Furthermore, we elucidated the relationship between the cell cycle/DNA repair regulatory events and tumour cell survival which might contribute to the optimisation of cancer treatment.

4 Materials and Methods

4.1 Materials

4.1.1 Cell Lines

WT and CDK2$^{-/-}$ MEFs were generated as described in (Berthet et al., 2003) and were kindly provided by Prof. E. Aleem, Alexandria University, Egypt. Human SAS, FaDu, HSC4, Cal33, UTSCC5 and UTSCC8 HNSCC cell lines were a kind gift of Prof. R. Grenman, Turku University Central Hospital, Finland and Prof. M. Baumann, Dresden University of Technology, Germany.

SAS-CDK9-EGFP and SAS-EGFP cells were generated as described in section 4.4.

4.1.2 Bacteria

XL1-Blue competent *Escherichia coli* (Agilent Technologies, Inc., California, United States) was used as host organism. The genotype of these cells is: *recA1 endA1 gyrA96 thi-1 hsdR17 supE44 relA1 lac* [F' *proAB lacI^{q}ZΔM15* Tn*10*(Tet^r)].

4.1.3 Plasmid

In order to amplify the CDK9 gene, the full coding DNA sequence of human WT CDK9 was cloned between the cytomegalovirus (CMV) promoter region and the enhanced green fluorescence protein (EGFP) encoding region of the pEGFP-N1 plasmid (Invitrogen, Karlsruhe, Germany) (Section 4.4).

4.1.4 Equipments

Device	Model	Manufacturer
Autoclave	V-65	Systec, Wettenberg, Germany
Bacterial incubator		Memmert, Schwabach, Germany
Barometer		Conrad Electronics, Hirschau, Germany
Bio Imaging System	Gene Genius	Syngene, Cambridge, Great Britain
Centrifuge	5804R	Eppendorf, Hamburg, Germany
Centrifuge	5810R	Eppendorf, Hamburg, Germany
Centrifuge	Minispin$^®$	Eppendorf, Hamburg, Germany
CO$_2$ incubator	Heracell	Heraeus Holding GmbH, Hanau, Germany
Cooled vertical electrophoresis Unit	SE 600	Hoefer, San Francisco, USA
Counting chamber	Neubauer bright line	Paul Marienfeld GmbH & Co. KG, Lauda-Königshofen, Germany

Device	Model	Manufacturer
Dosimeter	PTW Unidos	PTW, Freiburg, Germany
Flow cytometer	CyFlow	Partec GmbH, Münster, Germany
Fluorescence microscope	Axioskop 2 plus	Carl Zeiss, Jena, Germany
Freezer -20 ºC	KX1011	Liebherr, Ochsenhausen, Germany
Freezer -80 ºC		Heraeus Holding GmbH, Hanau, Germany
Ice machine	AT910	Scotsman, London, Great Britain
Incubation shaker	CERTOMAT®IS	B. Braun Melsungen AG, Melsungen, Germany
Incubator for cell culture solutions		Heraeus Holding GmbH, Hanau, Germany
Inverted microscope	Axiovert 25	Carl Zeiss, Jena, Germany
Inverted fluorescence microscope	Axiovert 40 CFL	Carl Zeiss, Jena, Germany
Inverted fluorescence microscope	Axio Observer Z1	Carl Zeiss, Jena, Germany
Laminar flow cabinet	Clean Air	Heraeus Holding GmbH, Hanau, Germany
Laser scanning microscope (LSM)	Axiovert 200M, LSM 510 Meta	Carl Zeiss, Jena, Germany
Magnetic stirrer with heater	MR 3001	Heidolph, Schwabach, Germany
Manual piece counter	T 120	IVO, Villingen-Schwenningen, Germany
Microcentrifuge	5415R	Eppendorf, Hamburg, Germany
Microwave		Sharp Electronics (Europe) GmbH, Hamburg, Germany
Mini-vertical electrophoresis unit	SE 250	Hoefer, San Francisco, USA
Multidimensional platform shaker	Polymax 1040	Heidolph, Schwabach, Germany
Nanodrop® Spektrophotometer	ND-1000	PeqLab Biotechnologie GmbH, Erlangen, Germany
Orbital shaker	KS 260 basic	IKA, Staufen, Germany
Plastic sealer machine	Dual Electronic	Jencons-PLS, London, Great Britain
pH meter	ph Level 1	inoLab, Weilheim, Germany
Photo scanner	Perfection 4490 PHOTO	Epson, Meerbusch, Germany
Power supply	EPS601	Amersham, Freiburg, Germany
Precision balance	LE244S-0CE	Sartorius, Göttingen, Germany
Refrigerator		Liebherr, Ochsenhausen, Germany
Roller mixer	SRT1	Stuart Scientific Ltd., Bath, Great Britain
Scale	BL 1500 S	Sartorius, Göttingen, Germany
Semi-dry transfer unit	TE77	Amersham, Freiburg, Germany
Stereo-microscope with light source	Stemi-2000	Carl Zeiss, Jena, Germany
Tecan microplate reader	Genios Pro	Tecan, Crailsheim, Germany
Thermocycler	Mastercycler epgradient	Eppendorf, Hamburg, Germany
Thermomixer	Comfort 1.5 ml	Eppendorf, Hamburg, Germany
Vacuum pump	Vacusafe comfort	VacuSafe IBS Integra Bioscience, Chur, Switzerland
Vortex mixer	Reax control	VWR, Darmstadt, Germany
Washer disinfector	Compact disinfector G7783 CD	Miele & Cie. KG, Gütersloh, Germany
Water bath	SW22	Julabo Labortechnik GmbH, Seelbach, Germany
Water purification system	Milli-Q®	Millipore, Schwalbach/Ts., Germany

Device	Model	Manufacturer
X-ray irradiator	Xylon Y.TU 320	Xylon, Zurich, Switzerland

4.1.5   Computer Software

Software	Version	Developer
AxioVision	Release 4.8.2	Carl Zeiss, Jena, Germany
FloMax	2.70	Quantum Analysis GmbH, Münster, Germany
Gap4		STADEN Software Package (Staden et al., 2000)
GraphPad Prism	4.03	GraphPad Software Inc., San Diego, USA
ImageJ	1.47g	Wayne Rasband, National Institutes of Health, USA
Magellan	5.0	Tecan, Crailsheim, Germany
Microsoft Excel	2003	Microsoft Corp., Redmond, WA, USA
ND-1000	3.3.0	NanoDrop Technologies, Inc. Wilmington, DE, USA
Zeiss LSM image browser	3,5,0,376	Carl Zeiss GmbH, Jena, Germany

4.1.6   Other Materials

Name	Manufacturer
Caliper	OBI, Wermelskirchen, Germany
Cell scraper (18, 40 cm)	BD, Heidelberg, Germany
Conical centrifuge tube (15, 50 ml)	BD, Heidelberg, Germany
Cover glass	Menzel GmbH & Co. KG, Braunschweig, Germany
Cover slips (round)	Glaswarenfabrik Karl Hecht KG, Sondheim, Germany
Cryotubes	Biochrom, Berlin, Germany
Eppendorf® Safe-Lock microcentrifuge tube (0.5, 1.5, 2 ml)	Eppendorf, Hamburg, Germany
Filter tips, sterile (10, 100, 200, 1000 µl)	Fisher Scientific GmbH, Schwerte, Germany
Freezing box	Nalgene, Rochester, NY, USA
Glass Pasteur pipette	Brand GmbH u. Co. KG, Wertheim, Germany
Hamilton 700 Series Microliter™ syringe (50, 100 µl)	Hamilton Bonaduz AG, Bonaduz, GR, Switzerland
HyperFilm® ECL™	Amersham, Freiburg, Germany
Ice tub	Roth, Karlsruhe, Germany
Insulin syringe, 0.3 mm x 12 mm	Braun, Melsungen, Germany
Laboratory bottles	Schott AG, Mainz, Germany
Metal plates	Eigenbau, UKD, Dresden, Germany
Microscopic slide	Roth, Karlsruhe, Germany
Protran® nitrocellulose membrane, 0.2 µm	Whatman, Dassel, Germany
Non-tissue culture plate (96-well)	Corning Life Science, Wiesbaden, Germany
Pipette (1, 5, 10, 25 ml)	BD, Heidelberg, Germany
Pipette controller, accu-jet® pro	Brand, Herrenberg, Germany
Thermometer	Conrad Electronics, Hirschau, Germany
Tissue culture dish (60, 100 mm)	Greiner Bio-one GmbH, Frickenhausen, Germany
Tissue culture flask (T25, T75, T175)	BD, Heidelberg, Germany
Tissue culture plate (6-, 12-, 24-, 48-, 96-well)	Roth, Karlsruhe, Germany
Whatman-filter paper	Bender-Hobein, Zurich, Switzerland
X-ray cassette	Amersham, Freiburg, Germany

4.1.7 Small interfering RNAs (siRNAs)

Name	Sequence		siRNA ID	Company
hCDK2 siRNA#1	Sense:	5'-GGAGCUUAACCAUCCUAAUtt-3'	#42820	Applied Biosystems (Darmstadt, Germany)
	Antisense:	3'-AUUAGGAUGGUUAAGCUCCtt-5'		
hCDK2 siRNA#2	Sense:	5'-GGAAGUUUCAGUAUUAGAUtt-3'	#1409	Applied Biosystems (Darmstadt, Germany)
	Antisense:	3'-AUCUAAUACUGAAACUUCCtt-5'		
hCDK9 siRNA#1	Sense:	5'-GGAGAAUUUUACUGUGUUUtt-3'	#104	Applied Biosystems (Darmstadt, Germany)
	Antisense:	3'-AAACACAGUAAAAUUCUCCtg-5'		
hCDK9 siRNA#2	Sense:	5'-GGUGCUGAUGGAAAACGAGtt-3'	#103	Applied Biosystems (Darmstadt, Germany)
	Antisense:	3'-CUCGUUUUCCAUCAGCACCtt-5'		
Control siRNA	Sense:	5'-GCAGCUAUAUGAAUGUUGUtt-3'		Applied Biosystems (Darmstadt, Germany)
	Antisense:	3'-CGUACGCGGAAUACUUCGAtt-5'		

4.1.8 Primers

Name	Sequence	Melting temperature (Tm)	Company
hCDK9-*Nhe*I forward	5'- cta GCTAGC gccgcc ATGGCAAAGCAGTACGACTCGG-3'	68°C	Eurofins MWG Operon
hCDK9-*Bam*HI reverse	5'- cg GGATCC cg GAAGACGCGCTCAAACTCCG -3'	64°C	Eurofins MWG Operon

4.1.9 Enzymes

Polymerase chain reaction (PCR) was performed using a HotStarTaq® *Plus* Polymerase, 10x Buffer, MgCl$_2$, dNTPs (Qiagen, Hilden, Germany) mixture. DNA restriction digest was performed using *Nhe*I, *Bam*HI and *Apa*LI. T4 ligase (Invitrogen, Karlsruhe, Germany) was used to ligate digested DNA fragments.

4.1.10 Protein and DNA Ladders

The Benchmark™ protein ladder (Invitrogen, Karlsruhe, Germany) served as a molecular weight standard for sodium dodecyl sulphate-polyacrylamide gel electrophoresis (SDS-PAGE). For agarose gel electrophoresis, the Range mix DNA ladder (0.08-10.0 kb) (PEQLAB Biotechnologie, Erlangen, Germany) was used for evaluation of DNA fragment size.

4.1.11   Kits

Name	Purpose	Company
Pierce® BCA Protein Assay Kit	Protein concentration measurement	Thermo Fisher Scientific p/a Perbio Science Deutschland Zweigniederlassung der Thermo Fisher Scientific Germany BV & Co KG, Bonn, Germany
NucleoSpin® Plasmid	Plasmid Miniprep	Macherey-Nagel, Düren, Germany
NucleoSpin® Extract II	PCR product purification	Macherey-Nagel, Düren, Germany
Nucleobond® AX	Plasmid Midiprep	Macherey-Nagel, Düren, Germany
Super Signal West Dura Extended	Western blot horse reddish peroxidase signal detection	Thermo Fisher Scientific p/a Perbio Science Deutschland Zweigniederlassung der Thermo Fisher Scientific Germany BV & Co KG, Bonn, Germany

4.1.12   Primary Antibodies

Name [Clone]	Source, Isotype	Application	Dilution	Supplier
β-actin [AC-15]	Mouse IgG1, Monoclonal	Western Blotting	1:10,000	Sigma-Aldrich, Taufkirchen, Germany
ATM [D2E2]	Rabbit IgG, Monoclonal	Western Blotting	1:1000	Cell Signaling, Frankfurt a.M., Germany
5-Bromo-2´-deoxyuridine (BrdU) [B44]	Mouse IgG1, Monoclonal	Flow Cytometry	1:10	BD, Heidelberg, Germany
CDK2 [78B2]	Rabbit IgG, Monoclonal	Western Blotting	1:500	Cell Signaling, Frankfurt a.M., Germany
CDK9 [C12F7]	Rabbit IgG, Monoclonal	Western Blotting	1:1000	Cell Signaling, Frankfurt a.M., Germany
CHK2	Rabbit, Polyclonal	Western Blotting	1:500	Cell Signaling, Frankfurt a.M., Germany
Cyclin A	Rabbit IgG, Polyclonal	Western Blotting	1:1000	Santa Cruz, Heidelberg, Germany
Cyclin D1 [D1-72-13G]	Mouse IgG1, Monoclonal	Western Blotting	1:500	Zymed Laboratories Inc., California, USA
Cyclin E [HE12]	Mouse IgG1, Monoclonal	Western Blotting	1:1000	Cell Signaling, Frankfurt a.M., Germany
DNA-PK	Rabbit, Polyclonal	Western Blotting	1:1000	Cell Signaling, Frankfurt a.M., Germany
GFP	Rabbit, Polyclonal	Western Blotting	1:2000	Abcam, Cambridge, UK
ORC1 [7A7]	Rabbit IgG1, Monoclonal	Western Blotting	1:1000	Cell Signaling, Frankfurt a.M., Germany
p27(Kip1) [57/Kip1/p27]	Mouse IgG1, Monoclonal	Western Blotting	1:1000	BD, Heidelberg, Germany

Name [Clone]	Source, Isotype	Application	Dilution	Supplier
p53 binding protein 1 (53BP1)	Rabbit, Polyclonal	Immunofluorescence	1:2000	Novus Biologicals, Littelton, USA
P95/NBS1	Rabbit Polyclonal	Western Blotting	1:1000	Cell Signaling, Frankfurt a.M., Germany
phospho-ATM(S1981) [10H11.E12]	Mouse IgG1, Monoclonal	Western Blotting	1:500	Cell Signaling, Frankfurt a.M., Germany
phospho-CHK2(T86)	Rabbit, Polyclonal	Western Blotting	1:500	Cell Signaling, Frankfurt a.M., Germany
phospho-Histone 2AX(S139) (γH2AX) [JBW301]	Mouse IgG1, Monoclonal	Immunofluorescence	1:1000	Millipore, Darmstadt, Germany
phospho-Rb(S795)	Rabbit, Polyclonal	Western Blotting	1:1000	Cell Signaling, Frankfurt a.M., Germany
phospho-Rpb1-CTD(S2/5)	Rabbit, Polyclonal	Western Blotting	1:1000	Cell Signaling, Frankfurt a.M., Germany
PCNA [F-2]	Mouse IgG2a, Monoclonal	Western Blotting	1:500	Santa Cruz, Heidelberg, Germany
RAD50	Rabbit, Polyclonal	Western Blotting	1:1000	Cell Signaling, Frankfurt a.M., Germany
Rb	Rabbit, Polyclonal	Western Blotting	1:1000	Santa Cruz, Heidelberg, Germany
RPA70	Rabbit Polyclonal	Western Blotting	1:1000	Cell Signaling, Frankfurt a.M., Germany
Rpb1-CTD [4H8]	Mouse IgG1, Monoclonal	Western Blotting	1:1000	Cell Signaling, Frankfurt a.M., Germany

4.1.13   Secondary Antibodies

Antibody name	Application	Dilution	Company
Alexa488 anti-rabbit	Immunofluorescence	1:2000	Invitrogen, Karlsruhe, Germany
Alexa594 anti-mouse	Immunofluorescence	1:2000	Invitrogen, Karlsruhe, Germany
Anti-mouse IgG FITC	Flow Cytometry	1:100	Sigma-Aldrich, Taufkirchen, Germany
Anti-rat-peroxidase	Western Blotting	1:5000	Sigma-Aldrich, Taufkirchen, Germany
Goat anti-mouse (HRP-conjugated)	Western Blotting	1:5000, 1:10,000	Amersham, Freiburg, Germany
Goat anti-rabbit (HRP-conjugated)	Western Blotting	1:5000	Amersham, Freiburg, Germany

4.1.14   Reagents

4.1.14.1   Cell Culture and Transfection

Name	Composition	Storage	Company
Agarose (1%)	1 g Agarose, Typ I-A in 100 ml ddH$_2$O 100 ml ddH$_2$O	RT	Sigma, Taufkirchen, Germany
Complete medium	500 ml DMEM	4°C	PAA, Cölbe, Germany
	50 ml FBS		PAA, Cölbe, Germany
	5.5 ml NEAA		PAA, Cölbe, Germany
Complete medium (1.5 mg/ml G418)	500 ml complete medium 7.5 ml G418 (100 mg/ml)	4°C	
Coomassie stain	0.5 g Coomassie G250	RT	J.T. Baker, Deventer, Netherland
	75 ml Glacial acetic acid		Merck, Darmstadt, Germany
	200 ml Methanol		Merck, Darmstadt, Germany
	725 ddH$_2$O		
Dulbecco's modified Eagle's medium (DMEM)	Glucose (4.5 g/l) with stable Glutamine	4°C	PAA, Cölbe, Germany
Ethanol (80%)	800 ml 99% Ethanol	RT	Berkel, Berlin, Germany
	200 ml ddH$_2$O		
Fetal bovine serum (FBS)		-20°C	PAA, Cölbe, Germany
Freezing medium	8.5 ml Complete medium	-20°C	
	1 ml FBS		PAA, Cölbe, Germany
	0.5 ml DMSO		AppliChem GmbH, Darmstadt, Germany
Geneticin® (G418) (100 mg/ml)	25 g G418 Sulphate ddH$_2$O to a final volume of 250 ml	-20°C	PAA, Cölbe, Germany
Matrigel™ basement membrane matrix high concentration (lrECM) (20 mg/ml)		-20°C	BD, Heidelberg, Germany
Matrigel™ basement membrane matrix in DMEM (10 mg/ml)	5 ml Matrigel™ basement membrane matrix high concentration 5 ml DMEM	4°C	
Matrigel™ basement membrane matrix in complete medium (5 mg/ml)	1 ml Matrigel™ basement membrane matrix (10 mg/ml) 1 ml complete medium	4°C	
MEM non-essential amino acids (NEAA) 10 mM (100x)		4°C	PAA, Cölbe, Germany
Oligofectamine® transfection reagent		4°C	Invitrogen, Karlsruhe, Germany
Opti-MEM® (20% FBS)	8 ml Opti-MEM®	RT	Invitrogen, Karlsruhe, Germany
	2 ml FBS		PAA, Cölbe, Germany
Opti-MEM® I reduced serum medium, GlutaMAX™		4°C	Invitrogen, Karlsruhe, Germany

Name	Composition	Storage	Company
Phosphate-buffered saline (PBS) (1x)		RT	PAA, Cölbe, Germany
Trypsin-EDTA (1x)		-20°C	PAA, Cölbe, Germany

- ▪ Note: Used FBS was heated to 56°C for 30 min in a water bath to destroy heat-labile complement proteins.

4.1.14.2   Flow Cytometry

Name	Composition	Storage	Company
BrdU (1 mM)	15.35 mg BrdU in 50 ml PBS, filtered (sterile)	-20°C	Serva, Heidelberg, Germany
BSA in 1xPBS (PBSA) (1%)	1 g BSA 1x PBS to a final volume of 100 ml	4°C	Sigma, Taufkirchen, Germany
Ethanol (80%)	80 ml 99% Ethanol 20 ml ddH$_2$O	-20°C	Berkel, Berlin, Germany
Hydrochloric acid (HCl) (2N)	16.6 ml 37% HCl ddH$_2$O to a final volume of 100 ml	RT	Merck, Darmstadt, Germany
Pepsin solution (0.05%) (Freshly prepared)	50 mg Pepsin 100 ml ddH$_2$O	4°C	Merck, Darmstadt, Germany
Propidium Iodide (PI) solution (25 µg/ml)	2.5 mg PI 100 ml 1x PBS	4°C (Dark)	Serva, Heidelberg, Germany
Ribonuclease A (RNase) solution (0.01%)	10 mg RNase 100 ml 1x PBS	4°C	Sigma, Taufkirchen, Germany

4.1.14.3   SDS-PAGE and Western Blotting

Name	Composition	Storage	Company
Acrylamide-bisacrylamide solution (30%)		4°C	Serva, Heidelberg, Germany
Ammonium persulphate (APS) solution (10%)	10 g APS ddH$_2$O to a final volume of 100 ml	-20°C	AppliChem GmbH, Darmstadt, Germany
BSA in PBST (5%)	0.5 g BSA PBST to a final volume of 10 ml	4°C	Sigma, Taufkirchen, Germany
Complete™ protease inhibitor (25x)	One tablet in 2 ml ddH$_2$O	-20°C	Roche Diagnostics GmbH, Mannheim, Germany
EDTA (500 mM) (pH 8.0)	7.306 g EDTA ddH$_2$O to a final volume of 50 ml pH adjusted to 8.0	RT	Roth, Karlsruhe, Germany

Name	Composition	Storage	Company
Film developer (GBX Developer Kodak)	250 ml GBX Developer Kodak 750 ml ddH$_2$O	RT, Dark	Kodack, Stuttgart, Germany
Film fixer (GBX Fixer Kodak)	250 ml GBX Fixer Kodak 750 ml ddH$_2$O	RT	Kodack, Stuttgart, Germany
Gycerol (50%)	25 ml Gycerol 25 ml ddH$_2$O	RT	Roth, Karlsruhe, Germany
Isopropanol (Propan-2-ol)		RT	Merck, Darmstadt, Germany
Milk buffer (5%)	5 g Milk powder PBS (1x) to a final volume of 100 ml	4°C	AppliChem GmbH, Darmstadt, Germany
Maniatis-SDS blotting buffer (10x)	29 g Glycine 58 g Tris ddH$_2$O to a final volume of 1 l	RT	Roth, Karlsruhe, Germany Roth, Karlsruhe, Germany
Maniatis-SDS blotting buffer (1x)	100 ml Maniatis-SDS Blotting buffer (10x) 200 ml Methanol 700 ml ddH$_2$O	RT	J.T. Baker, Deventer, Netherland
Modified RIPA lysis buffer	951 µl RIPA stock solution 40 µl Complete™ Protease Inhibitor (25x) 5 µl Na$_3$VO$_4$ (200 mM) 4 µl NaF (500 mM)	4°C	
Na$_3$VO$_4$ (200 mM)	3.678 g Na$_3$VO$_4$ ddH$_2$O to a final volume of 100 ml	-20°C	Sigma, Taufkirchen, Germany
NaCl (5 M)	14.61 g NaCl ddH$_2$O to a final volume of 50 ml	RT	Merck, Darmstadt, Germany
NaF (500 mM)	2.1 g NaF ddH$_2$O to a final volume of 100 ml, activated at pH 10.0	-20°C	Sigma, Taufkirchen, Germany
PBS (1x)	100 ml PBS (20x) 1900 ml ddH$_2$O	RT	
PBS(1x)/0.05% Tween 20 (PBST)	0.5 ml Tween 20 1 l PBS (1x)	RT	Serva, Heidelberg, Germany
PBS stock solution (20x) (pH 7.4)	160 g NaCl 4 g KCl 36 g Na$_2$HPO$_4$ 4.8 g KH$_2$PO$_4$ ddH$_2$O to a final volume of 1 l pH adjusted at 7.4	RT	Merck, Darmstadt, Germany Merck, Darmstadt, Germany Merck, Darmstadt, Germany Merck, Darmstadt, Germany
Ponceau S		RT	Sigma, Taufkirchen, Germany

Name	Composition	Storage	Company
Reduced electrophoresis loading buffer (1x)	200 µl Reduced electrophoresis loading buffer (6x) 1 ml ddH$_2$O	-20°C	
Reduced electrophoresis loading buffer (6x)	5 ml Glycerol (50%) 925 mg DTT 1.03 g SDS 3.5 ml Tris-HCl (1 M) pH 6.8 1.2 mg Bromophenol blue ddH$_2$O to a final volume of 10 ml	-20°C	AppliChem GmbH, Darmstadt, Germany Roth, Karlsruhe, Germany AppliChem GmbH, Darmstadt, Germany
RIPA stock solution	12.5 ml Tris-HCl (1 M) (pH 7.4) 2.5 ml NP-40 6.25 ml Sodium deoxycholate (10%) 7.5 ml NaCl (5 M) 0.5 ml EDTA (0.5 M) (pH 8.0) ddH$_2$O to a final volume of 250 ml	4°C	Roth, Karlsruhe, Germany Fluka, München, Germany
SDS (10%)	5 g SDS ddH$_2$O to a final volume of 50 ml	RT	Roth, Karlsruhe, Germany
SDS-PAGE running buffer (10x)	30.3 g Tris 144.1 g Glycine 10 g SDS ddH$_2$O to a final volume of 1 l	RT	Roth, Karlsruhe, Germany Roth, Karlsruhe, Germany Roth, Karlsruhe, Germany
Sodium deoxycholate (10%)	5 g Sodium deoxycholate ddH$_2$O to a final volume of 50 ml	RT	Sigma, Taufkirchen, Germany
Tetramethylethylenediamine (TEMED)		4°C	Merck, Darmstadt, Germany
Tris-HCl (0.5 M) (pH 6.8)	60.57 g Tris ddH$_2$O to a final volume of 1 l pH adjusted to 6.8	RT	Roth, Karlsruhe, Germany
Tris-HCl (1 M) (pH 6.8)	12.11 g Tris ddH$_2$O to a final volume of 100 ml pH adjusted to 6.8	RT	Roth, Karlsruhe, Germany
Tris-HCl (1 M) (pH 7.4)	12.11 g Tris ddH$_2$O to a final volume of 100 ml pH adjusted to 7.4	RT	Roth, Karlsruhe, Germany
Tris-HCl (3 M) (pH 8.8)	363.42 g Tris ddH$_2$O to a final volume of 1 l pH adjusted to 8.8	RT	Roth, Karlsruhe, Germany

4.1.14.4 Immunofluorescence Staining

Name	Composition	Storage	Company
Bovine serum albumin (BSA) (1%)	0.25 g BSA 25 ml ddH$_2$O	4°C	Sigma, Taufkirchen, Germany
Formaldehyde (3%)	3 ml 37% Formaldehyde 34 ml 1x PBS	4°C	Merck, Darmstadt, Germany
Triton X-100 (0.25%)	62.5 µl Triton X-100 25 ml 1x PBS	4°C	Merck, Darmstadt, Germany
Vectashield® mounting medium with DAPI		4°C	Vector Laboratories, Burlingame, USA

4.1.14.5 Molecular Cloning and Transformation

Name	Composition	Storage	Company
Agarose (electrophoresis grade)		RT	Invitrogen, Karlsruhe, Germany
Agarose probe buffer (10x)	250 mg Bromphenol blue 33 ml Tris (150 mM) (pH 7.6) 60 ml Glycerol ddH$_2$O to a final volume of 100 ml	4°C	AppliChem GmbH, Darmstadt, Germany Roth, Karlsruhe, Germany Roth, Karlsruhe, Germany
SOC medium (pH 7.0)	20 g Trypton/Pepton 5 g Yeast Extract 0.5 g NaCl 2.5 ml 1 M KCl 10 ml 1 M MgCl$_2$ 20 ml 1 M Glucose ddH$_2$O to a final volume of 1 l Autoclaved	4°C	Roth, Karlsruhe, Germany Roth, Karlsruhe, Germany Fluka, München, Germany Merck, Darmstadt, Germany Merck, Darmstadt, Germany
Kanamycin sulphate (30 mg/ml)	3 g 100 ml ddH$_2$O	-20°C	Roth, Karlsruhe, Germany
Lysogeny broth (LB) medium (pH 7.0)	20 g Trypton/Pepton 5 g Yeast extract 10 g NaCl ddH$_2$O to a final volume of 1 l Autoclaved	4°C	Roth, Karlsruhe, Germany Roth, Karlsruhe, Germany Merck, Darmstadt, Germany
LB agar	15 g Agar 1 l LB Medium Autoclaved	4°C	AppliChem GmbH, Darmstadt, Germany

Name	Composition	Storage	Company
Lipofectamine® 2000 reagent		4°C	Invitrogen, Karlsruhe, Germany
RedSafe™ nucleic acid staining solution		4°C	iNtRON Biotechnology, Kyungki-Do, Korea
TBE buffer (10x) (pH 8.0)	108 g Tris 55 g Boric acid 40 ml EDTA (0.5 M) ddH$_2$O to a final volume of 1 l	RT	Roth, Karlsruhe, Germany Merck, Darmstadt, Germany
TBE buffer (1x)	100 ml TBE buffer (10x) (pH 8.0) 900 ml ddH$_2$O	RT	

4.2   Methods

4.2.1   Cell Culture

4.2.1.1   Cell Culture Conditions

Cells were cultured in complete medium under standard cell culture conditions in incubators with humidified atmosphere containing 7% carbon dioxide (CO_2) (pH 7.4) at 37°C. In all experiments, asynchronously and exponentially growing cells (~60% confluence) were used.

4.2.1.2   Cell Freezing

Cell cultures (~60% confluence) were trypsinised using Trypsin/EDTA (trypsinisation time was cell line dependent: 7-15 min), resuspended in complete medium, collected in 50 ml Falcon tube and centrifuged (130 rcf, 4°C, 5 min). The supernatant was removed and the cell pellet was resuspended in ice-cold freezing medium (T25 Flask: 1 ml, T75: 3 ml, T175: 6 ml) and transferred into pre-cooled Cryovials (1 ml of the cell suspension per Cryovial). Finally, the Cryovials were stored in a -80°C freezer.

4.2.1.3   Cell Thawing

Frozen Cryovials were removed from -80°C freezer and warmed by hand until the frozen cell suspension melted (~5 min). The cell suspension was transferred using a 5 ml pipette into a sterile T75 flask containing 25 ml complete medium. The medium was replaced after 5 h.

4.2.1.4   Passaging of Cells

50-70% confluent cell cultures were split into new cell culture flasks. Cells were washed once with PBS, trypsinised and resuspended in complete medium. The cell suspension was split 1:3-1:30 (splitting ratio was cell line dependent) into a new cell culture flask containing fresh complete medium. The new flask was controlled using an inverted microscope and placed inside the cell culture incubator. In all experiments, cell cultures with a maximum passage number of 12 passages were used to minimise the genetic drift.

4.2.1.5   Cell Counting

A cell counting chamber (Haemocytometer) was used to count cells in cell suspensions. Both the counting slide and the cover slip were carefully cleaned with 70% ethanol. The coverslip was moistened by exhaled breath and placed over the counting slide. 10 µl of cell suspension were pipetted at the coverslip's edge and allowed to run

between the coverslip and the counting slide. Cells in each of the four large corner squares of the Haemocytometer were counted using 10x objective of the inverted microscope. The mean cell count per square was calculated and multiplied by 10,000 to obtain the total cell count per ml.

4.2.2   Radiation Exposure

Cells were irradiated at room temperature (RT) with single doses of X-rays using X-ray irradiator (Yxlon Y.TU 320, Yxlon, Copenhagen, Denmark) yielding a dose rate of ~1.2 Gy/min at 200 kV and 20 mA. The X-ray radiation was filtered with 0.5 mm copper filter. Applied doses ranged from 0 to 8 Gy. The delivered dose was measured using a Duplex dosimeter (PTW, Freiburg, Germany).

4.2.3   Small interfering RNA-mediated Knockdown

Small interfering ribonucleic acids (siRNAs) are a class of single- or double-stranded RNA molecules which interfere with the expression of specific target genes with complementary nucleotide sequences (Elbashir et al., 2001; Kim et al., 2005). In this study, the expression of CDK2 or CDK9 was downregulated using CDK2 or CDK9 siRNAs. In all experiments, a non-specific siRNA transfection was used as control.

siRNA transfection was performed in 6-well plates, 60 mm cell culture dishes or 100 mm cell culture dishes. The number of seeded cells was cell line dependent (Table 4.1).

Table 4.1. The number of seeded cells 24 h prior to siRNA transfection

Cell line	Seeded number of cells		
	6-well plate	60 mm dish	100 mm dish
SAS	150,000/Well	80,000	600,000
FaDu	250,000/Well	80,000	700,000
HSC4	250,000/Well	-----	-----
Cal33	250,000/Well	-----	-----
UTSCC5	300,000/Well	-----	-----
UTSCC8	400,000/Well	-----	-----

Twenty-four hours after seeding the cells, the siRNA/Opti-MEM® I mixture (Mixture A) and Oligofectamine/Opti-MEM® I mixture (Mixture B) were prepared and incubated for 10 min at RT. Both mixtures (A and B) were pooled together and incubated for 20 min at RT (Table 4.2).

Seeded sells (30-50% confluent) were washed once with Opti-MEM® I (6-well: 1 ml/Well, 60 mm dish: 1.5 ml, 100 mm dish: 6 ml) and fresh Opti-MEM® I (6-well: 800 µl/Well, 60 mm dish: 1.2 ml, 100 mm dish: 4.8 ml) was added to the cells. siRNA mixture

was added to the cells (6-well: 200 µl/Well, 60 mm dish: 300 µl, 100 mm dish: 1.2 ml). After 8 h incubation at standard cell culture conditions, Opti-MEM® I containing 20% FBS was pipetted to the transfected cells (6-well: 1 ml/Well, 60 mm dish: 1.5 ml, 100 mm dish: 6 ml). The transfected cell cultures were used for colony formation assay (Section 4.2.4), γH2AX/53PB1 foci assay (Section 4.2.5), apoptosis assay (Section 4.2.6), cell cycle analysis (Section 4.2.7) and protein analysis (Section 4.2.8).

Table 4.2. Dilution scheme of siRNA transfection mixture.

Tissue culture vessel	Initial siRNA conc.	Final siRNA conc.	Mixture A		Mixture B		Total volume
			Required amount of siRNA	Required amount of Opti-MEM® I	Required amount of Oligofectamine	Required amount of Opti-MEM® I	
1 well in 6-well plate	20 µM	20 nM	1 µl	184 µl	4 µl	11 µl	200 µl
60 mm dish	20 µM	20 nM	1.5 µl	276 µl	6 µl	16.5 µl	300 µl
100 mm dish	20 µM	20 nM	6 µl	1104 µl	24 µl	66 µl	1.2 ml

4.2.4   Colony Formation Assay

Colony formation assays were applied for the measurement of clonogenic cell survival. This assay is based on the ability of a single cell to undergo at least 5-6 successive divisions and grow into a colony as published (Palyi et al., 1995; Puck & Marcus, 1956; Storch et al., 2010).

4.2.4.1   Two Dimensional (2D) Colony Formation Assay

Single cells were seeded in polystyrene 6-well plates (Cordes et al., 2006). Cells were washed with 1x PBS, trypsinised, resuspended in complete medium and counted. Volume X (Equation 4.1) of the cell suspension was diluted in 5 ml complete medium in a 50 ml Falcon tube to obtain a 20,000 cell/ml single cell suspension.

$$X = \frac{100,000}{\text{Total cell count}}$$

Equation 4.1

The required number of cells was seeded in each well of the 6-well plate as indicated in Table 4.3. Two ml of complete medium were added into each well. The plates

were shaken back-and-forth and right-to-left to ensure the uniform distribution of cells in each well. The cell distribution was microscopically controlled.

After 24 h, the plates were irradiated with a single dose of X-rays (0, 2, 4, 6 or 8 Gy) at RT. After the specific incubation time (Table 4.3), the colony formation assay was stopped by fixing the cells with 80% ethanol for 10 min. The fixed cells were stained for 1 h with Coomassie blue stain. Finally, the 6-well plates were washed with running tap water and dried at RT.

Table 4.3. The optimal number of cells and the corresponding incubation times for colony formation assays.

Cell line	Number of cells per X-ray dose (Volume of 20,000/ml cell suspension)					Incubation time (Days after plating)
	0 Gy	2 Gy	4 Gy	6 Gy	8 Gy	
WT MEF	1250 (62.5 µl)	1250 (62.5 µl)	2500 (125 µl)	5000 (250 µl)	6200 (310 µl)	7
CDK2$^{-/-}$ MEF	1250 (62.5 µl)	1250 (62.5 µl)	2500 (125 µl)	5000 (250 µl)	6200 (310 µl)	7
SAS	700 (35 µl)	700 (35 µl)	1400 (70 µl)	2800 (140 µl)	3200 (210 µl)	7
FaDu	1000 (50 µl)	1000 (50 µl)	2000 (100 µl)	4000 (200 µl)	6000 (300 µl)	11
HSC4	1000 (50 µl)	1000 (50 µl)	2000 (100 µl)	4000 (200 µl)	6000 (300 µl)	8
Cal33	1200 (60 µl)	1200 (60 µl)	2400 (120 µl)	4800 (240 µl)	7200 (360 µl)	13
UTSCC5	1500 (75 µl)	1500 (75 µl)	3000 (150 µl)	6000 (300 µl)	9000 (450 µl)	14
UTSCC8	2000 (100 µl)	2000 (100 µl)	4000 (200 µl)	8000 (400 µl)	12000 (600 µl)	14
SAS-EGFP	700 (35 µl)	700 (35 µl)	1400 (70 µl)	2800 (140 µl)	3200 (210 µl)	7
SAS-CDK9-EGFP	700 (35 µl)	700 (35 µl)	1400 (70 µl)	2800 (140 µl)	3200 (210 µl)	7

4.2.4.2   Three Dimensional (3D) Colony Formation Assay

In 3D colony formation assay, single cells were plated in 0.5 g/l Matrigel™ laminin-rich extracellular matrix (lrECM)/complete medium mixture in 96-well plates (Hehlgans et al., 2008). The wells of the 96-well plate were coated with 50 µl sterile 1% agarose. Cells were mixed with the appropriate amount of 0.5 g/l lrECM/complete medium mixture to obtain a final cell count of 2000 cell/100 µl and each well was plated with 100 µl of the cell/lrECM/complete medium mixture. The plates were incubated in the incubator under standard conditions. Three hours later, 100 µl of complete medium was added to each

well. To avoid evaporation and dryness, 200 µl of sterile 1x PBS was pipetted to the empty wells around the wells in which cells were seeded.

After 24 h, cells were irradiated and incubated for seven days (SAS) or nine days (FaDu). Formed colonies were fixed by adding 100 µl of 3% formaldehyde in 1x PBS into each well.

4.2.4.3   Evaluation of Colony Formation Assay

The number of colonies formed under 2D conditions was counted using binuclear microscope. Under 3D conditions, formed colonies were counted using an inverted microscope. Only colonies of more than 50 cells were scored as viable colonies.

Plating efficiencies (PEs) were calculated by dividing the number of colonies the originate from single cells by the number of seeded cells (Equation 4.2). The plating efficiency varied between the cell lines.

$$PE = \frac{\text{Number of colonies}}{\text{Number of seeded cells}}$$ **Equation 4.2**

The surviving fraction (SF) of each irradiation dose was calculated by dividing the PE of irradiated cells by the PE of unirradiated cells according to Equation 4.3.

$$SF = \frac{PE_{irradiated}}{PE_{unirradiated}}$$ **Equation 4.3**

Representative images of 2D and 3D colony formation were acquired using an Epson Perfection 4490 PHOTO scanner (Epson, Meerbusch, Germany) or using an Axiovert 40 CFL microscope (Zeiss, Jena, Germany) respectively. Each point on the survival curves represents the mean surviving fraction ± standard deviation from three independent experiments.

4.2.5 γH2AX/53BP1 Foci Assay

γH2AX/53BP1 foci assay was performed to evaluate the number of radiation-induced γH2AX and p53 binding protein 1 (53BP1) colocalised foci at sites of DNA DSBs (Kinner et al., 2008; Rothkamm & Lobrich, 2003).

γH2AX/53BP1 foci assay was performed by seeding certain number of cells (SAS: 150,000, FaDu: 300,000) in T25 flasks. After 24 h, cells were irradiated with a single dose of X-rays (0 or 6 Gy) and incubated under standard cell culture conditions. Twenty-four hours after irradiation, cells were trypsinised, harvested in 5 ml complete medium in a 15

ml falcon tube, centrifuged (130 rcf, 4°C, 3 min) and fixed by resuspending the cell pellet in 0.5 ml 3% formaldehyde in 1x PBS and stored at 4°C until analysis.

γH2AX/53BP1-positive nuclear foci of 50 cells were counted using the Axioscope 2 plus fluorescence microscope (Zeiss, Jena, Germany) and defined as residual DSBs.

4.2.5.1 Immunofluorescence Staining

Fixed cell suspension was washed by adding 4 ml 1x PBS and centrifuged (200 rcf, 4°C, 5 min). The supernatant was removed carefully using a suction pump. The pellet was resuspended in 1 ml 0.25% Triton X-100 and incubated at RT for 10 min. In order to remove excess Triton X-100, cell suspension was washed by adding 4 ml 1x PBS and centrifuged (200 rcf, 4°C, 5 min). The supernatant was discarded and the pellet was resuspended in 100 µl 1% PBSA (Blocking, 1 h, RT). Cells were centrifuged (200 rcf, 4°C, 5 min), and the supernatant was carefully removed using a 100 µl Pipette.

All antibodies were diluted in 1% PBSA. The 1st primary antibody against γH2AX was added for 2 h at RT. Cells were washed by adding 5 ml 1x PBS and centrifuged (200 rcf, 4°C, 5 min). The supernatant was discarded and the 1st secondary Alexa Fluor anti-mouse (red) antibody was added (1 h, RT, dark). After washing with 5 ml 1x PBS and centrifugation (200 rcf, 4°C, 5 min), the supernatant was removed and cells were stained with the second antibody against 53BP1 (1 h, RT, dark). Cells were washed with 5 ml 1x PBS, centrifuged to discard the supernatant and incubated with the 2nd secondary Alexa Fluor anti-rabbit (green) antibody (1 h, RT, dark). Finally, 5 ml 1x PBS were added and followed by centrifugation and removal of the supernatant. The samples were stored in dark refrigerator at 4°C.

4.2.5.2 Mounting of stained Cells on Glass Slides

Stained cells were fixed on slides using a 100 µl pipette. After resuspending the pellet, 7 µl of cell suspension were spread on a microscopic glass slide using a 100 µl pipette tip. A small drop of Vectrashield® fluorescence specialised mounting media containing 4',6-diamidino-2-phenylindole (DAPI) was added and mounted by a cover slip. The slides were then stored in dark at -20°C.

4.2.5.3 Evaluation of γH2AX/53BP1 positive Foci

The evaluation was carried out using an Axioskop 2 plus fluorescence microscope (Zeiss, Jena, Germany). The number of γH2AX/53BP1 positive foci was defined in nuclei of 50 cells (foci-free nuclei were also counted). The mean number of foci per cell was evaluated as described in (Eke et al., 2007). Data were expressed as means ± standard

deviation of three independent experiments. Representative fluorescence images were obtained using a LSM 510 Meta equipped with Zeiss LSM 510 Software (Zeiss).

4.2.6 Apoptosis assay

For analysing apoptosis, transfected cells were irradiated with X-rays (0 or 6 Gy, single dose). Twenty-four hours later, cells were trysinised and mounted with Vectashield/DAPI mounting medium. Apoptotic nuclei of 100 cells were counted using the Axioscope 2 plus fluorescence microscope (Zeiss, Jena, Germany).

4.2.7 Cell Cycle Analysis

BrdU is a thymidine base analogue that is able to incorporate into the newly synthesised DNA during the S phase of the cell cycle (Ross et al., 2008). Incorporated BrdU into cellular DNA was detected using specific anti-BrdU/FITC antibodies and the S phase cell population was distinguished. The total DNA content of cells was stained with propidium iodide (PI).

4.2.7.1 Cell Cycle Analysis after Irradiation with X-rays

Cells were seeded in a 100 mm cell culture dish (MEFs: 150,000, SAS: 40,000 cell/dish, FaDu: 45,000 cell/dish), and after 72 h were irradiated with X-rays (0 or 6 Gy). At certain time points after irradiation (0, 10, 14, 18, 24 or 48 h), cells were pulse-labelled with 10 µM BrdU in complete medium (10 min, 37°C). The BrdU-containing medium was discarded, and cells were washed twice with 1x PBS and trypsinised. Cell suspension was collected in a 15 ml Falcon tube and centrifuged (150 rcf, 4°C, 8 min). The cell pellet was resupended in 1 ml of -20°C-cold 80% ethanol (added drop by drop with vortex) and stored at -20°C until analysis.

4.2.7.2 Cell Cycle Analysis after CDK2 or CDK9 Depletion

Cells were seeded in a 60 mm cell culture dish (SAS: 80,000 cell/dish, FaDu: 80,000 cell/dish). After 24 h, cells were transfected with CDK2 or CDK9 siRNAs. At 0, 1, 2, 3 or 4 days after transfection, cells were treated with 10 µM BrdU, fixed in -20°C-cold 80% ethanol and stored at -20°C until analysis.

### 4.2.7.3 Cell Cycle Analysis after CDK2 or CDK9 Knockdown combined with Irradiation

Cells were plated in a 60 mm cell culture dish (SAS: 80,000 cell/dish, FaDu: 80,000 cell/dish) and after 24 h were transfected against CDK2 or CDK9. Later, 0 or 6 Gy single dose of X-rays was applied 24 h after transfection. Fourteen hours later, cells were pulse-labelled with 10 µM BrdU, fixed in -20°C-cold 80% ethanol and stored at -20°C until analysis.

4.2.7.4   Extraction of Nuclei and Immunofluorescence Staining

Extraction of nuclei was performed as described in (Cordes et al., 2006). Cells were centrifuged (150 rcf, 4°C, 8 min) and the pellet was resuspended in 2 ml of 0.01% RNase solution (shaking, 37°C, 10 min). After re-centrifugation, the pellet was resuspended in 2 ml of freshly prepared 0.05% pepsin solution (shaking, 37°C,10 min) and incubated for 5 min in ice. Next, 4 ml of 1x PBS were added to the cell suspension followed by centrifugation. Extraction of cell nuclei was accomplished by resuspending the pellet in 2 ml of 2N HCl for 10 min. Cell nuclei were washed by adding 4 ml of cold 1x PBS and centrifugation (repeated twice). Nuclei were resuspended in PBSA, centrifuged and incubated with 200 µl of 1:10 anti-BrdU (dark, RT, 30 min). After PBS washing and centrifugation, the sample was resuspended in 200 µl of FITC-conjugated anti-mouse IgG antibody (dark, RT, 30 min). Finally, the total DNA content was stained by 1 ml of 25 µg/ml PI solution (dark, 1 h).

Using a CyFlow flow cytometer, the following parameters were recorded for each sample: size of nuclei [Forward scatter, FSC], granularity of nuclei [Side scatter, SSC], BrdU-FITC [FL1], total DNA content (PI) [FL3].

Using the FloMax software, a dot blot of FL1 (logarithmic scale) on the y axis and FL3 (linear scale) on the x axis was generated and gated to obtain the cell cycle distribution of the sample as shown in Figure 4.1.
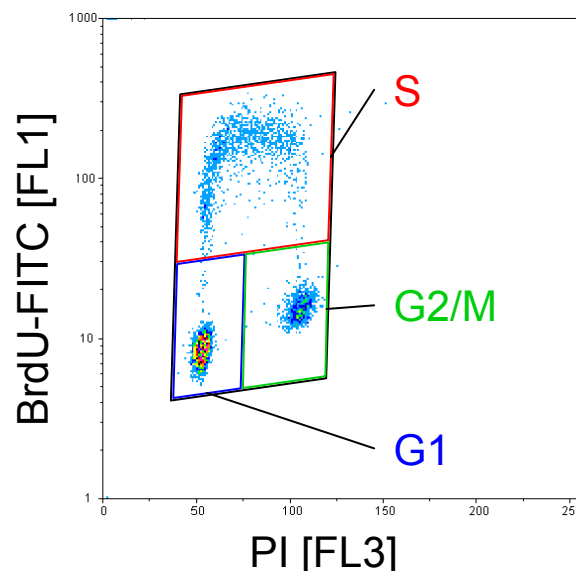
Figure 4.1. Flow cytometric cell cycle analysis. Dot blot showing the proportion of BrdU-FITC [FL1] positive cells as a function of PI [FL3]. Proportions of different cell cycle phases were defined and calculated as a percentage of the total count of events.

4.2.8 Protein Analysis

4.2.8.1 Western Blot Analysis after CDK2 Knockdown

Transfected cells were seeded in 100 mm cell culture dishes (1.2 million cell/dish). After 24 h, whole cell lysates were prepared by harvesting cells in modified Radioimmunoprecipitation Assay (RIPA) lysis buffer. These lysates were used to monitor the level and phosphorylation status of a panel of cell cycle- and transcription-related proteins.

4.2.8.2 Western Blot Analysis of DNA Damage Response Protein after CDK2 or CDK9 Knockdown combined with Irradiation

In order to investigate the effects of depletion of CDK2 or CDK9 on DNA damage response proteins, transfected cell cultures were irradiated with 0 or 6 Gy single dose of X-rays and whole cell lysates were prepared 15 min after irradiation.

4.2.8.3 Protein Kinetic Analysis after CDK9 Knockdown

Cells were seeded in 60 mm cell culture dishes (SAS: 100,000 cell/dish, FaDu: 150,000 cell/dish) and transfected after 24 h. At certain time points (0, 12, 24 and 48 h), cells were harvested in modified RIPA lysis buffer and total cell lysates were prepared. Cell lysates were subjected to SDS-PAGE and immunoblotted with antibodies against cell cycling and transcription related proteins.

4.2.9 Total Protein Extraction

Protein lysates were prepared from adherent cell cultures in 60 mm or 100 mm dishes. After placing the dishes on an ice-cold metal plate, the cell culture medium was discarded and cells were washed twice with ice-cold 1x PBS. 80 µl (for 60 mm dish) or 200 µl (for 100 mm dish) of modified RIPA buffer were pipetted to the cells. Next, cells were scraped off the dish using a cell scraper and cell lysate was collected in a 1.5 ml Eppendorf tube. After 30 min incubation on ice, cell lysate was forced through a small needle (4 times) using an insulin syringe. The sample was incubated for 1 h on ice and centrifuged (16000 rcf, 20 min, 4°C). The supernatant was transferred into a new ice-cold 1.5 ml Eppendorf tube and stored in -80°C freezer.

4.2.10 Determination of Protein Concentration

For accurate determination of protein concentration, the Pierce® Bicinchoninic Acid (BCA) Protein Assay Kit was used (Hehlgans et al., 2008). In this assay, protein samples were diluted 1:10 in RIPA solution (2 µl of sample in 18 µl of RIPA solution). Protein standards of 0.025, 0.5, 1.0, 2.0 mg/ml of bovine serum albumin (BSA) were prepared. Standards and unknown samples were pipetted into 96-well plate (flat bottom). BCA

working reagents were mixed 50 parts of BCA Reagent A with 1 part of BCA Reagent B (50:1, Reagent A:B). 200 µl of the working reagent mixture was then added to each sample and the plate was incubated at 37°C. After 30 min incubation time, the absorbance of the loaded samples was measured using a TECAN microplate reader (Excitation filter: 560 nm) and the Magellan 5.0 software.

4.2.11   Sodium Dodecyl Sulphate Polyacrylamide Gel Electrophoresis

SDS-PAGE is a technique used to separate charged protein molecules through a gel matrix using an electric current. These charged protein molecules migrate by different rates through the gel matrix according to size, charge and shape (Frederick et al., 2002).

SDS-PAGE was performed using Hoefer SE 250 Mini-Gel System with a 1.5 mm comb. After assembling the gel sandwich, 6.9 ml of ice-cold resolving gel mixture was casted inside, covered by a layer of isopropanol and allowed to gelatinise at RT. Twenty minutes later, the isopropanol layer was discarded, and the gel surface was washed three times with double distilled water (ddH$_2$O) and dried. After drying, the 1.5 mm comb was inserted and 1.5 ml of ice-cold 5% stacking gel mixture was loaded and allowed to gelatinise. Gel-forming mixtures with different acrylamide concentrations were prepared according to the formulations given in Table 4.4.

Before loading the samples, the gel comb was removed and the slots were washed three times with 1x running buffer.

Table 4.4. Composition of resolving and stacking gels.

Components (ml)	Resolving gel			Components (ml)	Stacking gel (5%)
	4%	8%	10%		
ddH$_2$O	4.52	3.46	2.93	ddH$_2$O	1.63
Tris-HCl (3M) pH 8.8	2.00	2.00	2.00	Tris-HCl (0.5 M) pH 6.8	0.72
Acrylamide (30%)	1.06	2.13	2.67	Acrylamide (30%)	0.50
Glycerol (50%)	0.16	0.16	0.16	Glycerol (50%)	0.06
SDS (10%)	0.08	0.08	0.08	SDS (10%)	0.03
APS (10%)	0.16	0.16	0.16	APS (10%)	0.06
TEMED	0.0064	0.0064	0.0064	TEMED	0.0048

The separation of proteins was performed by applying a constant electric current of 30 mA/Gel for ~2 h.

4.2.11.1   Sample Preparation and Loading

20-25 µg of protein were mixed with 3 µl of loading buffer (6x) and denatured by heating at 90°C for 5 min. After short centrifugation (3 sec, 16000 rcf), the sample was loaded into the gel slot using a Microliter™ syringe.

4.2.12 Western Blotting

Using Western blotting, SDS-PAGE separated protein bands were electrophoretically transferred to an immobilising membrane. A semi-dry transfer unit was used to transfer proteins to a nitrocellulose membrane (Hehlgans et al., 2008).

After SDS-PAGE, the polyacrylamide gel sandwich was disassembled and covered by a transfer buffer-wetted nitrocellulose membrane and three pieces of transfer buffer-wetted Whatman filter papers. The other side of the polyacrylamide gel was covered by three transfer buffer-wetted Whatman filter papers, and the sandwich was gently squeezed on both sides to get red of the air bubbles. The sandwich was placed on the blotter (the nitrocellulose membrane side of the sandwich was placed on the positive (anode) plate). The transfer of proteins was performed by applying a constant electric current (0.8 mA/cm^2 nitrocellulose membrane) for 3 h.

After blotting, the membrane was washed twice with ddH$_2$O and rinsed in Ponceau S solution for 1 min to visualise the protein bands. The stained membrane was washed again with ddH$_2$O and after the molecular weight bands of Benchmark™ protein ladder were marked, the membrane was scanned using Epson Perfection 4490 PHOTO scanner.

4.2.13 Immunodetection

The membrane was cut into smaller stripes of desired range of molecular weight. The Benchmark™ protein ladder bands served as a molecular weight reference. The desired stripe was destained from Ponceau S using 1x PBS and blocked with 5% milk buffer (agitated, 30 rpm, 1 h). The blocked membrane stripe was welded together with the desired primary antibody in an air bubble-free thin plastic foil and incubated overnight at 4°C (agitated, 10 rpm). Later, the membrane stripe was washed three times (10 min each) with PBST and incubated with the horseradish peroxidase (HRP)-conjugated secondary antibody (agitated, 10 rpm, RT, 1.5 h).

The membrane stripe was washed five times with PBST and once with PBS (10 min each). The HRP activity of the membrane-attached secondary antibody was observed using SuperSignal® West Dura Extended Duration substrate kit. The two reagents of the kit were mixed together in equal ratios and slowly pipetted over the membrane stripe (0.05 ml substrate mixture per cm^2 of the membrane stripe). After 3 min, the substrate mixture was discarded and the stripe was placed between two transparent pieces of foil in an X-ray detection cassette. The chemiluminescent signal was detected using Amersham Hyperfilm ECL X-ray films in a red lightened dark room. Films were developed with Kodak GBX developer, fixed in Kodak GBX fixer, rinsed in tap water and dried.

4.2.14   Analysis of Protein Expression

The X-ray films were scanned using Epson Perfection 4490 PHOTO scanner and the intensities of protein bands were analysed by ImageJ (Version 1.47g) software. The measured intensity values of detected protein bands were normalised to the intensity values of β-actin. The relative phosphorylation ratio of a protein was calculated by normalising the intensity value of phospho-protein versus total protein.

4.3   Synthesis of recombinant DNA and Molecular Cloning

The construction of recombinant DNA and molecular cloning were performed according to (Sambrook, 2001) or according to the manufacturer's protocols of used kits.

4.3.1   Polymerase Chain Reaction

Amplification of human CDK9 (hCDK9) gene sequence (PCR product: 1119 bp) was performed using HotStarTaq® *Plus* Polymerase. PCR reaction mixture consisted of: 2 μl 10x PCR amplification buffer, 1 μl dNTPs, 1 μl hCDK9-*Nhe*I forward primer, 1 μl hCDK9-*Bam*HI reverse primer, 0.6 μl $MgCl_2$, 2 μl of DNA, 0.4 μl HotStarTaq® *Plus* Polymerase and 12 μl ddH_2O were mixed in a thin-walled PCR tube. Placental DNA (UKD, Dresden, Germany) was used as a template for PCR amplification. The optimal annealing temperature (Ta = 64°C) was determined by a gradient-PCR. The PCR started with a single denaturing cycle (4 min, 95°C), 35 cycles (30 sec, 95°C; 45 sec, 64°C; 45 sec, 72°C); single extension phase (5 min, 72°C), reaction hold at ∞ 4°C. The PCR product size was analysed by agarose gel electrophoresis.

4.3.2   Agarose Gel Electrophoresis

To check whether the PCR generated the desired DNA fragment, agarose gel electrophoresis was used to separate the PCR products.

DNA samples were mixed with agarose probe buffer (10x) and loaded into 1% agarose gel containing RedSafe™ nucleic acid stain. Loaded DNA samples were electrophoretically separated at 160 V for 1 h. The gel was placed on a UV-Transilluminator and the image was acquired using a Bio Imaging System. The captured image was printed out and saved as an image file.

The presence of the PCR product of expected size (1.1 kb, the size of the coding sequence of hCDK9) was verified by comparing the size of fractionated PCR product DNA fragments with a DNA ladder (Figure 4.2).
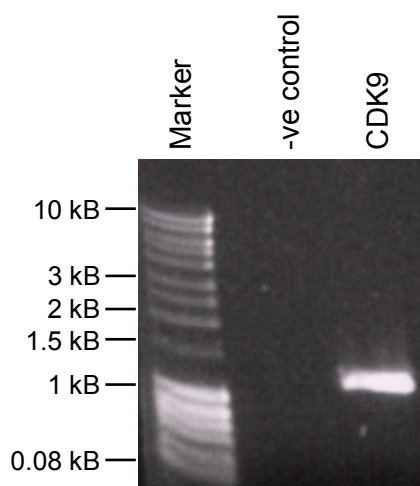
Figure 4.2. RedSafe™-stained PCR products after agarose gel electrophoresis. PCR products were separated in RedSafe™-supplemented 1% agarose gel in 1x TBE buffer. The gel image indicates successful amplification of hCDK9 target sequence. No amplification was present in the -ve control sample.

4.3.3 Restriction Digestion of the PCR Product and pEGFP-N1 Vector

The pEGFP-N1 vector and the CDK9 PCR product were digested with *Nhe*I and *Bam*HI restriction enzymes. The reaction mixture consisted of: 20 µg DNA, 1 µl 100x BSA, 10 µl 10x NEBuffer 4, 3 µl *Nhe*I, 3 µl *Bam*HI, x µl ddH$_2$O (Total volume = 100 µl).

4.3.4 Purification of Digested DNA Fragments

Purification of restricted PCR product and pEGFP-N1 vector was performed according to PCR clean-up protocol from Macherey-Nagel using NucleoSpin® Extract II Kit.

4.3.5 Ligation

Purified digested PCR hCDK9 fragments and pEGFP-N1 vectors were ligated to form the new recombinant hCDK9-pEGFP-N1 plasmids (Figure 4.3). The ligation mixture composed of: 1 µl purified digested hCDK9 DNA, 2 µl purified digested pEGFP-N1 plasmid DNA, 1 µl 10x ligation buffer, 10 µl T4 DNA ligase, 5 µl ddH$_2$O. The ligation mixture was incubated for 4 h at 14°C in the PCR cycler.

4.3.6 Transformation

Introduction of the recombinant DNA into the competent bacterial cells was performed through a heat shock. Frozen bacterial cells were thawed on ice and 2 µl of plasmid DNA were mixed with bacteria. After 30 min incubation on ice, the transformation mixture was incubated at 42°C for 45 sec. The mixture was incubated again on ice. After 2

min, 450 µl of SOC medium were added and the transformation mixture was shaken at 37°C for 2 h. The transformed bacteria were plated on kanamycin (Roth, Karlsruhe, Germany) (30 µg/ml) containing agar plates, spread using a sterile spreader and incubated overnight at 37°C.
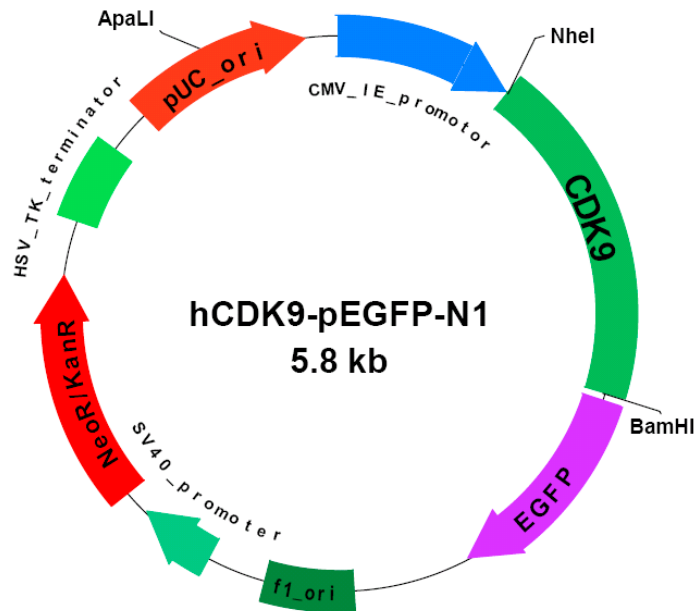
Figure 4.3. Vector map of the hCDK9-pEGFP-N1 plasmid. This verctor is generated by cloning the coding sequence of CDK9 gene into pEGFP-N1 plasmid (Invitrogen, Karlsruhe, Germany).

4.3.7   Plasmid Preparation

Selection of positive clones was established by culturing single clones from the transformed-bacteria agar plates in SOC medium containing antibiotic. Single clones were picked up using a sterile pipette tip and grown in 5 ml SOC medium containing 30 µg/ml kanamycin (Roth, Karlsruhe, Germany) in 15 ml Falcon tubes. The Falcon tubes were incubated at 37°C in the shaking incubator for 8 h (Starter culture). Plasmid preparation was performed using the NucleoSpin® Plasmid Kit according to manufacturer's instructions. In order to prepare a large amount of the plasmid DNA, 1 ml of ready prepared starter culture was inoculated into 200 ml SOC medium containing kanamycin (Roth, Karlsruhe, Germany) (30 µg/ml) in an Erlenmeyer flask and incubated at 37°C overnight in the shaking incubator (Overnight culture).

Next day, the overnight culture was centrifuged (10 min, 394 rcf, 4°C). The supernatant was discarded and the plasmid DNA was isolated according to the manufacturer's protocol using the NucleoBond® AX from Macherey-Nagel.

4.3.8 Determination of DNA Concentration

The plasmid DNA concentration was determined using NanoDrop[®] spectrometer (PeqLab Biotechnologie GmbH, Erlangen, Germany) and ND-1000 software (Version 3.3.0).

4.3.9 Sequencing

The sequence of plasmid DNA was determined by Eurofins MWG Operon sequencing department (Martinsried, Germany) and evaluated using the Gap4 program.

4.3.10 Linearisation of Plasmids

Both hCDK9-pEGFP-N1 and pEGFP-N1 plasmids were linearised using *Apa*LI restriction enzyme before stable transfection. The reaction mixture consisted of: 20 µg DNA, 1 µl 100x BSA, 10 µl 10x NEBuffer 4, 3 µl *Apa*LI, x µl ddH$_2$O (Total volume = 100 µl).

4.4 Stable Transfection

Stable transfection was used to permanently integrate the hCDK9-pEGFP-N1 expression vector or pEGFP-N1 empty vector into the genome of SAS HNSCC cells. Plasmid DNA transfer was performed using the lipid-based gene delivery reagent Lipofectamine™. Stably transfected cells were selected using G418 (Hehlgans et al., 2009; Sambrook, 2001; Storch, 2010).

SAS cells were trypsinised, counted and 100,000 cell/well were seeded in 1 ml complete medium in a 12-well plate. Plated cells were cultured at standard condition in a cell culture incubator. After 24 h, cells were transfected using a stable transfection mixture that was prepared as described in Table 4.5. The linearised plasmid DNA/Opti-MEM[®] I mixture A and Lipofectamine™/Opti-MEM[®] I mixture B were prepared and incubated at RT. After 5 min, both mixtures (A and B) were pooled together and incubated for 20 min at RT.

Table 4.5. Dilution scheme of stable transfection mixture.

Plasmid	Initial plasmid DNA conc.	Mixture A		Mixture B	
		Required amount of DNA (2 µg)	Required amount of Opti-MEM[®] I	Required amount of Lipofectamine™	Required amount of Opti-MEM[®] I
pEGFP-N1 empty vector (linearised)	0.857 µg/µl	2.3 µl	125 µl	5 µl	125 µl
hCDK9-pEGFP-N1 (linearised)	0.929 µg/µl	2.2 µl	125 µl	5 µl	125 µl

After changing the medium, 250 µl of the transfection mixture was pipetted to the cells and the medium was replaced again after 5 h with fresh complete medium. Twenty-four hours after transfection, cells in each well were trypsinised and equally split into five 100 mm dishes under selection pressure in complete medium containing 1.5 mg/ml G418. Untransfected SAS cells were seeded in 100 mm dish in complete medium containing 1.5 mg/ml G418 and were used as control for selection. All cells in the 100 mm control dish died within 8 days after treatment with G418. The G418-resistant transfected cells were found growing into colonies, and were isolated using sterile cloning cylinders 16 days after transfection. Each isolated clone was transferred to a well in a 24-well plate and grown in complete medium containing 1.5 mg/ml G418. The medium was routinely changed every 3-4 days. A glass cover slip seeded with cells was prepared for each single clone. These cover slips were examined using the Axioscope 2 plus fluorescence microscope (Zeiss, Jena, Germany) to control the transfection efficiency of isolated clones.

Positive clones (with more than 80% EGFP positive cells) were identified, and the levels of exogenous expression of CDK9 and EGFP were controlled for each single clone by Western blot.

Single positive clones were frozen and stored at -80 C and a pool of three positive clones of SAS-CDK9-EGFP cells as well as SAS-EGFP cells was prepared, cultured and used for further experiments.

Fluorescence images of SAS-CDK9-EGFP and SAS-EGFP control cells were obtained using LSM 510 Meta equipped with Zeiss LSM 510 Software. Cells were seeded for 24 h on glass coverslips and fixed with 3% formaldehyde (10 min). The fixed coverslips were mounted with Vectashield/DAPI mounting medium, examined and photographed.

4.5   Statistical Analysis

Experimental data were expressed as mean ± standard deviation (s.d.) of three independent repeats. The statistical significance of the data was evaluated by Student's t-test using Microsoft$^{®}$ Excel 2003. Results were considered statistically significant if the P value was less than 0.05. Graphical representations were created using GraphPad Prism 4.03.

5   Results

5.1   CDK2 Targeting enhances the Radiosensitivity of HNSCC Cancer Cells

Radiotherapy eliminates cancer cells by inducing genetic damage to stop the proliferative integrity of cells. CDK2 is involved in regulating cell cycle progression, cell cycle checkpoints (G1/S as well as G2/M) and DNA damage repair response (Aleem et al., 2004; Deans et al., 2006; Kaldis & Aleem, 2005; Neganova et al., 2011; Satyanarayana & Kaldis, 2009b; Sherr & Roberts, 2004). These functions are essential for maintaining genomic integrity and cell survival. Therefore, we investigated the role of CDK2 in the cellular radiosensitivity. CDK2$^{-/-}$ and WT MEFs as well as six human HNSCC cell lines were used.

5.1.1   CDK2 Deficiency is associated with increased Radiosensitivity in MEFs

To examine whether CDK2 is involved in cellular radiation survival of MEFs, we performed 2D colony formation assays using CDK2$^{-/-}$ and WT MEFs and measured the clonogenic survival upon irradiation using 2D colony formation assay. CDK2 deficiency was confirmed by Western blotting (Figure 5.1A). Our results showed a significant ($P <$ 0.05) dose dependent decrease in the clonogenic survival fraction of irradiated CDK2$^{-/-}$ MEFs as compared to WT MEFs (Figure 5.1B) (Soffar et al., 2013).
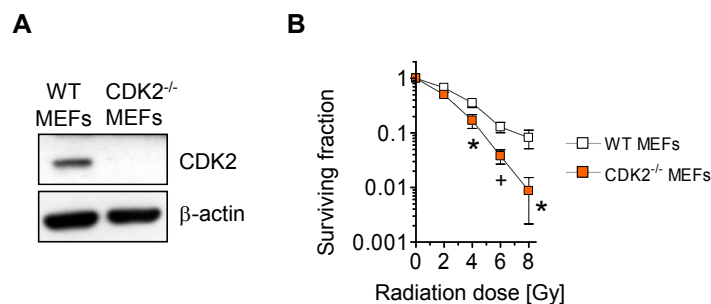
Figure 5.1. CDK2 deficiency mediates increased radiosensitivity relative to CDK2 WT status. CDK2$^{-/-}$ and WT MEFs were plated for colony formation and irradiated with X-rays (0 - 8 Gy, single dose) after 24 h. After 7 days, formed colonies were fixed, stained and counted. **(A)** Western blot of CDK2 in CDK2$^{-/-}$ and WT MEF cultures. β-actin served as loading control. **(B)** Clonogenic survival of irradiated CDK2$^{-/-}$ and WT MEFs. Results show mean ± s.d. (n = 3; student's t-test; * $P <$ 0.05; + $P <$ 0.01). (Soffar et al., 2013).

5.1.2 Absence of CDK2 correlates with elevated Number of residual DSBs in MEFs

Several studies suggested that the main target for biological effect of irradiation is DNA (Hall & Giaccia, 2006; Han & Yu, 2010). Among different types of radiation-induced DNA lesions, DSBs are considered as one of the most severe forms of DNA damage and are lethal to cells if left unrepaired (Shaheen et al., 2011; Symington & Gautier, 2011). In order to investigate whether CDK2 deficiency affects DNA damage repair of DSBs, we performed γH2AX/53BP1 foci assay 24 h after irradiation. Visual γH2AX/53BP1-positive foci were defined as residual DSBs (Figure 5.2A). The mean number of γH2AX/53BP1-positive foci per cell was evaluated. Our results showed a significant ($P < 0.05$) increase in the number of residual DSBs in 6 Gy-irradiated CDK2$^{-/-}$ MEFs relative to WT MEFs (Figure 5.2B) (Soffar et al., 2013).
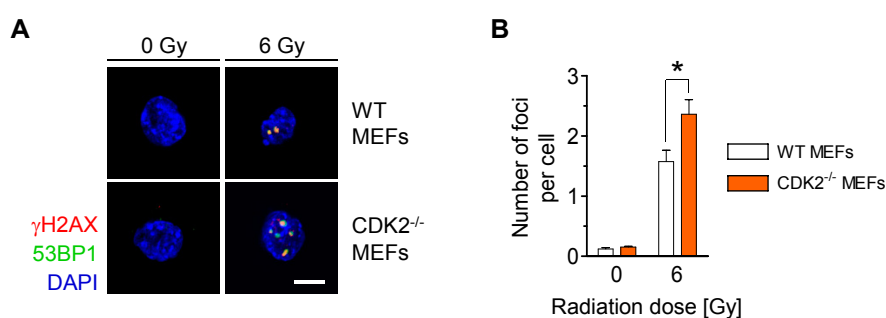
Figure 5.2. CDK2$^{-/-}$ MEFs show elevated number of radiation-induced residual DSBs as compared to WT MEFs. CDK2$^{-/-}$ and WT MEFs were plated and irradiated with X-rays (0 or 6 Gy, single dose). After 24 h, cells were harvested, fixed and immunostained against γH2AX and 53BP1. DAPI was used to stain nuclei. Double stained foci from 50 cell nuclei were counted by fluorescence microscopy and defined as residual DSBs. **(A)** Representative photographs of γH2AX/53BP1 double immunofluorescence staining. γH2AX (red), 53BP1 (green), DAPI (blue). Bar, 10 μm. **(B)** Number of γH2AX/53BP1-positive colocalised foci per cell 24 h after radiation. Results show mean ± s.d. (n = 3; student's *t*-test; * $P < 0.05$). (Soffar et al., 2013).

5.1.3 Loss of CDK2 mediates elevated Radiation-induced G2/M Phase Blockage

Activation of cell cycle checkpoints functions primarily to arrest cells transiently after genotoxic stress which provides sufficient time for DNA damage repair (Satyanarayana et al., 2008; Weinert et al., 1994; Weitzman et al., 2013; Yata & Esashi, 2009). As CDK2 is involved in cell cycle progression and checkpoint response, we performed cell cycle analysis to investigate whether CDK2 deficiency in MEFs affects cell cycle progression or cell cycle checkpoint response upon irradiation. In comparison to unirradiated controls, our results displayed a radiation-induced G2/M cell cycle phase arrest that peaks 10 h after irradiation in CDK2$^{-/-}$ MEFs as well as WT MEFs (differences between irradiated and unirradiated data points were statistically significant ($P < 0.05$) at

10, 14 and 18 h after irradiation) (Figure 5.3A). In parallel, we observed a significant ($P <$ 0.05) decrease in S phase populations. In addition, our results revealed a slight but significant ($P < 0.05$) increase in the G1 phase populations 24 h after irradiation. Comparing cell cycle distribution of unirradiated CDK2$^{-/-}$ to WT MEFs (0 h time point shown in Figure 5.3A) revealed that CDK2$^{-/-}$ MEFs possess significantly ($P < 0.01$) lower G1 phase and higher S phase populations as compared to WT MEFs (Figure 5.3B). In Figure 5.3C, we compared the cell cycle distribution of CDK2$^{-/-}$ to WT MEFs 10 h after irradiation (the time point at which the radiation-induced cell-cycle effects reached maximum). Interestingly, irradiation of CDK2$^{-/-}$ MEFs resulted in a significant ($P < 0.05$) increase in the percentage of cells accumulating in the G2/M phase as compared to WT MEFs (Figure 5.3C) (Soffar et al., 2013).

Taken together, our data suggest a possible role of CDK2 in radiation survival, repair of radiogenic DSBs and G2/M phase block in response to irradiation.

5.1.4   CDK2 Knockdown increases the Radiosensitivity of HNSCC Cancer Cells under 2D Growth Conditions

As CDK2 deficiency modulated the radiosensitivity of MEFs (Figure 5.1), we next studied the effect of CDK2 targeting on the cellular response of a panel of HNSCC cell lines to irradiation. The investigated cell lines were SAS, FaDu, HSC4, Cal33, UTSCC5 and UTSCC8. We evaluated the clonogenic survival upon CDK2 knockdown plus/minus irradiation using 2D colony formation assay. CDK2 knockdown was performed using two different CDK2 siRNAs (CDK2 siRNA#1 and CDK2 siRNA#2). A non-specific siRNA (Co siRNA) was used as control.

Our results displayed efficient CDK2 knockdown via CDK2 siRNA#1 (Figure 5.4A). The basal survival fraction of all tested cell lines upon CDK2 silencing was not affected (Figure 5.4B). Regarding the clonogenic radiation survival, we observed that SAS and FaDu CDK2 knockdown cell cultures are significantly ($P < 0.05$) more sensitive to X-rays as compared to siRNA control cultures (Figure 5.4C). The other tested cell lines (HSC4, Cal33, UTSCC5 and UTSCC8) lacked significant enhancement of radiosensitivity after CDK2 knockdown (Soffar et al., 2013).

We confirmed our findings in SAS and FaDu cells by depleting CDK2 using a second CDK2 siRNA (#2) (Figure 5.5A). We found that CDK2 knockdown results in an unchanged basal survival fraction and significantly ($P < 0.05$) enhances the radiosensitivity of SAS but not FaDu cells as compared to control cultures (Figure 5.5B, C) (Soffar et al., 2013).

Further investigations to evaluate the molecular role of CDK2 on radiation response were performed using CDK2 siRNA#1-depleted SAS and FaDu cell cultures.

A
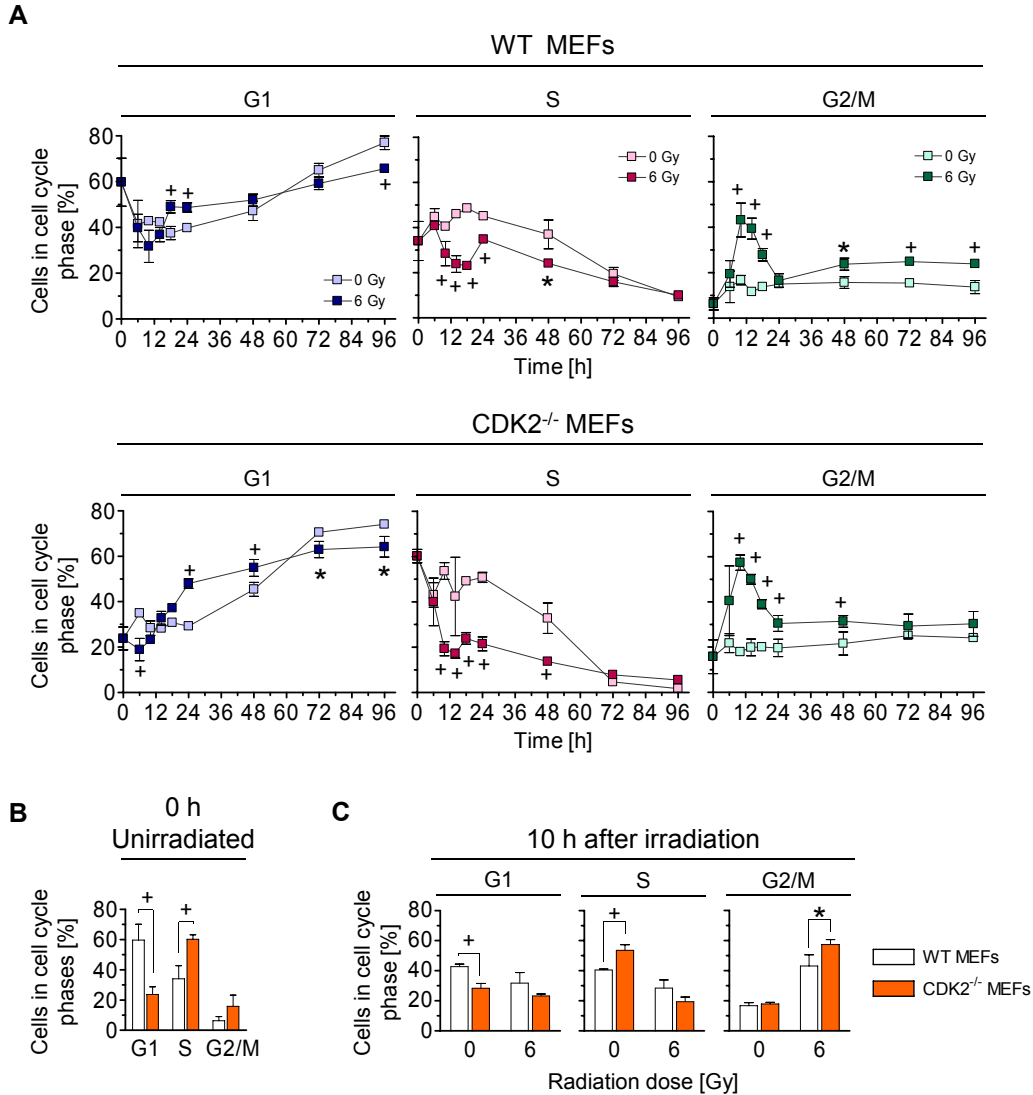
Figure 5.3. Absence of CDK2 in MEFs is associated with elevated radiation-induced G2/M arrest. CDK2^{-/-} and WT MEF cultures were irradiated with X-rays (0 or 6 Gy, single dose), pulse-labelled with BrdU at certain time points after irradiation (0, 10, 14, 18, 24 or 48 h) and fixed. Cell nuclei were extracted, stained with anti-BrdU/FITC and PI and analysed by CyFlow flow cytometer and FloMax software. **(A)** Cell cycle distribution analysis of unirradiated CDK2^{-/-} MEFs compared to WT MEFs. Results show mean ± s.d. (n = 3; student's *t*-test; * $P < 0.05$; + $P < 0.01$). **(B)** Cell cycle distribution of unirradiated CDK2^{-/-} MEFs relative to WT MEFs at 0 h. Results show mean ± s.d. (n = 3; student's *t*-test; + $P < 0.01$). **(C)** Cell cycle analysis of CDK2^{-/-} MEFs as compared to WT MEFs 10 h after irradiation. Results show mean ± s.d. (n = 3; student's *t*-test; * $P < 0.05$; + $P < 0.01$). ((B) and (C) were published in Soffar et al., 2013).
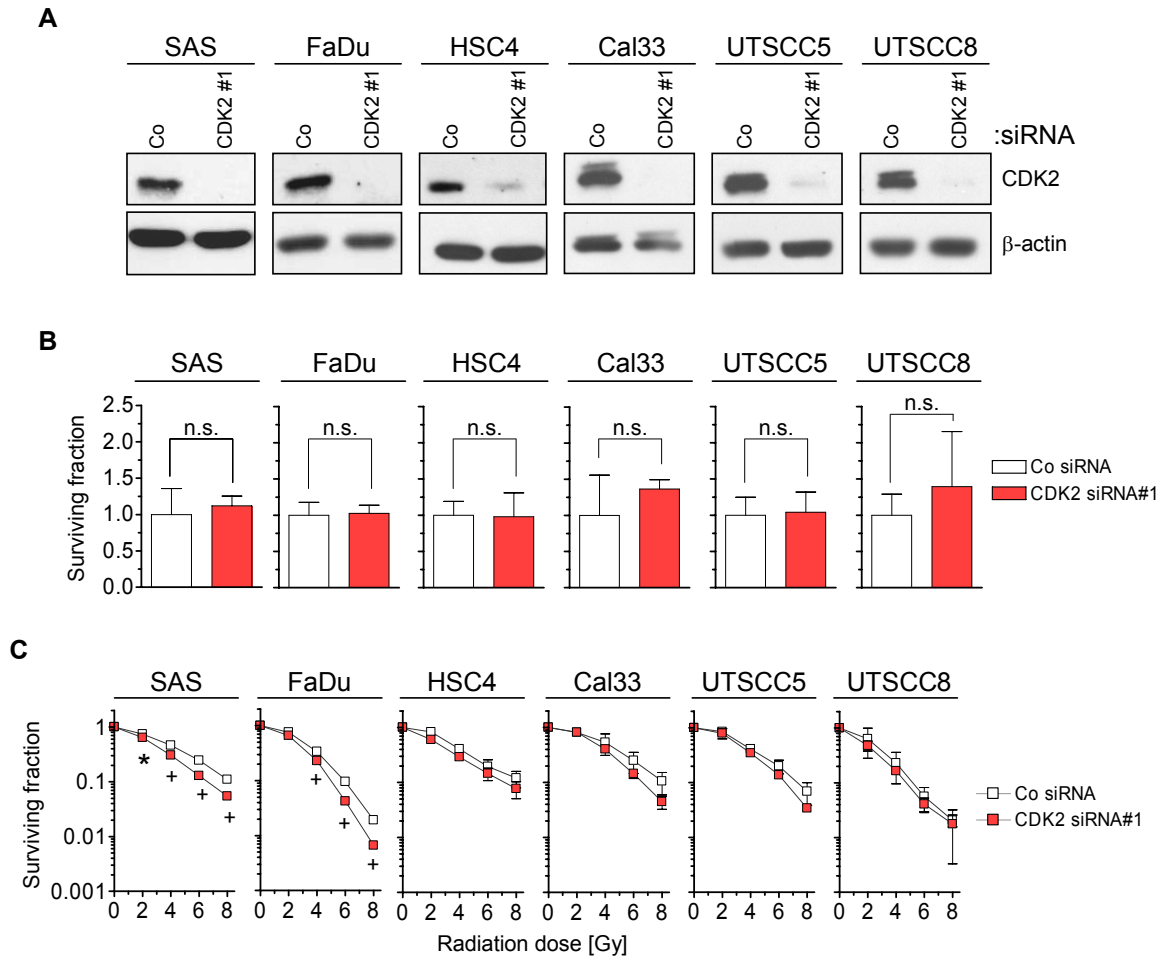
Figure 5.4. CDK2 knockdown enhances the radiosensitivity of 2D HNSCC cell cultures. CDK2 siRNA#1-transfected and control cultures were plated and after 24 h irradiated with X-rays (0 - 8 Gy, single dose). After certain incubation time (7 - 14 days, cell line dependent), formed colonies were microscopically counted. **(A)** Western blot analysis of CDK2 from whole cell lysates of CDK2 knockdown or control cell cultures. β-actin served as loading control. **(B)** Unaffected basal clonogenic survival of CDK2 knockdown or control cell cultures. Results show mean ± s.d. (n = 3; student's *t*-test; n.s. not significant). **(C)** Clonogenic survival of irradiated CDK2 knockdown or control cultures. Results show mean ± s.d. (n = 3; student's *t*-test; * $P <$ 0.05; [+] $P <$ 0.01). (Soffar et al., 2013).
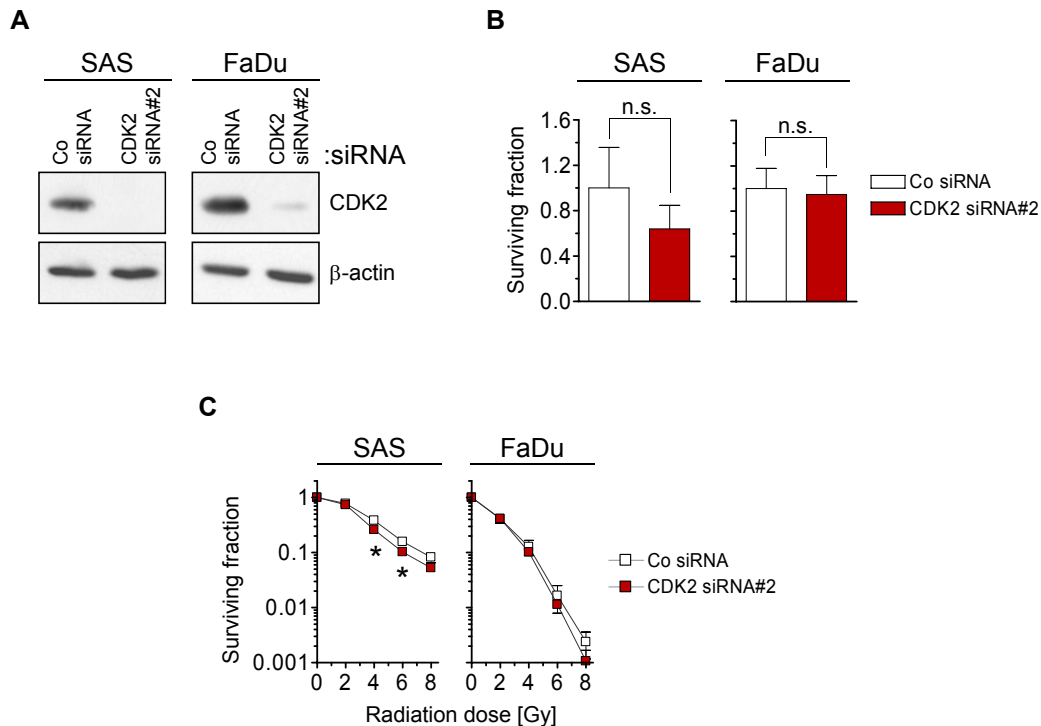
Figure 5.5. Depletion of CDK2 by CDK2 siRNA#2 increases the radiosensitivity of SAS but not FaDu cell cultures. CDK2 siRNA#2-transfected and control cultures were plated for colony formation and irradiated after 24 h with X-rays (0 - 8 Gy, single dose). **(A)** CDK2 Western blotting of whole cell lysate of CDK2 and control knockdown cultures. **(B)** Basal survival of CDK2 siRNA#2 knockdown cultures in comparison to control cultures. **(C)** Clonogenic radiation survival of CDK2 siRNA#2-transfected SAS and FaDu cell cultures as compared to control siRNA-transfected cultures. Results show mean ± s.d. (n = 3; student's *t*-test; * *P* < 0.05; + *P* < 0.01). (Soffar et al., 2013).

5.1.5 Depletion of CDK2 attenuates radiogenic DSB Repair in SAS and FaDu Cells

Our results revealed that CDK2$^{-/-}$ MEFs possess an elevated number of radiogenic residual DSBs as compared to WT cells (Figure 5.2). This indicates a possible role of CDK2 in DNA damage repair. In order to investigate whether CDK2 knockdown induces a similar effect in HNSCC cancer cells, we performed γH2AX/53BP1-positive foci assay and scored radiation-induced residual DSBs upon CDK2 knockdown in SAS and FaDu cell lines (Figure 5.6A). In line with our results from the colony formation assays, we observed a significant (*P* < 0.05) increase in the number of radiation-induced γH2AX/53BP1-positive foci per cell in CDK2 knockdown SAS and FaDu cell cultures as compared to control cultures (Figure 5.6B) (Soffar et al., 2013).

A

B
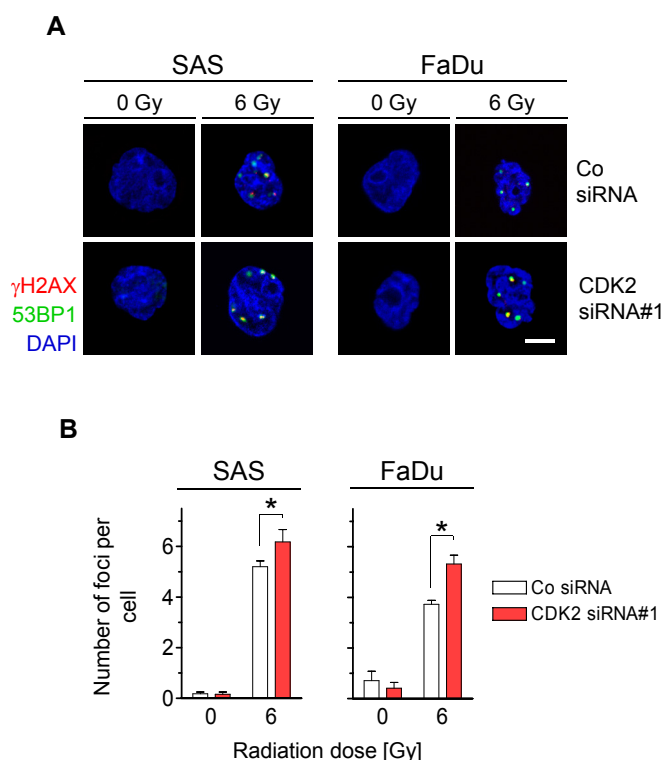
Figure 5.6. CDK2 knockdown increases the number of residual DSBs of irradiated SAS and FaDu cell cultures. CDK2 siRNA#1-transfected and control cultures were irradiated with X-rays (0 - 8 Gy, single dose). After 24 h, cells were trypsinised, fixed and immunostained against γH2AX and 53BP1. DAPI was used to stain nuclei. Double stained foci from 50 cell nuclei were counted by a fluorescence microscope and defined as residual DSBs. **(A)** Representative photographs show γH2AX/53BP1 double staining of unirradiated and irradiated CDK2-depleted and control cultures. γH2AX (red), 53BP1 (green), DAPI (blue). Bar, 10 µm. **(B)** Number of γH2AX/53BP1-positive foci per cell of CDK2 knockdown SAS and FaDu cells compared to controls. Results show mean ± s.d. (n = 3; student's *t*-test; * *P* < 0.05). (Soffar et al., 2013).

The increased number of radiogenic residual DSBs upon CDK2 knockdown in SAS and FaDu suggests that CDK2 is involved in DNA damage repair. To clarify this role, we investigated, by Western blotting, a panel of proteins involved in checkpoint signalling and DNA repair upon CDK2 knockdown 15 min after irradiation (0 or 6 Gy, X-rays, single dose) (Figure 5.7A). The 15 min time point was chosen to address the rapid changes in expression and phosphorylation of DNA damage repair proteins in response to irradiation. Densitometric analysis of Western blot signals of investigated proteins was performed using the ImageJ (Version 1.47g) software, and data were blotted as bar graphs in Figure 5.7B. All measured data values were normalised to β-actin as loading control, and values of phosphorylation levels of proteins were normalised to total protein levels. Despite efficient CDK2 knockdown, our results showed no apparent alterations in the levels of ATM, phospho-ATM(S1981), DNA-PK, CHK2, phospho-CHK2(T86), RAD50, NBS1 and PCNA (Figure 5.7A, B). Thus, these results cannot explain how CDK2 knockdown mediates DNA damage repair (Soffar et al., 2013).
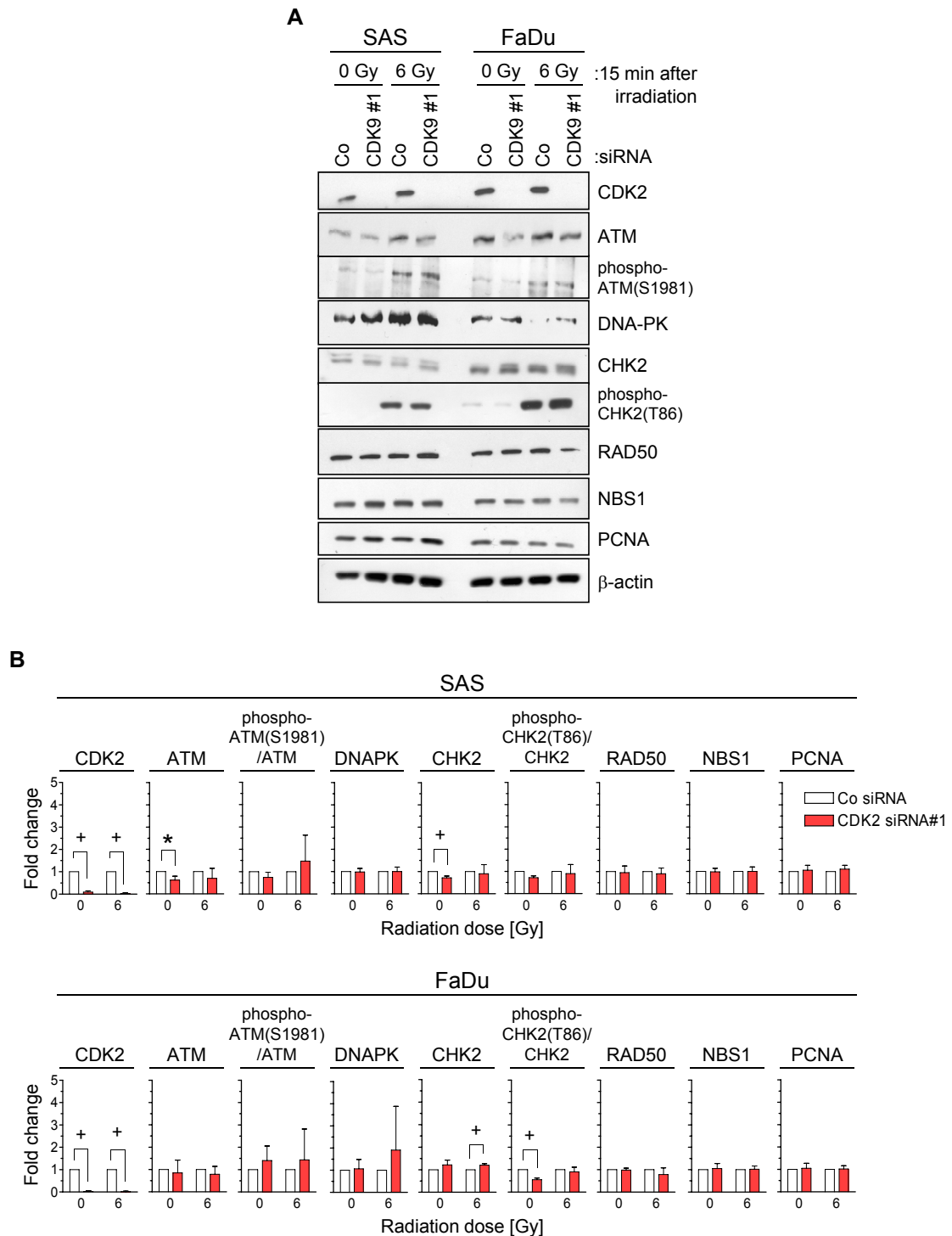
Figure 5.7. Impact of CDK2 silencing on expression and phosphorylation of DNA damage repair proteins. (A) Western blotting of whole cell protein lysates of CDK2 siRNA#1-transfected and control cultures harvested 15 min after irradiation (0 or 6 Gy, X-rays, single dose). β-actin served as loading control. **(B)** Densitometric analysis of Western blots of Figure A shows the fold change of expression or phosphorylation of proteins. Protein expression values were normalised to β-actin. Phosphorylation values of proteins were normalised to total protein expression. Results show mean ± s.d. (n = 3; student's *t*-test; * $P < 0.05$; + $P < 0.01$). (Soffar et al., 2013).

5.1.6 Silencing of CDK2 does not alter Apoptosis in SAS and FaDu Cells

DNA damage, such as DSBs, might induce cell death by activating apoptosis (Ciccia & Elledge, 2010). As CDK2 knockdown increased the number of radiogenic residual DSBs (Figure 5.6), we next evaluated the level of apoptosis in CDK2-depleted or control SAS and FaDu cells in response to ionising radiation. Our results showed that the level of apoptosis is very low in unirradiated as well as 6 Gy-irradiated SAS and FaDu cell cultures, and that CDK2 knockdown has no significant impact on apoptosis in both unirradiated and irradiated cells (Figure 5.8) (Soffar et al., 2013).
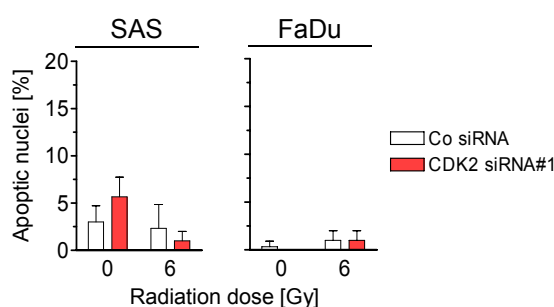

Figure 5.8. Apoptosis in unirradiated and irradiated CDK2-depleted or control SAS and FaDu cell cultures. CDK2 siRNA#1-transfected cells (non-specific siRNA was used as control) were irradiated with X-rays (0 or 6 Gy, single dose), fixed and stained with DAPI. The number of apoptotic nuclei per 100 cells was evaluated using fluorescence microscopy. Results show mean ± s.d. (n = 3). (Soffar et al., 2013).

5.1.7 CDK2 Knockdown has no impact on Cell Cycle Distribution of unirradiated and irradiated SAS and FaDu Cell Cultures

We showed that the absence of CDK2 in MEFs is associated with a significant induction of G2/M phase block after irradiation (Figure 5.3B). To address the possible role of CDK2 in cell cycling of SAS and FaDu cancer cells upon irradiation, we performed cell cycle analysis.

First, we investigated the effect of irradiation as monotherapy on the cell cycle of SAS and FaDu cell cultures. In this experiment, we analysed cell cycle distributions of unirradiated and 6 Gy-irradiated cell cultures. Our results revealed a typical radiation-induced G2/M cell cycle phase arrest that peaks at approximately 14 h after irradiation in both cell lines (the differences between irradiated and unirradiated data points were statistically significant ($P < 0.05$) at 10, 14 and 18 h after irradiation) (Figure 5.9). In parallel, we observed a significant ($P < 0.05$) decrease in the G1 and S phase cell populations in both cell lines. These data suggest that the appropriate time point to conduct further cell cycle distribution analysis after irradiation is 14 h (Soffar et al., 2013).
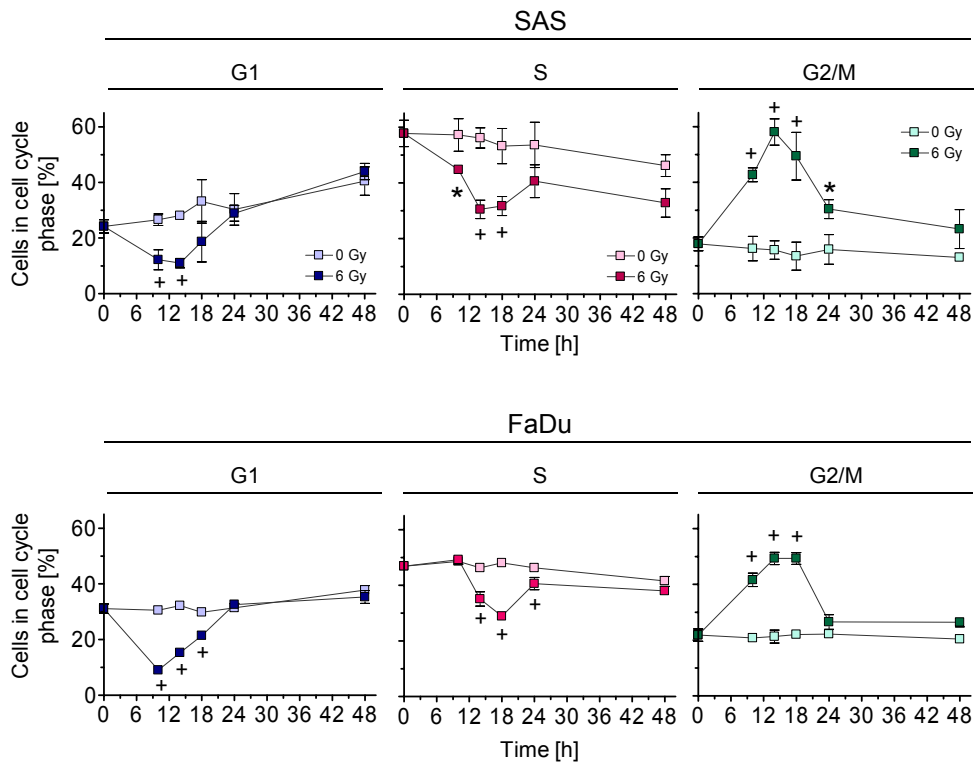
Figure 5.9. Irradiation induces G2/M cell cycle arrest in SAS and FaDu cell cultures. SAS and FaDu cells were plated and after 72 h were irradiated with X-rays (0 or 6 Gy, single dose). Cells were pulse-labelled with BrdU at indicated time points and fixed. Cell nuclei were extracted, immunostained with anti-BrdU/FITC and counterstained with PI. Results show mean ± s.d. (n = 3; student's *t*-test; * $P < 0.05$; + $P < 0.01$). (Soffar et al., 2013).

Next, we studied the effect of CDK2 knockdown as a single treatment (without irradiation) on the cell cycle distribution of SAS and FaDu cells. Our results showed unaffected cell cycle profiles after CDK2 knockdown as compared to controls (Figure 5.10) (Soffar et al., 2013).

In order to investigate whether CDK2 knockdown affects the response of SAS and FaDu cell cycles to ionising radiation, we performed cell cycle analysis of CDK2 knockdown and control cultures 14 h after irradiation (0 or 6 Gy, X-rays, single dose) as radiation-induced cell-cycle arrest in SAS and FaDu cells reaches the maximum at this time point (Figure 5.9). We observed that irradiation induces a typical G2/M cell cycle arrest in both cell lines (Figure 5.11), and that CDK2 knockdown did not modulate the cell cycle response to irradiation as compared to control cultures.

Taken together, our results showed that neither CDK2 knockdown nor combined CDK2 knockdown plus irradiation results in any significant alteration in the cell cycle distribution of SAS and FaDu cell cultures. In contrast with our results in MEFs, these data suggest that CDK2 is dispensable for the cell cycle of SAS and FaDu cells (Soffar et al., 2013).
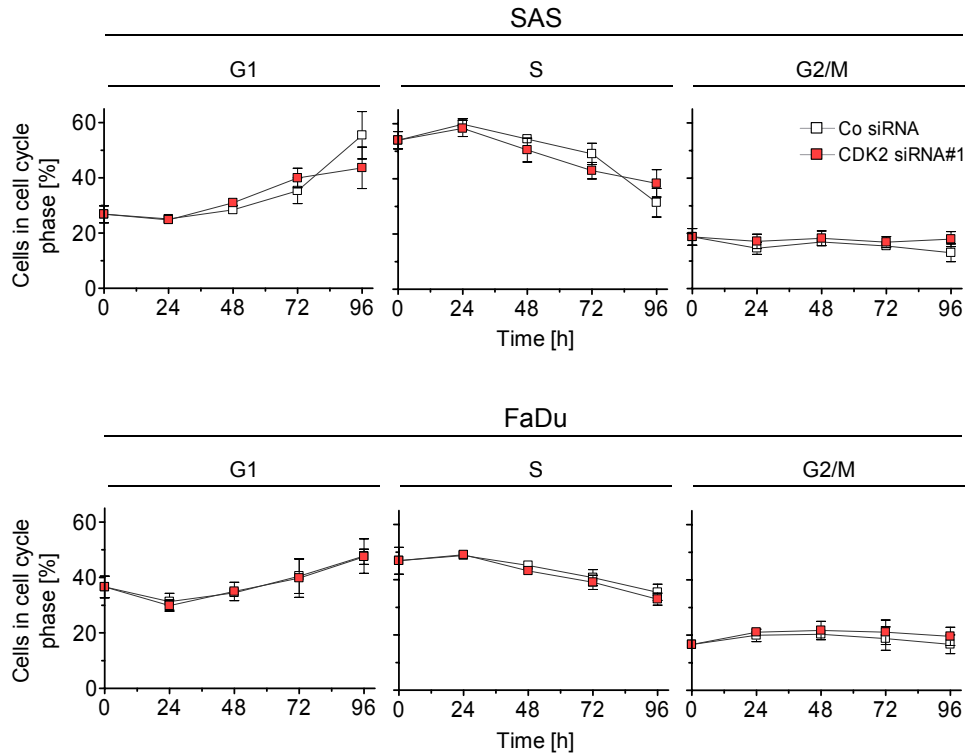
Figure 5.10. CDK2 is dispensable for the cell cycle of SAS and FaDu cells. Cell cycle analysis of CDK2-depleted SAS and FaDu cell cultures as compared to controls. Cells were transfected with CDK2 siRNA#1 (non-specific siRNA was used as control). At indicated time points, cells were pulse-labelled with BrdU and fixed. Cell nuclei were extracted, immunostained with anti-BrdU/FITC and counterstained with PI (n = 3). (Soffar et al., 2013).
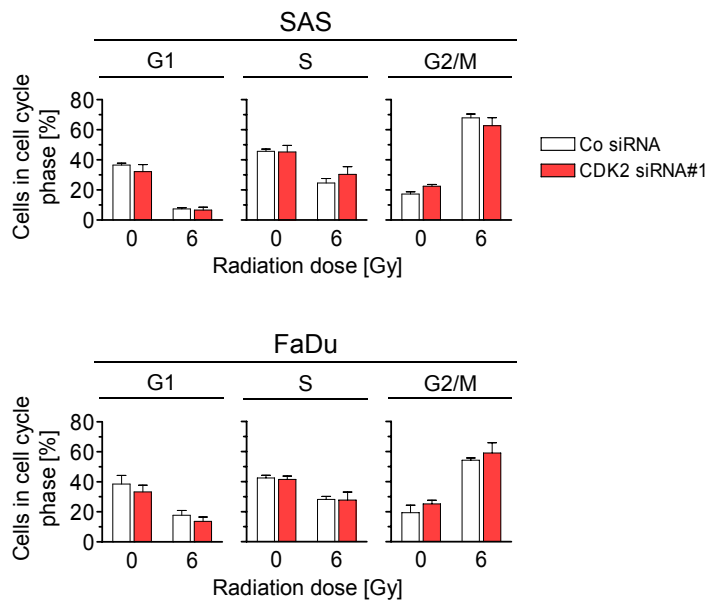
Figure 5.11. CDK2 is negligible for radiation-induced cell cycle arrest of SAS and FaDu cell cultures. Cell cycle analysis of unirradiated and 6 Gy-irradiated CDK2-depleted SAS and FaDu cell cultures as compared to controls. CDK2 siRNA#1-transfected and control cultures were irradiated with X-rays (0 or 6 Gy, single dose). After 14 h, cells were pulse-labelled with BrdU and fixed. Cell nuclei were extracted, immunostained with anti-BrdU/FITC and counterstained with PI. Results show mean ± s.d. (n = 3). (Soffar et al., 2013).

Next, we performed Western blot analysis to investigate the effect of CDK2 knockdown on the expression and phosphorylation levels of a panel of CDK2 interacting partners. Densitometric analysis of Western blots of investigated proteins was performed using the ImageJ (Version 1.47g) software, and data were blotted as bar graphs. All data values were normalised to β-actin as loading control, and density values of phosphorylation levels of proteins were normalised to total protein levels. Our results showed a 2-fold induction in the expression of Cyclin D1 and a 1.3-fold induction in the level of p27 in CDK2 knockdown cell cultures as compared to control cultures (Figure 5.12). Moreover, the level of Cyclin E was significantly elevated in SAS but not FaDu cells. No critical changes were observed in the expression levels of Cyclin A, RPA and ORC1. Most importantly, CDK2 knockdown had no impact on the phosphorylation of Rb, the main downstream substrate of CDK2, in both tested cell lines indicating a possible compensatory pathway for CDK2 functions (Soffar et al., 2013).
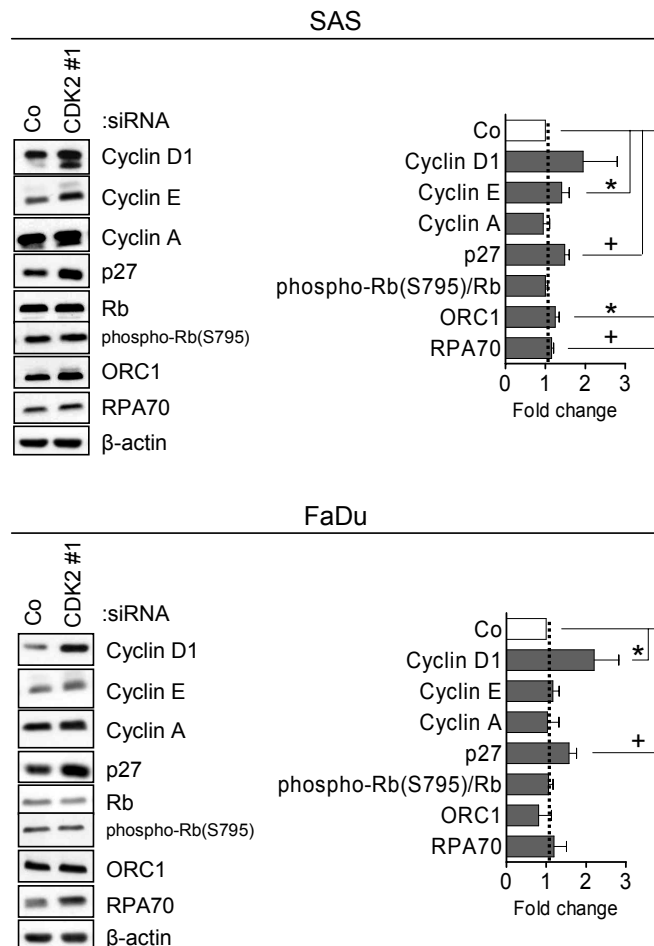
Figure 5.12. Knockdown of CDK2 modulates cell cycle proteins in SAS and FaDu cells. Western blot analysis of protein lysates of CDK2 siRNA#1-transfected SAS and FaDu cell cultures (non-specific siRNA was used as control) harvested 48 h after transfection. β-actin served as loading control. Bar graphs: Densitometric analysis displays the fold change of expression and phosphorylation of proteins after CDK2 knockdown relative to control. Results show mean ± s.d. (n = 3; student's *t*-test; * *P* < 0.05; + *P* < 0.01). (Soffar et al., 2013).

5.1.8   CDK2 Knockdown does not affect the Radiosensitivity of SAS and FaDu cells under 3D Growth Conditions

3D lrECM-based cell culture model better mimics the physiological growth conditions as compared to the traditional 2D monolayer culture (Eke et al., 2013). Therefore, we performed 3D lrECM colony formation assays to evaluate the clonogenic radiation survival of CDK2 knockdown and control SAS and FaDu cell cultures under 3D growth conditions. Our results showed that CDK2 knockdown (Figure 5.13A) has neither a significant effect on basal clonogenic survival (Figure 5.13B, C) nor on clonogenic radiation survival of SAS and FaDu cell cultures (Figure 5.13C, D) (Soffar et al., 2013).
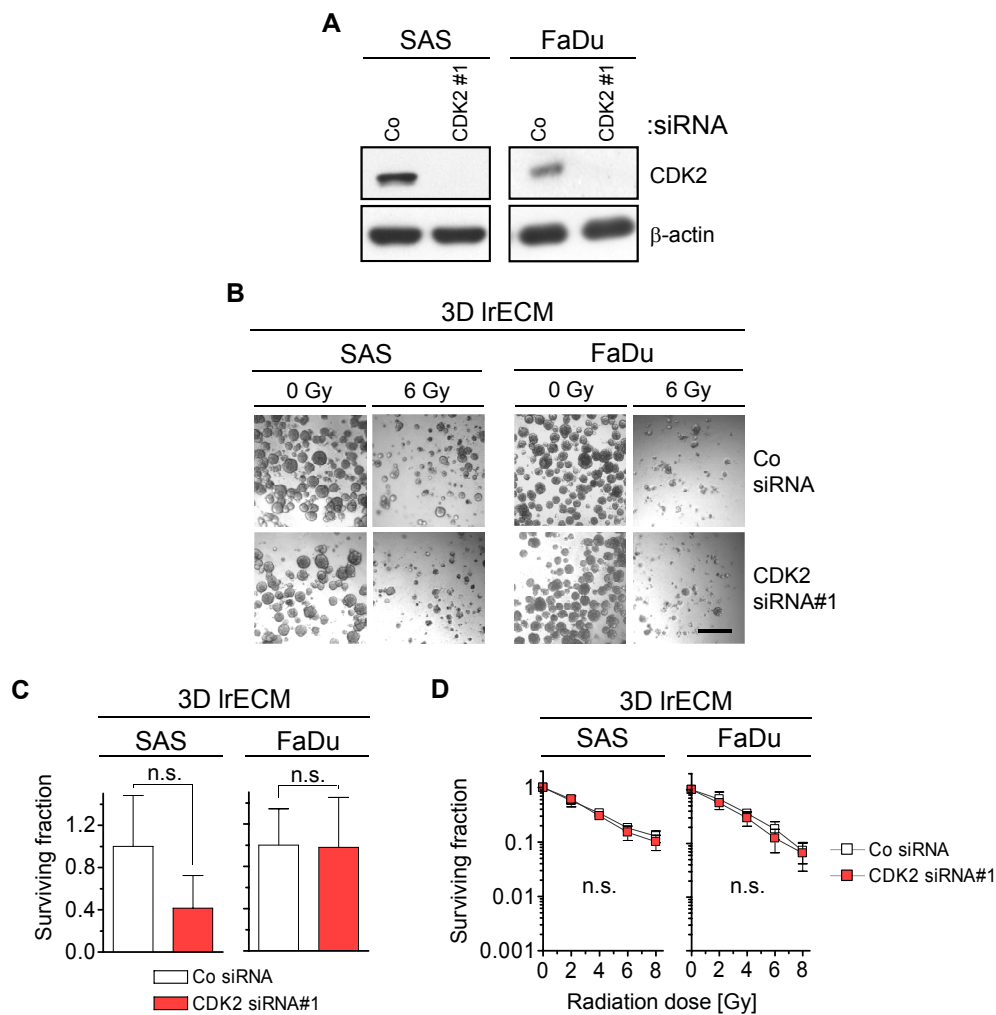
Figure 5.13. CDK2 knockdown does not impact the radiosensitivity of SAS and FaDu cell cultures under 3D growth conditions. CDK2 siRNA#1-transfected and control cultures were plated under 3D lrECM growth condition for colony formation assays. After 24, cells were irradiated with X-rays (0 - 8 Gy, single dose). After a certain incubation time (SAS: 7 days, FaDu: 9 days), formed colonies were microscopically counted. **(A)** CDK2 Western blot of CDK2 knockdown and control whole cell lysates. β-actin served as loading control. **(B)** Representative photographs show SAS and FaDu 3D colony formation assays after CDK2 knockdown plus/minus irradiation. Bar, 200 μm. **(C)** Basal survival fraction of 3D SAS and FaDu CDK2-depleted or control cell cultures. Results show mean ± s.d. (n = 3; student's *t*-test; n.s. not significant). **(D)** 3D colony formation of CDK2 knockdown or control SAS and FaDu cell cultures irradiated with X-rays (0 - 8 Gy, single dose). Results show mean ± s.d. (n = 3; student's *t*-test; n.s. not significant). (Soffar et al., 2013).

5.2 CDK9 regulates the Radiosensitivity, DNA Damage Repair and Cell Cycle of HNSCC Cancer Cells

Recently, Yu and colleagues reported that CDK9 plays a role in maintaining the genomic integrity in response to replication stress and promotes recovery from replication arrest (Yu et al., 2010). Such functions are necessary for cancer cell survival after radiation-induced genomic damage. Here, we investigated the potential role of CDK9 in the response of human HNSCC cancer cells to ionising radiation.

5.2.1 CDK9 Knockdown renders HNSCC Cells more radiosensitive to X-rays

To evaluate the role of CDK9 in the cellular radiation response, we investigated the clonogenic radiation survival upon CDK9 knockdown in a panel of 5 HNSCC cell lines using 2D colony formation assays. The investigated cell lines were SAS, FaDu, Cal33, HSC4 and UTSCC5. CDK9 knockdown was performed using two different CDK9 siRNAs (CDK9 siRNA#1, CDK9 siRNA#2). Non-specific siRNA was used as control. Our results showed that CDK9 siRNA-mediated knockdown results in an efficient reduction in the expression level of CDK9 in all cell lines (Figure 5.14A) except Cal33, in which CDK9 siRNA#1-mediated knockdown failed. As compared to controls, we observed unaffected basal survival fraction after CDK9 knockdown in all cell lines except SAS, in which the CDK9 knockdown significantly ($P < 0.05$) decreases the basal clonogenic survival (Figure 5.14B). Interestingly, CDK9 knockdown significantly decreased the radiosensitivity of all tested cell lines to ionising radiation as compared to controls (an exception was CDK9 siRNA#1-depleted UTSCC5 cell cultures) (Figure 5.14C). These results suggest a critical role for CDK9 in the clonogenic cell survival of investigated HNSCC cell lines upon irradiation.

Our further investigations to evaluate the role of CDK9 for radiation response were performed using CDK9 siRNA#1-depleted SAS and FaDu cell cultures.
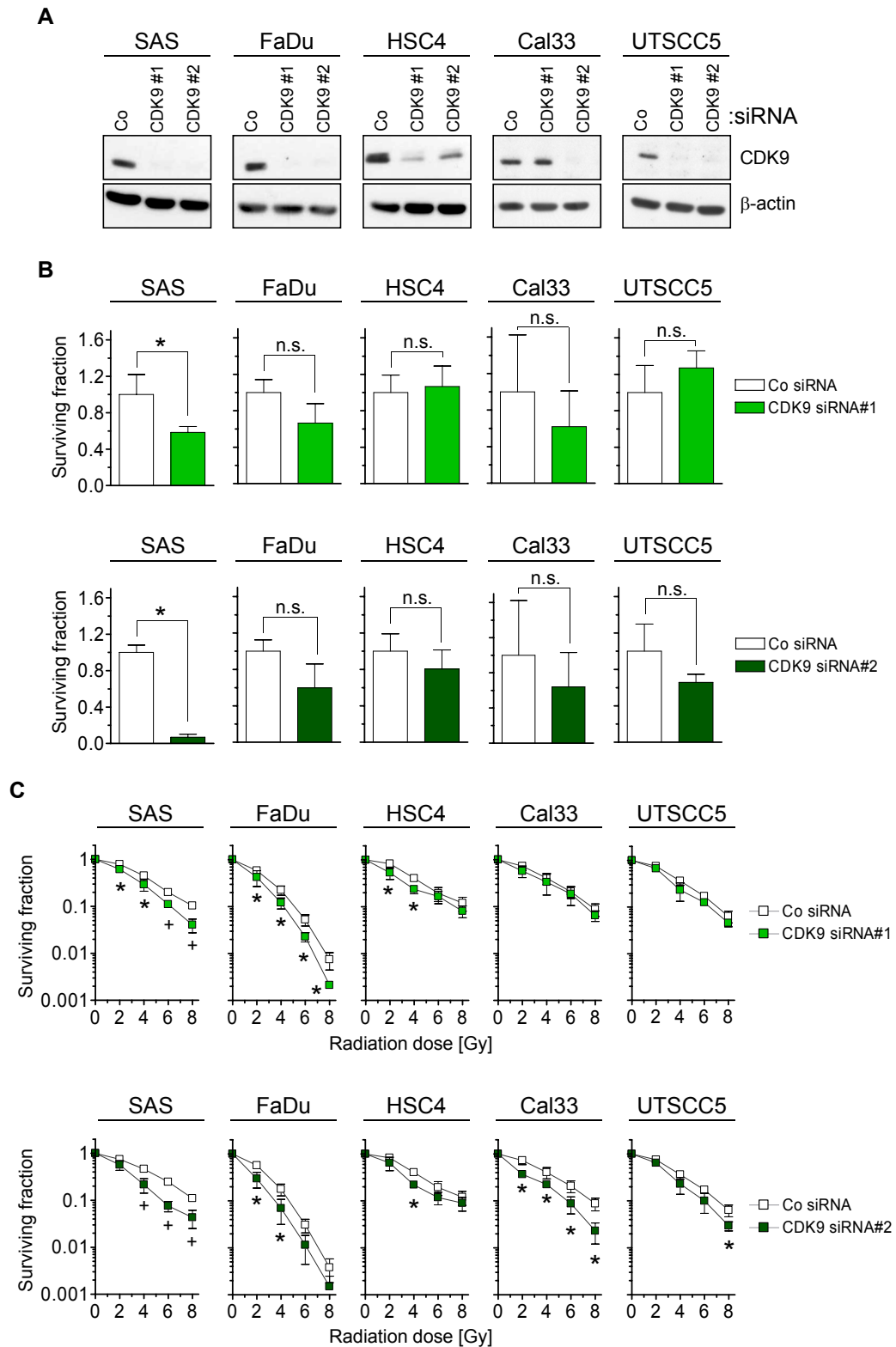
Figure 5.14. CDK9 knockdown modulates the sensitivity of HNSCC cancer cells to X-rays. Cells were transfected (CDK9 siRNA #1, CDK9 siRNA #2; Co siRNA) and plated for colony formation. After 24 h, the plated cells were irradiated with X-rays (0 - 8 Gy, single dose). Formed colonies were counted after 7 - 14 days (cell line dependent). **(A)** Efficient CDK9 depletion was confirmed by Western blotting. β-actin served as loading control. **(B)** Basal survival fraction after CDK9 knockdown. Results show mean ± s.d. (n = 3; student's *t*-test; n.s. not significant; * *P* < 0.05). **(C)** Clonogenic survival of indicated HNSCC cell lines upon CDK9 knockdown. Results show mean ± s.d. (n = 3; student's *t*-test; * *P* < 0.05; + *P* < 0.01).

5.2.2 Depletion of CDK9 contributes to Repair of radiation-induced DSBs in SAS and FaDu cells

Ionising radiation targets DNA and induces DNA damage (Hall & Giaccia, 2006; Han & Yu, 2010). A serious form of radiation-induced DNA damage is DSB which, if not properly repaired, may kill the cell (Shaheen et al., 2011; Symington & Gautier, 2011). In order to investigate whether CDK9 is involved in DNA damage repair of DSBs, we performed γH2AX/53BP1 foci assay to evaluate the number of radiogenic residual DSBs in CDK9-depleted and control SAS and FaDu cell cultures (Figure 5.15A). Our results displayed a significant ($P < 0.05$) increase in the number of residual DSBs in irradiated cells upon CDK9 silencing (Figure 5.15B).
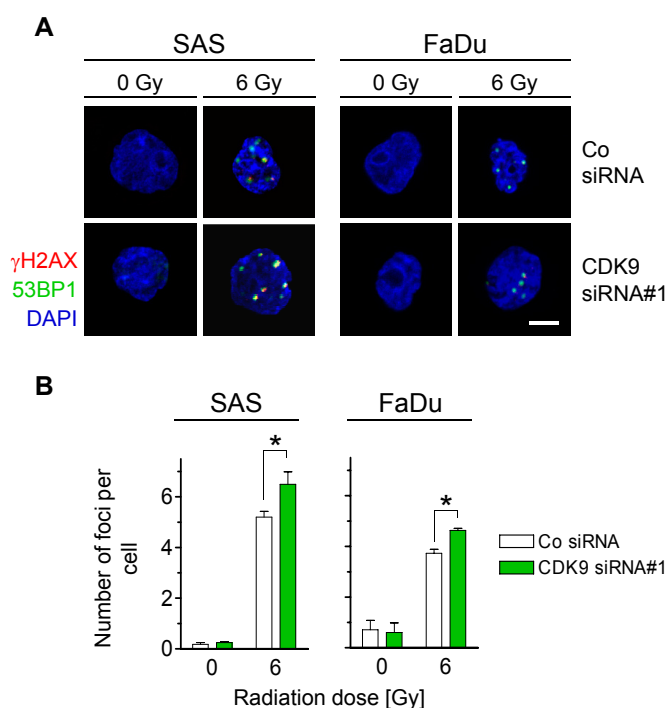

Figure 5.15. CDK9 silencing increases the number of radiation-induced residual DNA DSBs. CDK9 siRNA#1-transfected cells (non-specific siRNA was used as control) were irradiated with X-rays (0 or 6 Gy, single dose). After 24 h, cells were fixed and immunostained against γH2AX and 53BP1. DAPI was used to stain nuclei. Double stained foci from 50 cell nuclei were counted by a fluorescence microscope and defined as residual DSBs. **(A)** Representative images show γH2AX/53BP1 double staining of unirradiated and irradiated CDK9-depleted and control cultures. γH2AX (red), 53BP1 (green), DAPI (blue). Bar, 10 μm. **(B)** Number of γH2AX/53BP1-positive foci per cell of CDK9 knockdown SAS and FaDu cells as compared to controls. Results show mean ± s.d. (n = 3; student's *t*-test; * $P < 0.05$).

To better understand the role of CDK9 in DNA damage repair, we investigated the effect of CDK9 knockdown on the checkpoint signalling and DNA damage repair proteins by Western blotting. In this experiment, we prepared total cell lysates of CDK9 knockdown and control cultures 15 min after irradiation (0 or 6 Gy, X-rays, single dose). Densitometric analysis of Western blot signals of investigated proteins was performed using the ImageJ (Version 1.47g) software, and data were blotted as bar graphs in Figure 5.16B. All

measured data values were normalised to β-actin as loading control, and values of phosphorylation levels of proteins were normalised to total protein levels. We did not observe considerable differences in expression and phosphorylation levels of the investigated proteins including ATM, phospho-ATM(S1981), DNA-PK, CHK2, phospho-CHK2(T86), RAD50, NBS1 and PCNA upon CDK9 knockdown in both non-irradiated and irradiated SAS and FaDu cell cultures (Figure 5.16A, B). These results cannot explain the molecular role of CDK9 in DNA damage repair.
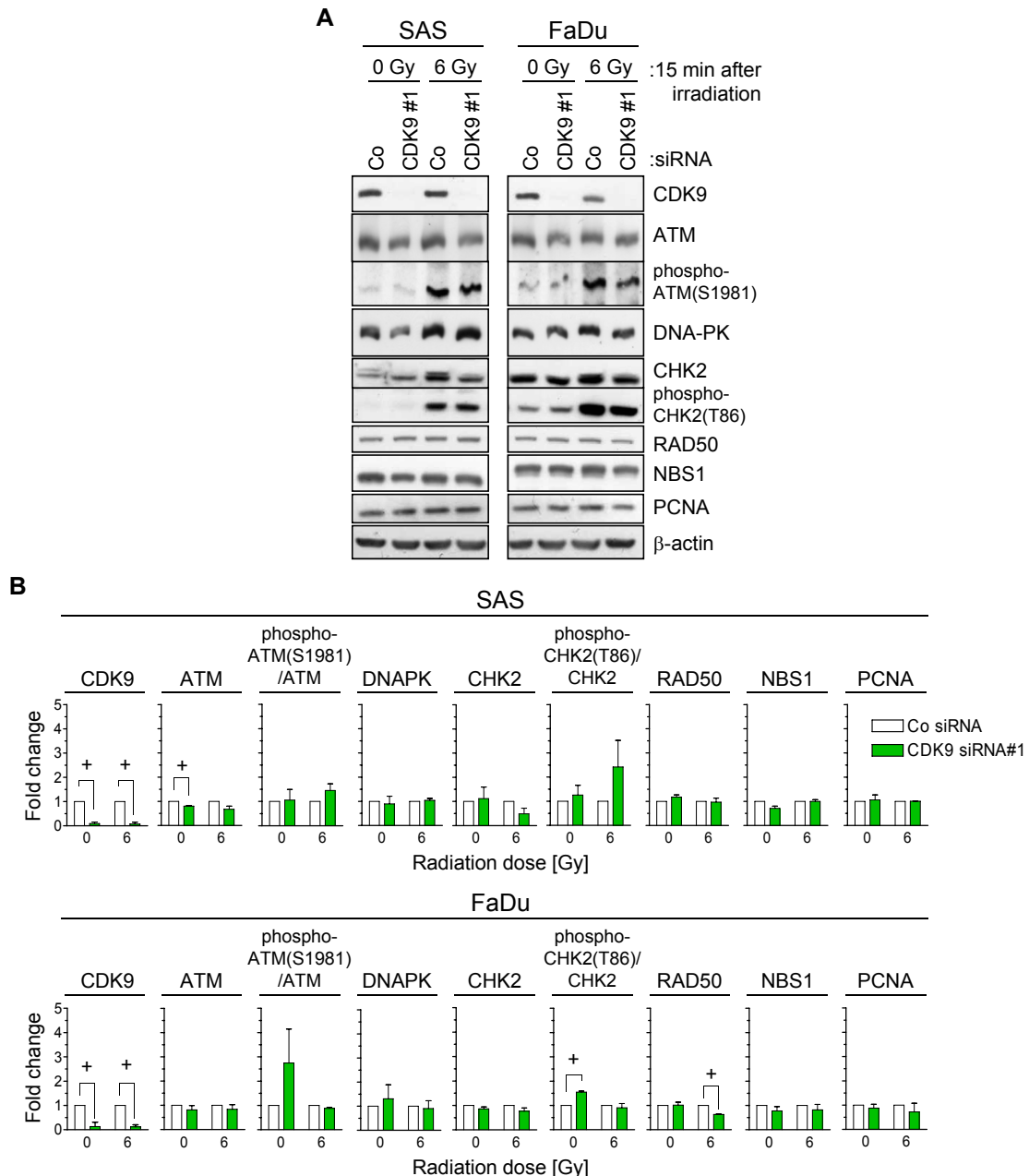
Figure 5.16. Effect of CDK9 depletion on DNA damage repair proteins. (A) Whole cell protein lysates of CDK9 siRNA#1-transfected cell cultures (non-specific siRNA was used as control) harvested 15 min after irradiation (0 or 6 Gy, X-rays, single dose) and analysed by SDS-PAGE and Western blotting. β-actin served as loading control. **(B)** Densitometric values of Western blots of Figure A. Data were normalised to β-actin. Results show mean ± s.d. (n = 2; student's *t*-test; [+] P < 0.01).

5.2.3 CDK9 silencing does not impact Apoptosis in SAS and FaDu Cells

Serious DNA damage, such as DSBs, may induce cell death by activating apoptosis (Ciccia & Elledge, 2010). Because of the increased number of radiogenic residual DSBs upon CDK9 knockdown, we performed apoptosis assay to evaluate whether CDK9 modulates the radiation-induced apoptosis in SAS and FaDu cells. Our results showed very low level of apoptosis in unirradiated as well as irradiated SAS and FaDu control cell cultures. Moreover, we observed that CDK9 depletion has no significant impact on apoptosis in both unirradiated and irradiated cell cultures (Figure 5.17).
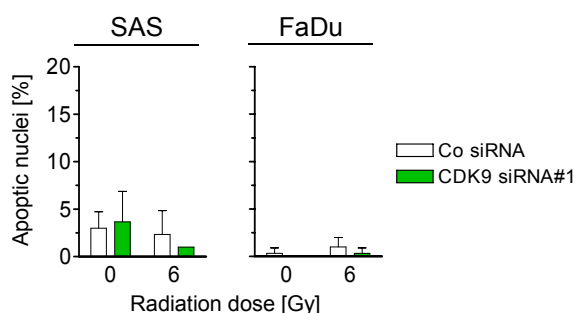
Figure 5.17. Apoptosis in unirradiated and irradiated CDK9 knockdown or control SAS and FaDu cell cultures. CDK9 siRNA#1-transfected cells (non-specific siRNA was used as control) were irradiated with X-rays (0 or 6 Gy, single dose). After 24 h, cells were fixed and stained with DAPI. The number of apoptotic nuclei per 100 cells was counted using a fluorescence microscope. Results show mean ± s.d. (n = 3).

5.2.4 Depletion of CDK9 modulates Cell Cycling in SAS and FaDu Cells

In addition to its well-known role in transcription elongation (Loyer et al., 2005; Malumbres & Barbacid, 2005; Ramanathan et al., 2001; Romano & Giordano, 2008; Zhou et al., 2000), CDK9 is able to phosphorylate the Rb (Simone et al., 2002). The Rb is an important cell cycle regulator through which CDK9 might play a role in cell cycle regulation. Therefore, we performed a cell cycle analysis at different time points following CDK9 knockdown in SAS and FaDu cell cultures. Our data showed that CDK9 knockdown leads to a significant increase ($P < 0.05$) in the G1 phase population (Figure 5.18). In consequence, the S phase population was significantly ($P < 0.05$) decreased. No changes were observed in the G2/M phase population.

In order to investigate whether CDK9 knockdown affects cell cycling in response to irradiation, we analysed the cell cycle of CDK9-depleted and control SAS and FaDu cell cultures 14 h after irradiation with X-rays (0 or 6 Gy, single dose).Our results showed that CDK9 knockdown has no impact on the cell cycle distribution of unirradiated as well as 6 Gy-irradiated SAS and FaDu cell cultures as compared to controls (Figure 5.19).
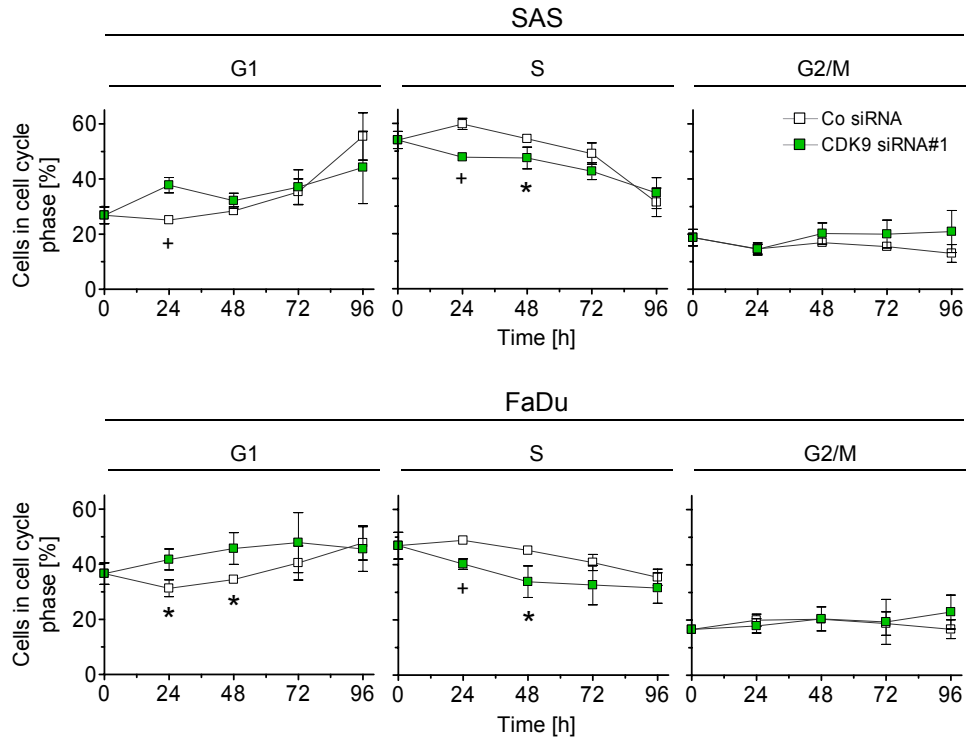
Figure 5.18. Depletion of CDK9 induces changes in cell cycles of SAS and FaDu cells. Cell cycle analysis of CDK9-depleted SAS and FaDu cell cultures as compared to controls. Cells were transfected with CDK9 siRNA#1 (non-specific siRNA was used as control). At indicated time points, cells were pulse-labelled with BrdU and fixed. Cell nuclei were extracted, immunostained with anti-BrdU/FITC and counterstained with PI. Results show mean ± s.d. (n = 3; student's *t*-test; * *P* < 0.05; + *P* < 0.01).
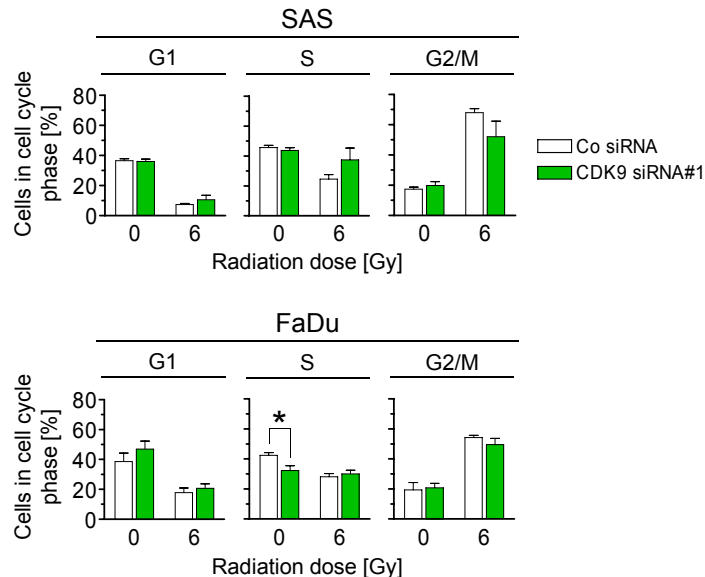
Figure 5.19. CDK9 knockdown does not affect the radiation-induced cell cycle arrest in SAS and FaDu cell cultures. Cell cycle analysis of unirradiated and 6 Gy-irradiated CDK9-depleted SAS and FaDu cell cultures as compared to controls. CDK9 siRNA#1-transfected and control cultures were irradiated with X-rays (0 or 6 Gy, single dose). After 14 h, cells were pulse-labelled with BrdU and fixed. Cell nuclei were extracted, immunostained with anti-BrdU/FITC and counterstained with PI. Results show mean ± s.d. (n = 3; student's *t*-test; * *P* < 0.05).

We next analysed the kinetic of expression and phosphorylation of a panel of cell cycle regulatory proteins as well as expression and phosphorylation of Rpb1-CTD of RNAPII upon CDK9 knockdown using Western blotting (Figure 5.20A). Densitometric analysis of Western blot signals of investigated proteins was performed using the ImageJ (Version 1.47g) software, and data were blotted as graphs in Figure 5.20B. All measured data values were normalised to β-actin as loading control, and values of phosphorylation levels of proteins were normalised to total protein levels. In parallel with the depletion of CDK9, we observed a rapid decline in the level of Cyclin D1, an induction in the level of Cyclin E and a slight reduction in the phosphorylation of Rb at residue S795 as compared to controls in both SAS and FaDu cell lines. However, no changes were observed on the levels of Rb, Rpb1-CTD or phospho-Rpb1-CTD(S2/5). These data suggests that CDK9 plays a role in the regulation of cell cycling in SAS and FaDu cell lines.

## 5.2.5 Characterisation of SAS-CDK9-EGFP and SAS-EGFP Transfectants

We showed that CDK9 knockdown is associated with increased radiosensitivity in SAS, FaDu, HSC4, Cal33 and UTSCC5 HNSCC cell lines (Figure 5.14). To better understand the possible role of CDK9 in the radiation response of cancer cells, we generated a SAS-CDK9-EGFP cell line by stable transfection of SAS cells with the hCDK9-pEGFP-N1 plasmid. Empty vector (pEGFP-N1) stably transfected cells (SAS-EGFP) were also generated and used as control.

To confirm CDK9-EGFP and EGFP expression, SAS-CDK9-EGFP and SAS-EGFP cell lines were subjected to microscopic analysis (Figure 5.21A). In addition, Western blot analysis showed that SAS-CDK9-EGFP cells express both the exogenous CDK9-EGFP fusion protein as well as the endogenous CDK9 protein (Figure 5.21B).

5.2.6 Ectopic Expression of CDK9 leads to radioresistance in SAS Cells

To better understand the role of CDK9 in the cellular radiation response, we performed colony formation assays using SAS-CDK9-EGFP cells (SAS-EGFP cells were used as control) to evaluate the effect of ectopic overexpression of CDK9 on the clonogenic radiation survival. Our results showed that exogenous expression of CDK9-EGFP in SAS cells is associated with a significantly ($P < 0.05$) increased basal survival (Figure 5.22A) as well as a significant ($P < 0.05$) increase in the clonogenic radiation survival of cells at high radiation dose (Figure 5.22B).
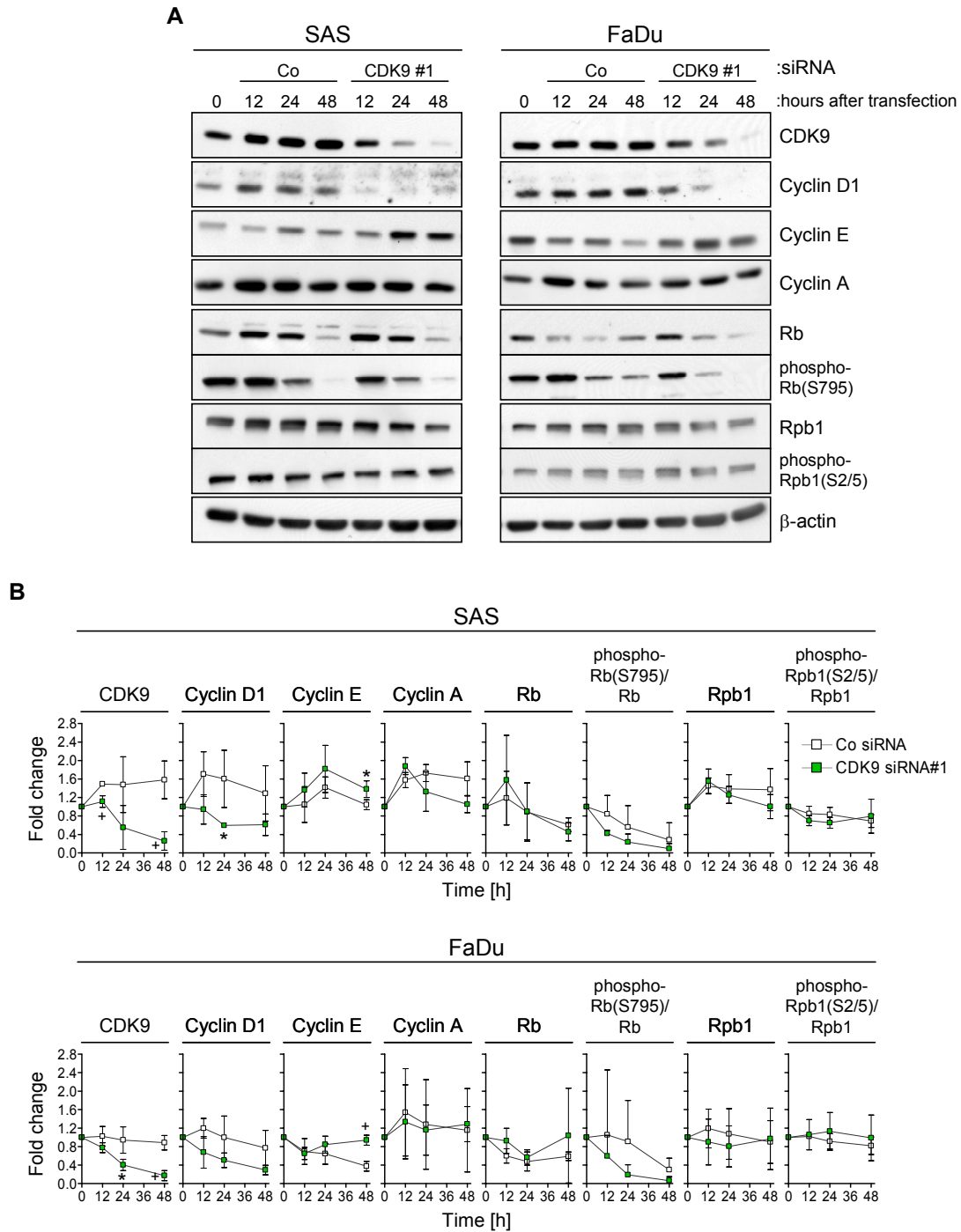
Figure 5.20. Protein analysis affirms a possible role for CDK9 on cell cycle regulation. CDK9 siRNA#1-transfected cell cultures (non-specific siRNA was used as control) were irradiated (0 or 6 Gy, X-rays, single dose), lysed in modified RIPA lysis buffer at indicated time points and analysed by SDS-PAGE and Western blotting. **(A)** Western blots for proteins regulate cell cycle and transcription. β-actin served as loading control. **(B)** Densitometric analysis of Western blots in Figure A. Data was normalised to 0 h values. Results show mean ± s.d. (n = 3; student's t-test; * $P < 0.05$; + $P < 0.01$).

A

| | EGFP | DAPI | Merge |

B
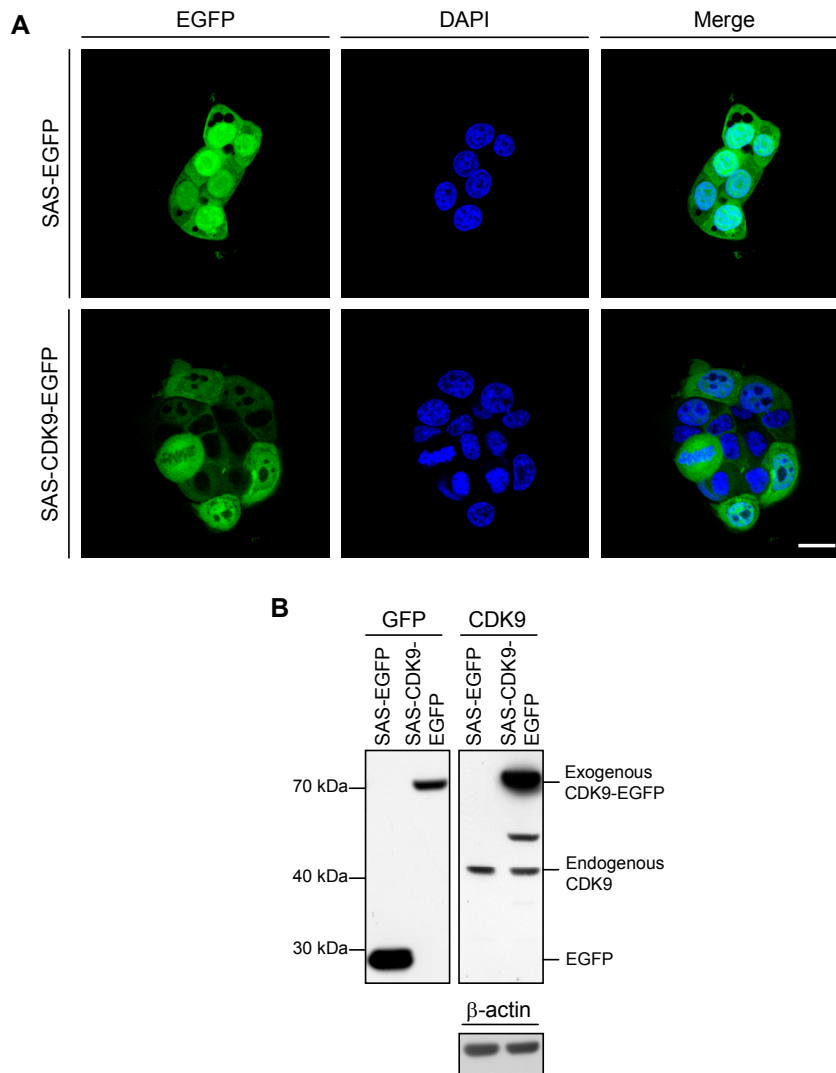
Figure 5.21. Expression and localisation of CDK9-EGFP in SAS transfectants. SAS-CDK9-EGFP and SAS-EGFP cells were generated by stable transfection of SAS cells with hCDK9-pEGFP-N1 or pEGFP-N1 plasmids respectively. **(A)** Fluorescence images of EGFP and CDK9-EGFP (green) expressing cells. Cell nuclei were stained with DAPI (blue). Bar, 20 µm. **(B)** Western blots of EGFP and CDK9 in EGFP and CDK9-EGFP transfectants. β-actin served as loading control.
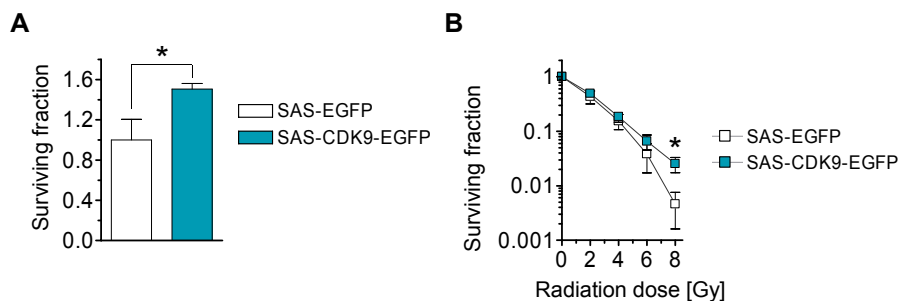
Figure 5.22. Exogenous expression of CDK9 induces radioresistance in SAS cells. SAS-CDK9-EGFP and SAS-EGFP (as control) transfectants were plated for colony formation and irradiated after 24 h with X-rays (0 - 8 Gy, single dose). After 7 days, formed colonies were microscopically counted. **(A)** Basal survival fraction of unirradiated cell cultures. Results show mean ± s.d. (n = 3; student's t-test; * P < 0.05). **(B)** Clonogenic radiation survival of SAS-CDK9-EGFP and SAS-EGFP cells. Results show mean ± s.d. (n = 3; student's t-test; * P < 0.05).

6 Discussion

Among other hallmarks (Hanahan & Weinberg, 2011), tumour cells are characterised by uncontrolled proliferation resulting from mutations in proto-oncogenes or tumour suppressor genes as well as environmental factors (Baumann et al., 2008; Burkhart & Sage, 2008; Finlay et al., 1989; Hahn & Weinberg, 2002; Hanahan & Weinberg, 2000; Hanahan & Weinberg, 2011; Jacks & Weinberg, 2002; Karnoub & Weinberg, 2008; Lodish et al., 2000b; Lu et al., 2012; Sandfort et al., 2007; Vogelstein & Kinzler, 2004). This allows cancer cells to escape cell death in response to potentially lethal damage and renders cells more resistant to standard cancer treatments such as radio- and chemotherapies (Hanahan & Weinberg, 2000; Johnstone et al., 2002). Disregulated activity of CDKs is common in many human cancers (Malumbres & Barbacid, 2001; Malumbres & Barbacid, 2009). Therefore, CDKs are regarded as potential targets for cancer therapy.

6.1 CDK2 Targeting enhances the Radiosensitivity of HNSCC Cancer Cells

CDK2 regulates important cellular events such as the G1/S phase transition, S phase progression, cell cycle checkpoints and apoptosis (Aleem et al., 2004; Deans et al., 2006; Kaldis & Aleem, 2005; Neganova et al., 2011; Satyanarayana & Kaldis, 2009b; Sherr & Roberts, 2004; Soffar et al., 2013). In addition, overexpression of CDK2 was found to be correlated with poorer prognosis and overall survival in head and neck cancers (Dong et al., 2001; Mihara et al., 2001; Shintani et al., 2002), ovarian cancer (Sui et al., 2001) and melanoma (Tang et al., 1999). Therefore, understanding the possible role of CDK2 in radiation response might be of utmost importance for advancement of anticancer therapies. In this study, we evaluated the significance of CDK2 for the cellular radiation response of MEFs as well as HNSCC cell lines (SAS, FaDu, HSC4, Cal33, UTSCC5 and UTSCC8). In order to address the role of CDK2, we performed a series of experiments to measure several key parameters such as clonogenic radiation survival, DNA damage repair, apoptosis and cell cycling (Soffar et al., 2013).

We showed that:
1. CDK2 deficiency is associated with increased cellular radiosensitivity in MEFs.
2. Loss of CDK2 in MEFs attenuates radiogenic DSBs repair.

3. CDK2 deficiency in MEFs correlates with higher radiation-induced G2/M arrest.

4. CDK2 knockdown enhances the radiosensitivity of 2D HNSCC cell cultures.

5. Silencing of CDK2 curbs radiogenic DSB repair in SAS and FaDu cells.

6. Depletion of CDK2 does not affect apoptosis in 0 and 6 Gy-irradiated SAS and FaDu cell cultures.

7. CDK2 knockdown has no impact on cell cycle distribution of unirradiated as well as irradiated SAS and FaDu cell cultures.

8. Silencing of CDK2 does not alter the radiosensitivity of SAS and FaDu cell cultures under 3D growth conditions.

Our results from the colony formation assays showed that loss of CDK2 is associated with increased cellular radiosensitivity of MEFs. In accordance, Satyanarayana and colleagues reported increased radiosensitivity in CDK2$^{-/-}$ mice relative to WT mice (Satyanarayana et al., 2008). A possible key factor in the cellular radiation survival is the efficiency of DNA damage repair (Chavaudra et al., 2004; Hedman, 2012). Therefore, we investigated the number of radiogenic residual DSBs, and found that CDK2$^{-/-}$ MEFs accumulates more radiogenic residual DSBs as compared to WT MEFs. These findings suggest a possible role of CDK2 in DNA damage repair of DSBs. Similar findings were reported by Satyanarayana and colleagues (Satyanarayana et al., 2008). In addition, a recent study suggested that treatment of A549 cells with *R*-Roscovitine, a small molecule CDK inhibitor, decreases their ability to repair DNA damage in a CDK2-dependent manner (Federico et al., 2010). Furthermore, Müller-Tidow and colleagues reported that Cyclin A1 plays a CDK2-mediated role in DSB repair (Muller-Tidow et al., 2004).

Another possible factor that might affect cellular radiation survival of cells is cell cycling and cell cycle checkpoint regulation. Our cell cycle profiles revealed a higher S phase population in CDK2$^{-/-}$ MEFs as compared to WT MEFs suggesting compromised S phase progression or S/G2 phase transition. In addition, our results showed a rapid radiation-induced G2/M arrest in both CDK2$^{-/-}$ and WT MEFs that peaks 10 h after irradiation. However, 24 h after irradiation, both CDK2$^{-/-}$ and WT MEFs displayed a slight increase in the G1 phase population which probably resulted from the release of cells from the G2/M arrest. Interestingly, comparing the cell cycle profiles of CDK2$^{-/-}$ MEFs to WT MEFs 10 h after irradiation revealed that the absence of CDK2 contributes to higher accumulation of cells in the G2/M phase. The increase in G2/M phase population in response to ionising radiation together with the elevated number of radiogenic residual DSBs in CDK2$^{-/-}$ MEFs as compared to WT MEFs suggest a possible disruption of DNA damage repair capacity in the absence of CDK2 (Satyanarayana et al., 2008).

Taken together, our findings suggest that CDK2 contributes to increased radiosensitivity of MEFs via modulating DNA damage repair and G2/M checkpoint response.

Based on our finding in MEFs, we hypothesised that CDK2 targeting improves cancer cell response to radiotherapy. Therefore, we investigated CDK2 as a potential cancer target in human HNSCC cell lines. In 2D colony formation assays, depletion of CDK2 clearly enhanced the radiosensitivity of SAS and FaDu cell lines. The other tested four HNSCC cell lines showed a non-significant radiosensitising trend upon CDK2 depletion. Concurrently, knockdown of CDK2 increased the number of radiation-induced residual DSBs in comparison to controls, which indicates a possible role of CDK2 in DNA damage repair in SAS and FaDu HNSCC cancer cells. Similarly, previous studies suggested that DSB repair function depends on CDK2 activity (Muller-Tidow et al., 2004; Satyanarayana et al., 2008). Moreover, recent reports indicated that CDK2 is a specific requirement for the DNA damage repair response, and that other CDKs, such as CDK1, might be unable to compensate the DNA repair functions of CDK2 in human cells (Satyanarayana & Kaldis, 2009b; Wohlbold et al., 2012). Despite elevated DSB levels, we did not observe a clear impact of CDK2 depletion on the expression and phosphorylation levels of DNA damage repair proteins. These results cannot explain how CDK2 mediates DNA damage repair and further studies are warranted to clarify this issue. Several studies reported a possible role of CDK2 in promoting apoptosis (Berthet et al., 2007; Hiromura et al., 2002; Maddika et al., 2008). However, we did not observe any signs of apoptosis as a consequence of CDK2 depletion in SAS and FaDu cancer cells. In accordance with our findings, Edamatsu and colleagues reported that treatment of CEM leukemic cells with Roscovitine does not induce apoptosis (Edamatsu et al., 2000).

As a next step, we investigated the cell cycle regulation and checkpoint response upon CDK2 knockdown plus/minus irradiation. Despite the typical radiation-induced G2/M arrest of untreated SAS and FaDu cells, knockdown of CDK2, as a single treatment or in combination with irradiation, had no impact on the cell cycle profiles of unirradiated as well as irradiated SAS and FaDu cells. These results suggest that the activity of CDK2 is dispensable for cell cycle progression and radiation-induced cell cycle arrest in SAS and FaDu cell lines. However, these findings are in contrast to our results in MEFs suggesting that CDK2 plays a more prominent role in cell cycling of MEFs than in HNSCC cells. Also, the difference in gene inhibition should be taken into consideration with a complete and stable gene knockout in MEFs and an almost complete and transient knockdown in HNSCC cells. Additionally, other CDK/Cyclin complexes may have the ability to compensate for the absence of CDK2 particularly under knockdown conditions (Aleem et al., 2005; Berthet et al., 2003; Cai et al., 2006; Ortega et al., 2003). We revealed, in

Western blot protein analysis, elevated levels of Cyclin D1 (in both SAS and FaDu cells) and Cyclin E (in SAS cells) upon CDK2 silencing. Similarly, Cai and colleageous reported an elevated Cyclin D level in NCI-H1299 and UTOS clones engineered to constitutively express CDK2 shRNA. Moreover, these clones also showed no apparent change in cell cycling (Cai et al., 2006). The elevated levels of the CDK inhibitor p27 may be attributed to the decreased CDK2 activity upon knockdown of CDK2 (Lacher et al., 2010; Li et al., 2011; Rodriguez-Ubreva et al., 2009). Intriguingly, no changes were observed in the phosphorylation of Rb protein, the main substrate of CDK2/Cyclin complexes, following knockdown of CDK2. This observation suggests a possible compensation of CDK2 kinase activity by other CDKs such as CDK1 which, in the absence of CDK2, is able to form complexes with Cyclin E and drive cells via the G1/S phase transition (Aleem et al., 2005; Kaldis & Aleem, 2005). CDK4 was also found to be able to phosphorylate the Rb even at CDK2 preferred phosphorylation sites (Tetsu & McCormick, 2003). Cyclin D1 binds to and activates CDK4 (Matsushime et al., 1994; Sherr, 1995; Sherr & Roberts, 2004). Therefore, the elevated Cyclin D1 and Cyclin E levels upon CDK2 knockdown might contribute to increased activities of CDK4 and CDK1 respectively that compensate for the absence of CDK2 activity (Aleem et al., 2005; Cai et al., 2006; Kaldis & Aleem, 2005; Tetsu & McCormick, 2003).

In short, our results suggest that CDK2 is dispensable for cell cycle progression and radiation-induced checkpoint response in SAS and FaDu cells. Subsequently, the elevated CDK2 knockdown-mediated radiosensitivity in SAS and FaDu cells is probably related to the impaired DNA repair (Satyanarayana et al., 2008).

Finally, we used a 3D lrECM based colony formation assay to stress the need of CDK2 for cellular radiation survival. This model is widely employed to investigate the possible role of cell-matrix interactions on the sensitivity of cancer cells to radio- and chemotherapy (Eke & Cordes, 2011; Eke et al., 2013; Hehlgans et al., 2012; Storch et al., 2010; Zschenker et al., 2012). Importantly, several studies reported that 3D ECM based cell culture models better mimic in vivo growth conditions than conventional 2D cell culture systems (Cordes et al., unpublished data; Eke et al., 2013; Kenny et al., 2007; Cordes et al., unpublished data, Lee et al., 2007; Pampaloni et al., 2007; Storch et al., 2010; Xu et al., 2009). Intriguingly, depletion of CDK2 failed to modulate the radiation survival of SAS and FaDu cancer cells cultured in a more physiologically 3D microenvironment indicating a non-essential role of CDK2 in the cellular radiation response of cells under 3D growth conditions. Further studies are warranted to explain why CDK2 is dispensable for the radiation survival of cells under 3D growth condition.

6.2 CDK9 regulates the Radiosensitivity, DNA Damage Repair and Cell Cycle of HNSCC Cancer Cells

DNA damage repair is the main priority of cells in response to genetic stress. The efficiency of DNA repair is crucial for the cellular response to genotoxic treatment such as radiotherapy. Recently, Yu and colleagues reported that CDK9 plays a role in maintaining the genomic integrity in response to replication stress and promotes recovery from replication arrest (Yu et al., 2010). Such functions are necessary for cancer cell survival after radiation-induced genomic damage. Therefore, we investigated the possible role of CDK9 in the radiation response of HNSCC cell lines via the measurement of key parameters such as clonogenic radiation survival, DNA damage repair, apoptosis and cell cycling.

In this study, we displayed that:

1. CDK9 knockdown mediates increased cellular radiosensitivity of HNSCC cancer cells.
2. Depletion of CDK9 attenuates the repair of radiogenic DSBs in SAS and FaDu cells.
3. Silencing of CDK9 has no impact on apoptosis in SAS and FaDu cells.
4. Knockdown of CDK9 modulates cell cycling in SAS and FaDu cells.
5. Ectopic CDK9 expression confers radioresistance in SAS cells.

We showed that depletion of CDK9 radiosensitises HNSCC cancer cells in a cell line dependent manner. As DSBs are considered a key determinant of cell survival in response to genotoxic stress (Shaheen et al., 2011; Symington & Gautier, 2011), we investigated the number of radiogenic residual DSBs upon CDK9 knockdown. Our data showed that silencing of CDK9 perturbs the repair of radiation-induced residual DSBs in SAS and FaDu cells. This indicates a possible role of CDK9 in DNA damage repair which may correlates with the enhanced radiosensitivity of cells upon depletion of CDK9 (Eke et al., 2007; Morawska, 2012; Rothkamm & Lobrich, 2003).

CDK9 is the catalytic part of pTEFb which stimulates transcription elongation by phosphorylating Rpb1-CTD of RNAPII (Loyer et al., 2005; Malumbres & Barbacid, 2005; Ramanathan et al., 2001; Romano & Giordano, 2008; Zhou et al., 2000). Previous studies reported a possible selective regulatory role of CDK9 on the expression of a restricted subset of genes instead of the expression of most genes by RNAPII (Garriga et al., 2010). Therefore, it is possible that CDK9 may specifically regulate one or more DNA damage response proteins. Consequently, we performed Western blot analysis in unirradiated and

irradiated CDK9-depleted and control SAS and FaDu cultures. We did not observe any critical changes in the expression or phosphorylation of DNA damage repair and checkpoint proteins. Our findings are in agreement with a previous study showed that depletion of CDK9 did not significantly upregulate or downregulate the DNA damage response genes in genome-wide expression analysis (Yu & Cortez, 2011). These findings cannot explain how CDK9 modulates the DNA damage repair of DSBs. Further investigations are required to clarify the role of CDK9 in DNA damage repair. Several studies suggested that CDK9 inhibition induces apoptosis in osteosarcoma, multiple myeloma and non-small cell lung cancer cells (Cai et al., 2006; Gojo et al., 2002). However, we could not observe any induction in apoptosis following CDK9 depletion in both SAS and FaDu HNSCC cells.

Our cell cycle analysis revealed that depletion of CDK9 delays cell cycle transition, which was indicated by an elevated G1-phase and declined S phase cell population. Similarly, Cai and colleagues reported that reduction of CDK9 activity was associated with changes in cell cycle distribution that were consistent with cell cycle delay (Cai et al., 2006). The S phase retardation after CDK9 silencing seems to be a consequence of the accumulation of cells in the G1 phase. Mammalian cells exhibit variation in their response to irradiation as they move through the cell cycle. Cells in the G2/M phase are the most radiosensitive while cells in the G1 phase show only moderate radiosensitivity (Sinclair & Morton, 1966). The S phase cell population is more radioresistant than cells in any other cell cycle phase (Sinclair & Morton, 1966). Accordingly, the retardation of S phase population might contribute to the enhanced radiosensitivity of cancer cells upon CDK9 knockdown.

On the molecular level, Rb is a known substrate for CDK9 (Simone et al., 2002). Therefore, it is not surprising that Rb was found to be hypophosphorylated after silencing of CDK9. In addition, CDK9 depletion was associated with a remarkable decrease in Cyclin D1 level in SAS and FaDu cells. Cyclin D1-dependent kinase activity promotes G1 phase progression by phosphorylating and inactivating Rb (Kato et al., 1993; Lundberg & Weinberg, 1998; Weinberg, 1995). Thus, the reduction of Cyclin D1 level might also contribute to hypophsphrylation of Rb. Moreover, because of the central role of Rb in cell cycle progression especially during the G1 phase, the observed cell cycle changes (the elevated G1 phase and decreased S phase populations) after CDK9 knockdown seems to be attributed to the hypophosphorylation of Rb (Cai et al., 2006; Zhang et al., 2008). In contrary with Cyclin D1, the level of Cyclin E, another G1 phase Cyclin, was elevated after CDK9 depletion which probably is an attempt of the cell to tune the cell cycle disturbance in response to the suppression of Cyclin D1-dependent kinase activity (Bowe et al., 2002).

Despite the well-known role of CDK9 in phosphorylating the Rpb1-CTD of RNAPII on S2 and S5 residues (Loyer et al., 2005; Malumbres & Barbacid, 2005; Palancade & Bensaude, 2003; Ramanathan et al., 2001; Romano & Giordano, 2008; Zhou et al., 2000), we unexpectedly did not observe any changes in the phosphorylation of Rpb1-CTD (S2/5) after depletion of CDK9. Several reports revealed that other CDKs, such as CDK12 and CDK13, regulate the transcription elongation by phosphorylating the Rpb1-CTD (Bartkowiak et al., 2010; Blazek et al., 2011). This may explain why CDK9 was negligible for Rpb1-CTD phosphorylation but cannot explain the CDK9-related changes in expression of Cyclin D1 and Cyclin E.

To better address the role of CDK9 in radiation response, we stably transfected SAS cells with CDK9-EGFP (hCDK9-pEGFP-N1 plasmid) or EGFP (pEGFP-N1 plasmid) constructs. Our results showed that ectopic expression of CDK9 confers radioresistance in SAS cells at high irradiation dose. This finding together with our previous findings upon CDK9 knockdown suggest a crucial role of CDK9 in the cellular response of HNSCC cells to ionising radiation. Further examinations are required to better understand this role on the molecular level and its consequences for DNA damage repair and cell cycle regulation.

7   Summary and Conclusion

Here, we revealed the possible roles of CDK2 and CDK9 in the response of HNSCC cancer cells to radiotherapy. Due to the lack of highly selective pharmacological inhibitors against CDK2 and CDK9, we employed siRNA interference technology to achieve selective depletion of these proteins. In order to achieve our goal, we performed a series of experiments to measure several key parameters such as clonogenic radiation survival, DNA damage repair, apoptosis and cell cycling

We found that loss of CDK2 radiosensitises MEFs as well as HNSCC 2D cell cultures. However, under more physiological 3D lrECM growth conditions, targeting of CDK2 failed to modulate the radiosensitivity of HNSCC cells. In addition, loss of CDK2 attenuated the repair of radiogenic DSBs in MEFs as well as SAS and FaDu cells indicating a possible role of CDK2 in DNA damage repair. Moreover, we found that CDK2 is dispensable for cell cycle and checkpoint regulation in SAS and FaDu cells. Taken together, these results suggest that targeting of CDK2 may not provide a therapeutic benefit to overcome HNSCC cell resistance to radiotherapy.

We also showed that depletion of CDK9 clearly enhances the radiosensitivity of HNSCC 2D cultures. In addition, the ectopic expression of CDK9 had a radioprotective effect on SAS cells. These findings suggest a critical role of CDK9 in the radiation response of HNSCC cells. Moreover, our results indicate a possible role of CDK9 in the DNA damage repair response and cell cycling of HNSCC cells. Conclusively, targeting of CDK9 might be a viable strategy to overcome cancer cell resistance to radiotherapy.

Future investigations are warranted to elucidate the role of CDK9 in cancer cell response to irradiation under 3D growth conditions and *in vivo* models, as well as other tumour entities.

List of Figures

List of Tables

References

Abraham, R.T. (2001). Cell cycle checkpoint signaling through the ATM and ATR kinases. *Genes Dev*, **15,** 2177-96.

Ahnesorg, P., Smith, P. & Jackson, S.P. (2006). XLF interacts with the XRCC4-DNA ligase IV complex to promote DNA nonhomologous end-joining. *Cell*, **124,** 301-13.

Akoulitchev, S., Chuikov, S. & Reinberg, D. (2000). TFIIH is negatively regulated by cdk8-containing mediator complexes. *Nature*, **407,** 102-6.

Aleem, E., Berthet, C. & Kaldis, P. (2004). Cdk2 as a master of S phase entry: fact or fake? *Cell Cycle*, **3,** 35-7.

Aleem, E. & Kaldis, P. (2006). Mouse models of cell cycle regulators: new paradigms. *Results Probl Cell Differ*, **42,** 271-328.

Aleem, E., Kiyokawa, H. & Kaldis, P. (2005). Cdc2-cyclin E complexes regulate the G1/S phase transition. *Nat Cell Biol*, **7,** 831-6.

Aprelikova, O., Xiong, Y. & Liu, E.T. (1995). Both p16 and p21 families of cyclin-dependent kinase (CDK) inhibitors block the phosphorylation of cyclin-dependent kinases by the CDK-activating kinase. *J Biol Chem*, **270,** 18195-7.

Arbes, S.J., Jr., Olshan, A.F., Caplan, D.J., Schoenbach, V.J., Slade, G.D. & Symons, M.J. (1999). Factors contributing to the poorer survival of black Americans diagnosed with oral cancer (United States). *Cancer Causes Control*, **10,** 513-23.

Argiris, A., Brockstein, B.E., Haraf, D.J., Stenson, K.M., Mittal, B.B., Kies, M.S., Rosen, F.R., Jovanovic, B. & Vokes, E.E. (2004). Competing causes of death and second primary tumors in patients with locoregionally advanced head and neck cancer treated with chemoradiotherapy. *Clin Cancer Res*, **10,** 1956-62.

Bakkenist, C.J. & Kastan, M.B. (2003). DNA damage activates ATM through intermolecular autophosphorylation and dimer dissociation. *Nature*, **421,** 499-506.

Banin, S., Moyal, L., Shieh, S., Taya, Y., Anderson, C.W., Chessa, L., Smorodinsky, N.I., Prives, C., Reiss, Y., Shiloh, Y. & Ziv, Y. (1998). Enhanced phosphorylation of p53 by ATM in response to DNA damage. *Science*, **281,** 1674-7.

Bartek, J. & Lukas, J. (2007). DNA damage checkpoints: from initiation to recovery or adaptation. *Curr Opin Cell Biol*, **19,** 238-45.

References

Bartkowiak, B., Liu, P., Phatnani, H.P., Fuda, N.J., Cooper, J.J., Price, D.H., Adelman, K., Lis, J.T. & Greenleaf, A.L. (2010). CDK12 is a transcription elongation-associated CTD kinase, the metazoan ortholog of yeast Ctk1. *Genes Dev*, **24,** 2303-16.

Bartova, I., Otyepka, M., Kriz, Z. & Koca, J. (2004). Activation and inhibition of cyclin-dependent kinase-2 by phosphorylation; a molecular dynamics study reveals the functional importance of the glycine-rich loop. *Protein Sci*, **13,** 1449-57.

Baskar, R., Lee, K.A., Yeo, R. & Yeoh, K.W. (2012). Cancer and radiation therapy: current advances and future directions. *Int J Med Sci*, **9,** 193-9.

Baumann, M., Cordes, N., Haase, M. & Zips, D. (2008). Molecular Cancer and Radiation Biology. In *Perez and Brady's Principles and Practice of Radiation Oncology*, Halperin, E.C., Perez, C.A. & Brady, L.W. (eds). Wolters Kluwer Health/Lippincott Williams & Wilkins.

Baumli, S., Hole, A.J., Wang, L.Z., Noble, M.E. & Endicott, J.A. (2012). The CDK9 tail determines the reaction pathway of positive transcription elongation factor b. *Structure*, **20,** 1788-95.

Baumli, S., Lolli, G., Lowe, E.D., Troiani, S., Rusconi, L., Bullock, A.N., Debreczeni, J.E., Knapp, S. & Johnson, L.N. (2008). The structure of P-TEFb (CDK9/cyclin T1), its complex with flavopiridol and regulation by phosphorylation. *Embo J*, **27,** 1907-18.

Berkovich, E., Monnat, R.J., Jr. & Kastan, M.B. (2007). Roles of ATM and NBS1 in chromatin structure modulation and DNA double-strand break repair. *Nat Cell Biol*, **9,** 683-90.

Berthet, C., Aleem, E., Coppola, V., Tessarollo, L. & Kaldis, P. (2003). Cdk2 knockout mice are viable. *Curr Biol*, **13,** 1775-85.

Berthet, C., Rodriguez-Galan, M.C., Hodge, D.L., Gooya, J., Pascal, V., Young, H.A., Keller, J., Bosselut, R. & Kaldis, P. (2007). Hematopoiesis and thymic apoptosis are not affected by the loss of Cdk2. *Mol Cell Biol*, **27,** 5079-89.

Blazek, D., Kohoutek, J., Bartholomeeusen, K., Johansen, E., Hulinkova, P., Luo, Z., Cimermancic, P., Ule, J. & Peterlin, B.M. (2011). The Cyclin K/Cdk12 complex maintains genomic stability via regulation of expression of DNA damage response genes. *Genes Dev*, **25,** 2158-72.

Bohgaki, T., Bohgaki, M. & Hakem, R. (2010). DNA double-strand break signaling and human disorders. *Genome Integr*, **1,** 15.

Boonstra, J. & Post, J.A. (2004). Molecular events associated with reactive oxygen species and cell cycle progression in mammalian cells. *Gene*, **337,** 1-13.

Bowe, D.B., Kenney, N.J., Adereth, Y. & Maroulakou, I.G. (2002). Suppression of Neu-induced mammary tumor growth in cyclin D1 deficient mice is compensated for by cyclin E. *Oncogene*, **21,** 291-8.

References

Bres, V., Yoh, S.M. & Jones, K.A. (2008). The multi-tasking P-TEFb complex. *Curr Opin Cell Biol*, **20,** 334-40.

Bristow, R.G. & Hill, R.P. (2008). Hypoxia and metabolism. Hypoxia, DNA repair and genetic instability. *Nat Rev Cancer*, **8,** 180-92.

Brock, W.A. & Williams, M. (1985). Kinetics of micronucleus expression in synchronized irradiated Chinese hamster ovary cells. *Cell Tissue Kinet*, **18,** 247-54.

Bruno, T., De Nicola, F., Iezzi, S., Lecis, D., D'Angelo, C., Di Padova, M., Corbi, N., Dimiziani, L., Zannini, L., Jekimovs, C., Scarsella, M., Porrello, A., Chersi, A., Crescenzi, M., Leonetti, C., Khanna, K.K., Soddu, S., Floridi, A., Passananti, C., Delia, D. & Fanciulli, M. (2006). Che-1 phosphorylation by ATM/ATR and Chk2 kinases activates p53 transcription and the G2/M checkpoint. *Cancer Cell*, **10,** 473-86.

Burkhart, D.L. & Sage, J. (2008). Cellular mechanisms of tumour suppression by the retinoblastoma gene. *Nat Rev Cancer*, **8,** 671-82.

Burki, H.J. (1980). Ionizing radiation-induced 6-thioguanine-resistant clones in synchronous CHO cells. *Radiat Res*, **81,** 76-84.

Byrd, J.C., Lin, T.S., Dalton, J.T., Wu, D., Phelps, M.A., Fischer, B., Moran, M., Blum, K.A., Rovin, B., Brooker-McEldowney, M., Broering, S., Schaaf, L.J., Johnson, A.J., Lucas, D.M., Heerema, N.A., Lozanski, G., Young, D.C., Suarez, J.R., Colevas, A.D. & Grever, M.R. (2007). Flavopiridol administered using a pharmacologically derived schedule is associated with marked clinical efficacy in refractory, genetically high-risk chronic lymphocytic leukemia. *Blood*, **109,** 399-404.

Cai, D., Latham, V.M., Jr., Zhang, X. & Shapiro, G.I. (2006). Combined depletion of cell cycle and transcriptional cyclin-dependent kinase activities induces apoptosis in cancer cells. *Cancer Res*, **66,** 9270-80.

Canavese, M., Santo, L. & Raje, N. (2012). Cyclin dependent kinases in cancer: potential for therapeutic intervention. *Cancer Biol Ther*, **13,** 451-7.

Canman, C.E., Lim, D.S., Cimprich, K.A., Taya, Y., Tamai, K., Sakaguchi, K., Appella, E., Kastan, M.B. & Siliciano, J.D. (1998). Activation of the ATM kinase by ionizing radiation and phosphorylation of p53. *Science*, **281,** 1677-9.

Chan, T.A., Hwang, P.M., Hermeking, H., Kinzler, K.W. & Vogelstein, B. (2000). Cooperative effects of genes controlling the G(2)/M checkpoint. *Genes Dev*, **14,** 1584-8.

Chary, S.R. & Jain, R.K. (1989). Direct measurement of interstitial convection and diffusion of albumin in normal and neoplastic tissues by fluorescence photobleaching. *Proc Natl Acad Sci U S A*, **86,** 5385-9.

References

Chavaudra, N., Bourhis, J. & Foray, N. (2004). Quantified relationship between cellular radiosensitivity, DNA repair defects and chromatin relaxation: a study of 19 human tumour cell lines from different origin. *Radiother Oncol*, **73,** 373-82.

Chehab, N.H., Malikzay, A., Stavridi, E.S. & Halazonetis, T.D. (1999). Phosphorylation of Ser-20 mediates stabilization of human p53 in response to DNA damage. *Proc Natl Acad Sci U S A*, **96,** 13777-82.

Chen, H.H., Wang, Y.C. & Fann, M.J. (2006). Identification and characterization of the CDK12/cyclin L1 complex involved in alternative splicing regulation. *Mol Cell Biol*, **26,** 2736-45.

Chen, H.H., Wong, Y.H., Geneviere, A.M. & Fann, M.J. (2007). CDK13/CDC2L5 interacts with L-type cyclins and regulates alternative splicing. *Biochem Biophys Res Commun*, **354,** 735-40.

Choy, H., MacRae, R. & Story, M. (2008). Basic Concepts of Chemotherapy and Irradiation Interaction. In *Perez and Brady's Principles and Practice of Radiation Oncology*, Halperin, E.C., Perez, C.A. & Brady, L.W. (eds). Wolters Kluwer Health/Lippincott Williams & Wilkins.

Chuang, Y.Y. & Liber, H.L. (1996). Effects of cell cycle position on ionizing radiation mutagenesis. I. Quantitative assays of two genetic loci in a human lymphoblastoid cell line. *Radiat Res*, **146,** 494-500.

Ciccia, A. & Elledge, S.J. (2010). The DNA damage response: making it safe to play with knives. *Mol Cell*, **40,** 179-204.

Cobrinik, D. (2005). Pocket proteins and cell cycle control. *Oncogene*, **24,** 2796-809.

Colevas, D., Blaylock, B. & Gravell, A. (2002). Clinical trials referral resource. Flavopiridol. *Oncology (Williston Park)*, **16,** 1204-5, 1210-2, 1214.

Cordes, N., Seidler, J., Durzok, R., Geinitz, H. & Brakebusch, C. (2006). beta1-integrin-mediated signaling essentially contributes to cell survival after radiation-induced genotoxic injury. *Oncogene*, **25,** 1378-90.

Couedel, C., Mills, K.D., Barchi, M., Shen, L., Olshen, A., Johnson, R.D., Nussenzweig, A., Essers, J., Kanaar, R., Li, G.C., Alt, F.W. & Jasin, M. (2004). Collaboration of homologous recombination and nonhomologous end-joining factors for the survival and integrity of mice and cells. *Genes Dev*, **18,** 1293-304.

Cruz, J.C. & Tsai, L.H. (2004). Cdk5 deregulation in the pathogenesis of Alzheimer's disease. *Trends Mol Med*, **10,** 452-8.

d'Adda di Fagagna, F., Reaper, P.M., Clay-Farrace, L., Fiegler, H., Carr, P., Von Zglinicki, T., Saretzki, G., Carter, N.P. & Jackson, S.P. (2003). A DNA damage checkpoint response in telomere-initiated senescence. *Nature*, **426,** 194-8.

References

Daniel, P. (2002). Deregulation von Zellzyklus und Apoptose als molekulare Grundlage der Therapieresistenz von Tumoren. In *Medizinischen Fakultät Charité*, Vol. Venia Legendi. Humboldt-Universität zu Berlin: Berlin.

De Bondt, H.L., Rosenblatt, J., Jancarik, J., Jones, H.D., Morgan, D.O. & Kim, S.H. (1993). Crystal structure of cyclin-dependent kinase 2. *Nature*, **363,** 595-602.

de Bruin, E.C. & Medema, J.P. (2008). Apoptosis and non-apoptotic deaths in cancer development and treatment response. *Cancer Treat Rev*, **34,** 737-49.

Deans, A.J., Khanna, K.K., McNees, C.J., Mercurio, C., Heierhorst, J. & McArthur, G.A. (2006). Cyclin-dependent kinase 2 functions in normal DNA repair and is a therapeutic target in BRCA1-deficient cancers. *Cancer Res*, **66,** 8219-26.

Deckbar, D., Jeggo, P.A. & Lobrich, M. (2011). Understanding the limitations of radiation-induced cell cycle checkpoints. *Crit Rev Biochem Mol Biol*, **46,** 271-83.

Deckbar, D., Stiff, T., Koch, B., Reis, C., Lobrich, M. & Jeggo, P.A. (2010). The limitations of the G1-S checkpoint. *Cancer Res*, **70,** 4412-21.

Deschner, E.E. & Gray, L.H. (1959). Influence of oxygen tension on x-ray-induced chromosomal damage in Ehrlich ascites tumor cells irradiated in vitro and in vivo. *Radiat Res*, **11,** 115-46.

Deshpande, A., Sicinski, P. & Hinds, P.W. (2005). Cyclins and cdks in development and cancer: a perspective. *Oncogene*, **24,** 2909-15.

Dewey, W.C., Furman, S.C. & Miller, H.H. (1970). Comparison of lethality and chromosomal damage induced by x-rays in synchronized Chinese hamster cells in vitro. *Radiat Res*, **43,** 561-81.

Dewey, W.C., Ling, C.C. & Meyn, R.E. (1995). Radiation-induced apoptosis: relevance to radiotherapy. *Int J Radiat Oncol Biol Phys*, **33,** 781-96.

Diaz-Padilla, I., Siu, L.L. & Duran, I. (2009). Cyclin-dependent kinase inhibitors as potential targeted anticancer agents. *Invest New Drugs*, **27,** 586-94.

Dickson, M.A. & Schwartz, G.K. (2009). Development of cell-cycle inhibitors for cancer therapy. *Curr Oncol*, **16,** 36-43.

Difilippantonio, M.J., Petersen, S., Chen, H.T., Johnson, R., Jasin, M., Kanaar, R., Ried, T. & Nussenzweig, A. (2002). Evidence for replicative repair of DNA double-strand breaks leading to oncogenic translocation and gene amplification. *J Exp Med*, **196,** 469-80.

Dikomey, E. & Brammer, I. (2000). Relationship between cellular radiosensitivity and non-repaired double-strand breaks studied for different growth states, dose rates and plating conditions in a normal human fibroblast line. *Int J Radiat Biol*, **76,** 773-81.

Dong, Y., Sui, L., Tai, Y., Sugimoto, K. & Tokuda, M. (2001). The overexpression of cyclin-dependent kinase (CDK) 2 in laryngeal squamous cell carcinomas. *Anticancer Res*, **21,** 103-8.

Drouet, J., Delteil, C., Lefrancois, J., Concannon, P., Salles, B. & Calsou, P. (2005). DNA-dependent protein kinase and XRCC4-DNA ligase IV mobilization in the cell in response to DNA double strand breaks. *J Biol Chem*, **280,** 7060-9.

Drouet, J., Frit, P., Delteil, C., de Villartay, J.P., Salles, B. & Calsou, P. (2006). Interplay between Ku, Artemis, and the DNA-dependent protein kinase catalytic subunit at DNA ends. *J Biol Chem*, **281,** 27784-93.

Durocher, D. & Jackson, S.P. (2001). DNA-PK, ATM and ATR as sensors of DNA damage: variations on a theme? *Curr Opin Cell Biol*, **13,** 225-31.

Dyson, N. (1998). The regulation of E2F by pRB-family proteins. *Genes Dev*, **12,** 2245-62.

Easton, J., Wei, T., Lahti, J.M. & Kidd, V.J. (1998). Disruption of the cyclin D/cyclin-dependent kinase/INK4/retinoblastoma protein regulatory pathway in human neuroblastoma. *Cancer Res*, **58,** 2624-32.

Edamatsu, H., Gau, C.L., Nemoto, T., Guo, L. & Tamanoi, F. (2000). Cdk inhibitors, roscovitine and olomoucine, synergize with farnesyltransferase inhibitor (FTI) to induce efficient apoptosis of human cancer cell lines. *Oncogene*, **19,** 3059-68.

Eke, I. & Cordes, N. (2011). Radiobiology goes 3D: how ECM and cell morphology impact on cell survival after irradiation. *Radiother Oncol*, **99,** 271-8.

Eke, I., Koch, U., Hehlgans, S., Sandfort, V., Stanchi, F., Zips, D., Baumann, M., Shevchenko, A., Pilarsky, C., Haase, M., Baretton, G.B., Calleja, V., Larijani, B., Fassler, R. & Cordes, N. (2010). PINCH1 regulates Akt1 activation and enhances radioresistance by inhibiting PP1alpha. *J Clin Invest*, **120,** 2516-27.

Eke, I., Sandfort, V., Storch, K., Baumann, M., Roper, B. & Cordes, N. (2007). Pharmacological inhibition of EGFR tyrosine kinase affects ILK-mediated cellular radiosensitization in vitro. *Int J Radiat Biol*, **83,** 793-802.

Eke, I., Schneider, L., Forster, C., Zips, D., Kunz-Schughart, L.A. & Cordes, N. (2013). EGFR/JIP-4/JNK2 signaling attenuates cetuximab-mediated radiosensitization of squamous cell carcinoma cells. *Cancer Res*, **73,** 297-306.

Elbashir, S.M., Harborth, J., Lendeckel, W., Yalcin, A., Weber, K. & Tuschl, T. (2001). Duplexes of 21-nucleotide RNAs mediate RNA interference in cultured mammalian cells. *Nature*, **411,** 494-8.

Endicott, J.A., Noble, M.E. & Tucker, J.A. (1999). Cyclin-dependent kinases: inhibition and substrate recognition. *Curr Opin Struct Biol*, **9,** 738-44.

Esashi, F., Christ, N., Gannon, J., Liu, Y., Hunt, T., Jasin, M. & West, S.C. (2005). CDK-dependent phosphorylation of BRCA2 as a regulatory mechanism for recombinational repair. *Nature*, **434,** 598-604.

Esposito, L., Indovina, P., Magnotti, F., Conti, D. & Giordano, A. (2013). Anticancer therapeutic strategies based on CDK inhibitors. *Curr Pharm Des*.

Federico, M., Symonds, C.E., Bagella, L., Rizzolio, F., Fanale, D., Russo, A. & Giordano, A. (2010). R-Roscovitine (Seliciclib) prevents DNA damage-induced cyclin A1 upregulation and hinders non-homologous end-joining (NHEJ) DNA repair. *Mol Cancer*, **9,** 208.

Ferlay, J., Shin, H.R., Bray, F., Forman, D., Mathers, C. & Parkin, D.M. (2010). Estimates of worldwide burden of cancer in 2008: GLOBOCAN 2008. *Int J Cancer*, **127,** 2893-917.

Finlay, C.A., Hinds, P.W. & Levine, A.J. (1989). The p53 proto-oncogene can act as a suppressor of transformation. *Cell*, **57,** 1083-93.

Fleck, O. & Nielsen, O. (2004). DNA repair. *J Cell Sci*, **117,** 515-7.

Forastiere, A., Koch, W., Trotti, A. & Sidransky, D. (2001). Head and neck cancer. *N Engl J Med*, **345,** 1890-900.

Frederick, M.A., Brent, R., Kingston, R.E., Moore, D., Seidman, J., Smith, J. & Struhl, K. (2002). Short protocols in molecular biology: a compendium of methods from Current protocols in molecular biology, Vol. 1. John Wiley & Sons, Inc.

Frouin, I., Toueille, M., Ferrari, E., Shevelev, I. & Hubscher, U. (2005). Phosphorylation of human DNA polymerase lambda by the cyclin-dependent kinase Cdk2/cyclin A complex is modulated by its association with proliferating cell nuclear antigen. *Nucleic Acids Res*, **33,** 5354-61.

Gadbois, D.M. & Lehnert, B.E. (1997). Temporal position of G1 arrest in normal human fibroblasts after exposure to gamma-rays. *Exp Cell Res*, **232,** 161-6.

Galons, H., Oumata, N. & Meijer, L. (2010). Cyclin-dependent kinase inhibitors: a survey of recent patent literature. *Expert Opin Ther Pat*, **20,** 377-404.

Garriga, J., Bhattacharya, S., Calbo, J., Marshall, R.M., Truongcao, M., Haines, D.S. & Grana, X. (2003). CDK9 is constitutively expressed throughout the cell cycle, and its steady-state expression is independent of SKP2. *Mol Cell Biol*, **23,** 5165-73.

Garriga, J. & Grana, X. (2004). Cellular control of gene expression by T-type cyclin/CDK9 complexes. *Gene*, **337,** 15-23.

Garriga, J., Xie, H., Obradovic, Z. & Grana, X. (2010). Selective control of gene expression by CDK9 in human cells. *J Cell Physiol*, **222,** 200-8.

Gojo, I., Zhang, B. & Fenton, R.G. (2002). The cyclin-dependent kinase inhibitor flavopiridol induces apoptosis in multiple myeloma cells through transcriptional repression and down-regulation of Mcl-1. *Clin Cancer Res*, **8,** 3527-38.

Goodarzi, A.A., Yu, Y., Riballo, E., Douglas, P., Walker, S.A., Ye, R., Harer, C., Marchetti, C., Morrice, N., Jeggo, P.A. & Lees-Miller, S.P. (2006). DNA-PK autophosphorylation facilitates Artemis endonuclease activity. *Embo J*, **25,** 3880-9.

Goodhead, D.T. (1994). Initial events in the cellular effects of ionizing radiations: clustered damage in DNA. *Int J Radiat Biol*, **65,** 7-17.

Gottlieb, T.M. & Jackson, S.P. (1993). The DNA-dependent protein kinase: requirement for DNA ends and association with Ku antigen. *Cell*, **72,** 131-42.

Graf, F., Wuest, F. & Pietzsch, J. (2011). Cyclin-Dependent Kinases (Cdk) as Targets for Cancer Therapy and Imaging. In *Advances in Cancer Therapy*, Gali-Muhtasib, H. (ed). InTech.

Hahn, W.C. & Weinberg, R.A. (2002). Rules for making human tumor cells. *N Engl J Med*, **347,** 1593-603.

Hall, E.J. (1972). Radiation dose-rate: a factor of importance in radiobiology and radiotherapy. *Br J Radiol*, **45,** 81-97.

Hall, E.J. & Giaccia, A.J. (2006). *Radiobiologie for the Radiologist*. Lippincott Williams & Wilkins.

Hallahan, D.E., Haimovitz-Friedman, A., Kufe, D.W., Fuks, Z. & Weichselbaum, R.R. (1993). The role of cytokines in radiation oncology. *Important Adv Oncol*, 71-80.

Halperin, E.C., Perez, C.A. & Brady, L.W. (2008). The Discipline of Radiation Oncology. In *Perez and Brady's Principles and Practice of Radiation Oncology*, Halperin, E.C., Perez, C.A. & Brady, L.W. (eds). Wolters Kluwer Health/Lippincott Williams & Wilkins

Han, W. & Yu, K.N. (2010). Ionizing Radiation, DNA Double Strand Break and Mutation. In *Advances in Genetics Research*, Urbano, K.V. (ed), Vol. 4. Nova Science Publishers, Inc.

Hanahan, D. & Weinberg, R.A. (2000). The hallmarks of cancer. *Cell*, **100,** 57-70.

Hanahan, D. & Weinberg, R.A. (2011). Hallmarks of cancer: the next generation. *Cell*, **144,** 646-74.

Hanks, S.K. & Hunter, T. (1995). Protein kinases 6. The eukaryotic protein kinase superfamily: kinase (catalytic) domain structure and classification. *Faseb J*, **9,** 576-96.

References

Harper, J.W., Adami, G.R., Wei, N., Keyomarsi, K. & Elledge, S.J. (1993). The p21 Cdk-interacting protein Cip1 is a potent inhibitor of G1 cyclin-dependent kinases. *Cell*, **75,** 805-16.

Harper, J.W. & Elledge, S.J. (2007). The DNA damage response: ten years after. *Mol Cell*, **28,** 739-45.

Harper, J.W., Elledge, S.J., Keyomarsi, K., Dynlacht, B., Tsai, L.H., Zhang, P., Dobrowolski, S., Bai, C., Connell-Crowley, L., Swindell, E. & et al. (1995). Inhibition of cyclin-dependent kinases by p21. *Mol Biol Cell*, **6,** 387-400.

Harrison, J.C. & Haber, J.E. (2006). Surviving the breakup: the DNA damage checkpoint. *Annu Rev Genet*, **40,** 209-35.

Hedman, M. (2012). TUMOR RADIOSENSITIVITY AND PROLIFERATION AS PARAMETERS FOR OPTIMIZING RADIOTHERAPY. In *DEPARTMENT OF ONCOLOGY-PATHOLOGY* pp. 47. Karolinska Institutet: Stockholm, Sweden.

Hehlgans, S., Eke, I. & Cordes, N. (2012). Targeting FAK radiosensitizes 3-dimensional grown human HNSCC cells through reduced Akt1 and MEK1/2 signaling. *Int J Radiat Oncol Biol Phys*, **83,** e669-76.

Hehlgans, S., Eke, I., Deuse, Y. & Cordes, N. (2008). Integrin-linked kinase: dispensable for radiation survival of three-dimensionally cultured fibroblasts. *Radiother Oncol*, **86,** 329-35.

Hehlgans, S., Eke, I., Storch, K., Haase, M., Baretton, G.B. & Cordes, N. (2009). Caveolin-1 mediated radioresistance of 3D grown pancreatic cancer cells. *Radiother Oncol*, **92,** 362-70.

Helleday, T., Lo, J., van Gent, D.C. & Engelward, B.P. (2007). DNA double-strand break repair: from mechanistic understanding to cancer treatment. *DNA Repair (Amst)*, **6,** 923-35.

Hengst, L. & Reed, S.I. (1998). Inhibitors of the Cip/Kip family. *Curr Top Microbiol Immunol*, **227,** 25-41.

Hiromura, K., Pippin, J.W., Blonski, M.J., Roberts, J.M. & Shankland, S.J. (2002). The subcellular localization of cyclin dependent kinase 2 determines the fate of mesangial cells: role in apoptosis and proliferation. *Oncogene*, **21,** 1750-8.

Hoeijmakers, J.H. (2001). Genome maintenance mechanisms for preventing cancer. *Nature*, **411,** 366-74.

Hu, D., Valentine, M., Kidd, V.J. & Lahti, J.M. (2007). CDK11(p58) is required for the maintenance of sister chromatid cohesion. *J Cell Sci*, **120,** 2424-34.

Hu, S.H., Parker, M.W., Lei, J.Y., Wilce, M.C., Benian, G.M. & Kemp, B.E. (1994). Insights into autoregulation from the crystal structure of twitchin kinase. *Nature*, **369,** 581-4.

IARC. (2008). *World Cancer Report, 2008*. **IARC Press**: Lyon.

References

Iliakis, G., Wang, Y., Guan, J. & Wang, H. (2003). DNA damage checkpoint control in cells exposed to ionizing radiation. *Oncogene*, **22,** 5834-47.

Jacks, T. & Weinberg, R.A. (2002). Taking the study of cancer cell survival to a new dimension. *Cell*, **111,** 923-5.

Jazayeri, A., Falck, J., Lukas, C., Bartek, J., Smith, G.C., Lukas, J. & Jackson, S.P. (2006). ATM- and cell cycle-dependent regulation of ATR in response to DNA double-strand breaks. *Nat Cell Biol*, **8,** 37-45.

Jeggo, P. & Lobrich, M. (2006a). Radiation-induced DNA damage responses. *Radiat Prot Dosimetry*, **122,** 124-7.

Jeggo, P.A. & Lobrich, M. (2006b). Contribution of DNA repair and cell cycle checkpoint arrest to the maintenance of genomic stability. *DNA Repair (Amst)*, **5,** 1192-8.

Johnson, L.N. & Lewis, R.J. (2001). Structural basis for control by phosphorylation. *Chem Rev*, **101,** 2209-42.

Johnstone, R.W., Ruefli, A.A. & Lowe, S.W. (2002). Apoptosis: a link between cancer genetics and chemotherapy. *Cell*, **108,** 153-64.

Jostes, R.F., Bushnell, K.M. & Dewey, W.C. (1980). X-ray induction of 8-azaguanine-resistant mutants in synchronous Chinese hamster ovary cells. *Radiat Res*, **83,** 146-61.

Kaldis, P. & Aleem, E. (2005). Cell cycle sibling rivalry: Cdc2 vs. Cdk2. *Cell Cycle*, **4,** 1491-4.

Karnoub, A.E. & Weinberg, R.A. (2008). Ras oncogenes: split personalities. *Nat Rev Mol Cell Biol*, **9,** 517-31.

Kasten, M. & Giordano, A. (2001). Cdk10, a Cdc2-related kinase, associates with the Ets2 transcription factor and modulates its transactivation activity. *Oncogene*, **20,** 1832-8.

Kato, J., Matsushime, H., Hiebert, S.W., Ewen, M.E. & Sherr, C.J. (1993). Direct binding of cyclin D to the retinoblastoma gene product (pRb) and pRb phosphorylation by the cyclin D-dependent kinase CDK4. *Genes Dev*, **7,** 331-42.

Kelland, L.R. (2000). Flavopiridol, the first cyclin-dependent kinase inhibitor to enter the clinic: current status. *Expert Opin Investig Drugs*, **9,** 2903-11.

Kenny, P.A., Lee, G.Y., Myers, C.A., Neve, R.M., Semeiks, J.R., Spellman, P.T., Lorenz, K., Lee, E.H., Barcellos-Hoff, M.H., Petersen, O.W., Gray, J.W. & Bissell, M.J. (2007). The morphologies of breast cancer cell lines in three-dimensional assays correlate with their profiles of gene expression. *Mol Oncol*, **1,** 84-96.

Kim, D.H., Behlke, M.A., Rose, S.D., Chang, M.S., Choi, S. & Rossi, J.J. (2005). Synthetic dsRNA Dicer substrates enhance RNAi potency and efficacy. *Nat Biotechnol*, **23,** 222-6.

References

Kim, J.H., Kang, M.J., Park, C.U., Kwak, H.J., Hwang, Y. & Koh, G.Y. (1999). Amplified CDK2 and cdc2 activities in primary colorectal carcinoma. *Cancer*, **85,** 546-53.

Kinner, A., Wu, W., Staudt, C. & Iliakis, G. (2008). Gamma-H2AX in recognition and signaling of DNA double-strand breaks in the context of chromatin. *Nucleic Acids Res*, **36,** 5678-94.

Kohoutek, J. & Blazek, D. (2012). Cyclin K goes with Cdk12 and Cdk13. *Cell Div*, **7,** 12.

Lacher, M.D., Pincheira, R., Zhu, Z., Camoretti-Mercado, B., Matli, M., Warren, R.S. & Castro, A.F. (2010). Rheb activates AMPK and reduces p27Kip1 levels in Tsc2-null cells via mTORC1-independent mechanisms: implications for cell proliferation and tumorigenesis. *Oncogene*, **29,** 6543-56.

Lans, H., Marteijn, J.A. & Vermeulen, W. (2012). ATP-dependent chromatin remodeling in the DNA-damage response. *Epigenetics Chromatin*.

Lapenna, S. & Giordano, A. (2009). Cell cycle kinases as therapeutic targets for cancer. *Nat Rev Drug Discov*, **8,** 547-66.

Latif, C., Harvey, S.H. & O'Connell, M.J. (2001). Ensuring the stability of the genome: DNA damage checkpoints. *ScientificWorldJournal*, **1,** 684-702.

Lawrence, T.S., Ten Haken, R.K. & Giaccia, A. (2008). *Principles of Radiation Oncology*. Cancer: Principles and Practice of Oncology. Lippincott Williams and Wilkins: Philadelphia.

Lea, D. (1955). *Actions of radiation on living cells*. Cambridge University Press: Cambridge, England.

Lee, G.Y., Kenny, P.A., Lee, E.H. & Bissell, M.J. (2007). Three-dimensional culture models of normal and malignant breast epithelial cells. *Nat Methods*, **4,** 359-65.

Lee, J. & Desiderio, S. (1999). Cyclin A/CDK2 regulates V(D)J recombination by coordinating RAG-2 accumulation and DNA repair. *Immunity*, **11,** 771-81.

Lee, M.H., Reynisdottir, I. & Massague, J. (1995). Cloning of p57KIP2, a cyclin-dependent kinase inhibitor with unique domain structure and tissue distribution. *Genes Dev*, **9,** 639-49.

Leonhardt, E.A., Trinh, M., Forrester, H.B., Johnson, R.T. & Dewey, W.C. (1997). Comparisons of the frequencies and molecular spectra of HPRT mutants when human cancer cells were X-irradiated during G1 or S phase. *Radiat Res*, **148,** 548-60.

Li, C., Zhao, X., Toline, E.C., Siegal, G.P., Evans, L.M., Ibrahim-Hashim, A., Desmond, R.A. & Hardy, R.W. (2011). Prevention of carcinogenesis and inhibition of breast cancer tumor burden by dietary stearate. *Carcinogenesis*, **32,** 1251-8.

Li, Y., Jenkins, C.W., Nichols, M.A. & Xiong, Y. (1994). Cell cycle expression and p53 regulation of the cyclin-dependent kinase inhibitor p21. *Oncogene*, **9,** 2261-8.

References

Lim, D.S., Kim, S.T., Xu, B., Maser, R.S., Lin, J., Petrini, J.H. & Kastan, M.B. (2000). ATM phosphorylates p95/nbs1 in an S-phase checkpoint pathway. *Nature*, **404,** 613-7.

Lin, W.C. & Desiderio, S. (1994). Cell cycle regulation of V(D)J recombination-activating protein RAG-2. *Proc Natl Acad Sci U S A*, **91,** 2733-7.

Linke, S.P., Harris, M.P., Neugebauer, S.E., Clarkin, K.C., Shepard, H.M., Maneval, D.C. & Wahl, G.M. (1997). p53-mediated accumulation of hypophosphorylated pRb after the G1 restriction point fails to halt cell cycle progression. *Oncogene*, **15,** 337-45.

Liu, H. & Herrmann, C.H. (2005). Differential localization and expression of the Cdk9 42k and 55k isoforms. *J Cell Physiol*, **203,** 251-60.

Lodish, H., Berk, A., Zipursky, S. & al., e. (2000a). Checkpoints in Cell-Cycle Regulation. In *Molecular Cell Biology*. W. H. Freeman and Company: New York.

Lodish, H., Berk, A., Zipursky, S. & al., e. (2000b). Proto-Oncogenes and Tumor-Suppressor Genes. In *Molecular Cell Biology*. W. H. Freeman: New York.

Loyer, P., Trembley, J.H., Katona, R., Kidd, V.J. & Lahti, J.M. (2005). Role of CDK/cyclin complexes in transcription and RNA splicing. *Cell Signal*, **17,** 1033-51.

Lu, C., Stewart, D.J., Lee, J.J., Ji, L., Ramesh, R., Jayachandran, G., Nunez, M.I., Wistuba, II, Erasmus, J.J., Hicks, M.E., Grimm, E.A., Reuben, J.M., Baladandayuthapani, V., Templeton, N.S., McMannis, J.D. & Roth, J.A. (2012). Phase I clinical trial of systemically administered TUSC2(FUS1)-nanoparticles mediating functional gene transfer in humans. *PLoS One*, **7,** e34833.

Lukas, J., Lukas, C. & Bartek, J. (2004). Mammalian cell cycle checkpoints: signalling pathways and their organization in space and time. *DNA Repair (Amst)*, **3,** 997-1007.

Lundberg, A.S. & Weinberg, R.A. (1998). Functional inactivation of the retinoblastoma protein requires sequential modification by at least two distinct cyclin-cdk complexes. *Mol Cell Biol*, **18,** 753-61.

Lunn, C.L., Chrivia, J.C. & Baldassare, J.J. (2010). Activation of Cdk2/Cyclin E complexes is dependent on the origin of replication licensing factor Cdc6 in mammalian cells. *Cell Cycle*, **9,** 4533-41.

Maddika, S., Ande, S.R., Wiechec, E., Hansen, L.L., Wesselborg, S. & Los, M. (2008). Akt-mediated phosphorylation of CDK2 regulates its dual role in cell cycle progression and apoptosis. *J Cell Sci*, **121,** 979-88.

Mailand, N., Falck, J., Lukas, C., Syljuasen, R.G., Welcker, M., Bartek, J. & Lukas, J. (2000). Rapid destruction of human Cdc25A in response to DNA damage. *Science*, **288,** 1425-9.

Mailand, N., Podtelejnikov, A.V., Groth, A., Mann, M., Bartek, J. & Lukas, J. (2002). Regulation of G(2)/M events by Cdc25A through phosphorylation-dependent modulation of its stability. *Embo J*, **21,** 5911-20.

Malumbres, M. & Barbacid, M. (2001). To cycle or not to cycle: a critical decision in cancer. *Nat Rev Cancer*, **1,** 222-31.

Malumbres, M. & Barbacid, M. (2005). Mammalian cyclin-dependent kinases. *Trends Biochem Sci*, **30,** 630-41.

Malumbres, M. & Barbacid, M. (2009). Cell cycle, CDKs and cancer: a changing paradigm. *Nat Rev Cancer*, **9,** 153-66.

Malumbres, M., Pevarello, P., Barbacid, M. & Bischoff, J.R. (2008). CDK inhibitors in cancer therapy: what is next? *Trends Pharmacol Sci*, **29,** 16-21.

Matsushime, H., Quelle, D.E., Shurtleff, S.A., Shibuya, M., Sherr, C.J. & Kato, J.Y. (1994). D-type cyclin-dependent kinase activity in mammalian cells. *Mol Cell Biol*, **14,** 2066-76.

McBride, W. & Withers, H. (2008). Biologic Basis of Radiation Therapy. In *Perez and Brady's Principles and Practice of Radiation Oncology*, Halperin, E.C., Perez, C.A. & Brady, L.W. (eds). Wolters Kluwer Health/Lippincott Williams & Wilkins.

McDonald, E.R., 3rd & El-Deiry, W.S. (2000). Cell cycle control as a basis for cancer drug development (Review). *Int J Oncol*, **16,** 871-86.

McGinn, C.J., Shewach, D.S. & Lawrence, T.S. (1996). Radiosensitizing nucleosides. *J Natl Cancer Inst*, **88,** 1193-203.

Melo, J. & Toczyski, D. (2002). A unified view of the DNA-damage checkpoint. *Curr Opin Cell Biol*, **14,** 237-45.

Michels, A.A., Fraldi, A., Li, Q., Adamson, T.E., Bonnet, F., Nguyen, V.T., Sedore, S.C., Price, J.P., Price, D.H., Lania, L. & Bensaude, O. (2004). Binding of the 7SK snRNA turns the HEXIM1 protein into a P-TEFb (CDK9/cyclin T) inhibitor. *Embo J*, **23,** 2608-19.

Mihara, M., Shintani, S., Nakahara, Y., Kiyota, A., Ueyama, Y., Matsumura, T. & Wong, D.T. (2001). Overexpression of CDK2 is a prognostic indicator of oral cancer progression. *Jpn J Cancer Res*, **92,** 352-60.

Mills, K.D., Ferguson, D.O., Essers, J., Eckersdorff, M., Kanaar, R. & Alt, F.W. (2004). Rad54 and DNA Ligase IV cooperate to maintain mammalian chromatid stability. *Genes Dev*, **18,** 1283-92.

Morawska, M.E. (2012). A role for CDK9 in UV damage response. *Cell Cycle*, **11,** 2229-30.

Mordes, D.A., Glick, G.G., Zhao, R. & Cortez, D. (2008). TopBP1 activates ATR through ATRIP and a PIKK regulatory domain. *Genes Dev*, **22,** 1478-89.

References

Moretti, L., Ocak, S., Hallahan, D.E. & Lu, B. (2010). Cell Cycle and Vascular Targets for Radiotherapy. In *Principles & Practice of Lung Cancer: The Official Reference Text of the IASLC, 4e*, Pass, H.I., Carbone, D.P., Johnson, D.H., Minna, J.D., Scagliotti, G.V. & Turrisi, A.T. (eds). LIPPINCOTT WILLIAMS & WILKINS, a WOLTERS KLUWER business.

Muller-Tidow, C., Ji, P., Diederichs, S., Potratz, J., Baumer, N., Kohler, G., Cauvet, T., Choudary, C., van der Meer, T., Chan, W.Y., Nieduszynski, C., Colledge, W.H., Carrington, M., Koeffler, H.P., Restle, A., Wiesmuller, L., Sobczak-Thepot, J., Berdel, W.E. & Serve, H. (2004). The cyclin A1-CDK2 complex regulates DNA double-strand break repair. *Mol Cell Biol*, **24,** 8917-28.

Murray, A. (1995). Cyclin ubiquitination: the destructive end of mitosis. *Cell*, **81,** 149-52.

Myers, J.S., Zhao, R., Xu, X., Ham, A.J. & Cortez, D. (2007). Cyclin-dependent kinase 2 dependent phosphorylation of ATRIP regulates the G2-M checkpoint response to DNA damage. *Cancer Res*, **67,** 6685-90.

Napolitano, G., Majello, B. & Lania, L. (2003). Catalytic activity of Cdk9 is required for nuclear co-localization of the Cdk9/cyclin T1 (P-TEFb) complex. *J Cell Physiol*, **197,** 1-7.

Neganova, I., Vilella, F., Atkinson, S.P., Lloret, M., Passos, J.F., von Zglinicki, T., O'Connor, J.E., Burks, D., Jones, R., Armstrong, L. & Lako, M. (2011). An important role for CDK2 in G1 to S checkpoint activation and DNA damage response in human embryonic stem cells. *Stem Cells*, **29,** 651-9.

Nevins, J.R. (2001). The Rb/E2F pathway and cancer. *Hum Mol Genet*, **10,** 699-703.

Nigg, E.A. (1995). Cyclin-dependent protein kinases: key regulators of the eukaryotic cell cycle. *Bioessays*, **17,** 471-80.

Nigg, E.A. (2001). Mitotic kinases as regulators of cell division and its checkpoints. *Nat Rev Mol Cell Biol*, **2,** 21-32.

Niida, H. & Nakanishi, M. (2006). DNA damage checkpoints in mammals. *Mutagenesis*, **21,** 3-9.

Norbury, C. & Nurse, P. (1992). Animal cell cycles and their control. *Annu Rev Biochem*, **61,** 441-70.

Nurse, P. (1994). Ordering S phase and M phase in the cell cycle. *Cell*, **79,** 547-50.

O'Connor, P.M. (1997). Mammalian G1 and G2 phase checkpoints. *Cancer Surv*, **29,** 151-82.

Obaya, A.J. & Sedivy, J.M. (2002). Regulation of cyclin-Cdk activity in mammalian cells. *Cell Mol Life Sci*, **59,** 126-42.

References

Ohtsubo, M., Theodoras, A.M., Schumacher, J., Roberts, J.M. & Pagano, M. (1995). Human cyclin E, a nuclear protein essential for the G1-to-S phase transition. *Mol Cell Biol*, **15,** 2612-24.

Orend, G., Huang, W., Olayioye, M.A., Hynes, N.E. & Chiquet-Ehrismann, R. (2003). Tenascin-C blocks cell-cycle progression of anchorage-dependent fibroblasts on fibronectin through inhibition of syndecan-4. *Oncogene*, **22,** 3917-26.

Ortega, S., Malumbres, M. & Barbacid, M. (2002). Cyclin D-dependent kinases, INK4 inhibitors and cancer. *Biochim Biophys Acta*, **1602,** 73-87.

Ortega, S., Prieto, I., Odajima, J., Martin, A., Dubus, P., Sotillo, R., Barbero, J.L., Malumbres, M. & Barbacid, M. (2003). Cyclin-dependent kinase 2 is essential for meiosis but not for mitotic cell division in mice. *Nat Genet*, **35,** 25-31.

Padera, T.P., Stoll, B.R., Tooredman, J.B., Capen, D., di Tomaso, E. & Jain, R.K. (2004). Pathology: cancer cells compress intratumour vessels. *Nature*, **427,** 695.

Palancade, B. & Bensaude, O. (2003). Investigating RNA polymerase II carboxyl-terminal domain (CTD) phosphorylation. *Eur J Biochem*, **270,** 3859-70.

Palyi, I., Fleischmann, T., Palyi, V., Daubner, D., Raposa, T., Paloczi, K., Benczur, M., Gergely, L., Csuka, O. & Bak, M. (1995). Establishment and characterization of an EBNA-negative human lymphoma cell line (BHL-89). *Haematologica*, **80,** 206-11.

Pampaloni, F., Reynaud, E.G. & Stelzer, E.H. (2007). The third dimension bridges the gap between cell culture and live tissue. *Nat Rev Mol Cell Biol*, **8,** 839-45.

Parker, S.L., Tong, T., Bolden, S. & Wingo, P.A. (1997). Cancer statistics, 1997. *CA Cancer J Clin*, **47,** 5-27.

Parkin, D.M., Bray, F., Ferlay, J. & Pisani, P. (2005). Global cancer statistics, 2002. *CA Cancer J Clin*, **55,** 74-108.

Pavletich, N.P. (1999). Mechanisms of cyclin-dependent kinase regulation: structures of Cdks, their cyclin activators, and Cip and INK4 inhibitors. *J Mol Biol*, **287,** 821-8.

Peng, J., Marshall, N.F. & Price, D.H. (1998). Identification of a cyclin subunit required for the function of Drosophila P-TEFb. *J Biol Chem*, **273,** 13855-60.

Pines, J. (1995). Cyclins and cyclin-dependent kinases: theme and variations. *Adv Cancer Res*, **66,** 181-212.

Pirngruber, J., Shchebet, A., Schreiber, L., Shema, E., Minsky, N., Chapman, R.D., Eick, D., Aylon, Y., Oren, M. & Johnsen, S.A. (2009). CDK9 directs H2B monoubiquitination and controls replication-dependent histone mRNA 3'-end processing. *EMBO Rep*, **10,** 894-900.

Polyak, K., Lee, M.H., Erdjument-Bromage, H., Koff, A., Roberts, J.M., Tempst, P. & Massague, J. (1994). Cloning of p27Kip1, a cyclin-dependent kinase inhibitor and a potential mediator of extracellular antimitogenic signals. *Cell*, **78,** 59-66.

Puck, T.T. & Marcus, P.I. (1956). Action of x-rays on mammalian cells. *J Exp Med*, **103,** 653-66.

Ramanathan, Y., Rajpara, S.M., Reza, S.M., Lees, E., Shuman, S., Mathews, M.B. & Pe'ery, T. (2001). Three RNA polymerase II carboxyl-terminal domain kinases display distinct substrate preferences. *J Biol Chem*, **276,** 10913-20.

Ren, S. & Rollins, B.J. (2004). Cyclin C/cdk3 promotes Rb-dependent G0 exit. *Cell*, **117,** 239-51.

Riabowol, K., Draetta, G., Brizuela, L., Vandre, D. & Beach, D. (1989). The cdc2 kinase is a nuclear protein that is essential for mitosis in mammalian cells. *Cell*, **57,** 393-401.

Rizzolio, F., Tuccinardi, T., Caligiuri, I., Lucchetti, C. & Giordano, A. (2010). CDK inhibitors: from the bench to clinical trials. *Curr Drug Targets*, **11,** 279-90.

Rodriguez-Ubreva, F.J., Cariaga-Martinez, A.E., Cortes, M.A., Romero-De Pablos, M., Ropero, S., Lopez-Ruiz, P. & Colas, B. (2009). Knockdown of protein tyrosine phosphatase SHP-1 inhibits G1/S progression in prostate cancer cells through the regulation of components of the cell-cycle machinery. *Oncogene*, **29,** 345-55.

Romano, G. & Giordano, A. (2008). Role of the cyclin-dependent kinase 9-related pathway in mammalian gene expression and human diseases. *Cell Cycle*, **7,** 3664-8.

Roninson, I.B., Broude, E.V. & Chang, B.D. (2001). If not apoptosis, then what? Treatment-induced senescence and mitotic catastrophe in tumor cells. *Drug Resist Updat*, **4,** 303-13.

Ross, H.H., Levkoff, L.H., Marshall, G.P., 2nd, Caldeira, M., Steindler, D.A., Reynolds, B.A. & Laywell, E.D. (2008). Bromodeoxyuridine induces senescence in neural stem and progenitor cells. *Stem Cells*, **26,** 3218-27.

Rothkamm, K., Kruger, I., Thompson, L.H. & Lobrich, M. (2003). Pathways of DNA double-strand break repair during the mammalian cell cycle. *Mol Cell Biol*, **23,** 5706-15.

Rothkamm, K. & Lobrich, M. (2003). Evidence for a lack of DNA double-strand break repair in human cells exposed to very low x-ray doses. *Proc Natl Acad Sci U S A*, **100,** 5057-62.

Roussel, M.F. (1999). The INK4 family of cell cycle inhibitors in cancer. *Oncogene*, **18,** 5311-7.

Ruffner, H., Jiang, W., Craig, A.G., Hunter, T. & Verma, I.M. (1999). BRCA1 is phosphorylated at serine 1497 in vivo at a cyclin-dependent kinase 2 phosphorylation site. *Mol Cell Biol*, **19,** 4843-54.

References

Saintigny, Y., Delacote, F., Vares, G., Petitot, F., Lambert, S., Averbeck, D. & Lopez, B.S. (2001). Characterization of homologous recombination induced by replication inhibition in mammalian cells. *Embo J*, **20,** 3861-70.

Saleh-Gohari, N. & Helleday, T. (2004). Conservative homologous recombination preferentially repairs DNA double-strand breaks in the S phase of the cell cycle in human cells. *Nucleic Acids Res*, **32,** 3683-8.

Sambrook, J., and Russell, D. W. (2001). *Molecular Cloning: A Laboratory Manual*. Cold Spring Harbor Laboratory Press.

Sancar, A., Lindsey-Boltz, L.A., Unsal-Kacmaz, K. & Linn, S. (2004). Molecular mechanisms of mammalian DNA repair and the DNA damage checkpoints. *Annu Rev Biochem*, **73,** 39-85.

Sanchez, I. & Dynlacht, B.D. (2005). New insights into cyclins, CDKs, and cell cycle control. *Semin Cell Dev Biol*, **16,** 311-21.

Sandfort, V., Koch, U. & Cordes, N. (2007). Cell adhesion-mediated radioresistance revisited. *Int J Radiat Biol*, **83,** 727-32.

Santamaria, D., Barriere, C., Cerqueira, A., Hunt, S., Tardy, C., Newton, K., Caceres, J.F., Dubus, P., Malumbres, M. & Barbacid, M. (2007). Cdk1 is sufficient to drive the mammalian cell cycle. *Nature*, **448,** 811-5.

Satyanarayana, A., Hilton, M.B. & Kaldis, P. (2008). p21 Inhibits Cdk1 in the absence of Cdk2 to maintain the G1/S phase DNA damage checkpoint. *Mol Biol Cell*, **19,** 65-77.

Satyanarayana, A. & Kaldis, P. (2009a). A dual role of Cdk2 in DNA damage response. *Cell Div*, **4,** 9.

Satyanarayana, A. & Kaldis, P. (2009b). Mammalian cell-cycle regulation: several Cdks, numerous cyclins and diverse compensatory mechanisms. *Oncogene*, **28,** 2925-39.

Schafer, K.A. (1998). The cell cycle: a review. *Vet Pathol*, **35,** 461-78.

Shaheen, F.S., Znojek, P., Fisher, A., Webster, M., Plummer, R., Gaughan, L., Smith, G.C., Leung, H.Y., Curtin, N.J. & Robson, C.N. (2011). Targeting the DNA double strand break repair machinery in prostate cancer. *PLoS One*, **6,** e20311.

Shapiro, G.I. (2006). Cyclin-dependent kinase pathways as targets for cancer treatment. *J Clin Oncol*, **24,** 1770-83.

Sherr, C.J. (1995). D-type cyclins. *Trends Biochem Sci*, **20,** 187-90.

Sherr, C.J. (1996). Cancer cell cycles. *Science*, **274,** 1672-7.

Sherr, C.J. & Roberts, J.M. (1999). CDK inhibitors: positive and negative regulators of G1-phase progression. *Genes Dev*, **13,** 1501-12.

Sherr, C.J. & Roberts, J.M. (2004). Living with or without cyclins and cyclin-dependent kinases. *Genes Dev*, **18,** 2699-711.

Shiloh, Y. (2003). ATM and related protein kinases: safeguarding genome integrity. *Nat Rev Cancer*, **3,** 155-68.

Shintani, S., Mihara, M., Nakahara, Y., Kiyota, A., Ueyama, Y., Matsumura, T. & Wong, D.T. (2002). Expression of cell cycle control proteins in normal epithelium, premalignant and malignant lesions of oral cavity. *Oral Oncol*, **38,** 235-43.

Siemeister, G., Luecking, U., Wagner, C., Detjen, K., Mc Coy, C. & Bosslet, K. (2006). Molecular and pharmacodynamic characteristics of the novel multi-target tumor growth inhibitor ZK 304709. *Biomed Pharmacother*, **60,** 269-72.

Simone, C., Bagella, L., Bellan, C. & Giordano, A. (2002). Physical interaction between pRb and cdk9/cyclinT2 complex. *Oncogene*, **21,** 4158-65.

Sinclair, W.K. (1968). Cyclic X-ray responses in mammalian cells in vitro. *Radiat Res*, **178,** AV112-24.

Sinclair, W.K. & Morton, R.A. (1963). Variations in X-Ray Response During the Division Cycle of Partially Synchronized Chinese Hamster Cells in Culture. *Nature*, **199,** 1158-60.

Sinclair, W.K. & Morton, R.A. (1966). X-ray sensitivity during the cell generation cycle of cultured Chinese hamster cells. *Radiat Res*, **29,** 450-74.

Smith, G.C., Divecha, N., Lakin, N.D. & Jackson, S.P. (1999). DNA-dependent protein kinase and related proteins. *Biochem Soc Symp*, **64,** 91-104.

Smith, G.C. & Jackson, S.P. (1999). The DNA-dependent protein kinase. *Genes Dev*, **13,** 916-34.

Soffar, A., Storch, K., Aleem, E. & Cordes, N. (2013). CDK2 knockdown enhances head and neck cancer cell radiosensitivity. *Int J Radiat Biol*.

Soule, B.P., Simone, N.L., DeGraff, W.G., Choudhuri, R., Cook, J.A. & Mitchell, J.B. (2010). Loratadine dysregulates cell cycle progression and enhances the effect of radiation in human tumor cell lines. *Radiat Oncol*, **5,** 8.

Staden, R., Beal, K.F. & Bonfield, J.K. (2000). The Staden package, 1998. *Methods Mol Biol*, **132,** 115-30.

Stell, P.M. (1989). Survival times in end-stage head and neck cancer. *Eur J Surg Oncol*, **15,** 407-10.

Stewart, R.D. (2001). Two-lesion kinetic model of double-strand break rejoining and cell killing. *Radiat Res*, **156,** 365-78.

Storch, K. (2010). Einfluss der Chromatinkondensation auf die zelluläre Strahlenempfindlichkeit unter dreidimensionalen Wachstumsbedingungen. In *der*

Fakultät Mathematik und Naturwissenschaften, Vol. Dr. rer. nat. pp. 128. Technischen Universität Dresden.

Storch, K., Eke, I., Borgmann, K., Krause, M., Richter, C., Becker, K., Schrock, E. & Cordes, N. (2010). Three-dimensional cell growth confers radioresistance by chromatin density modification. *Cancer Res*, **70,** 3925-34.

Stratford, I.J. (1992). Concepts and developments in radiosensitization of mammalian cells. *Int J Radiat Oncol Biol Phys*, **22,** 529-32.

Su, T.T. (2006). Cellular responses to DNA damage: one signal, multiple choices. *Annu Rev Genet*, **40,** 187-208.

Sui, L., Dong, Y., Ohno, M., Sugimoto, K., Tai, Y., Hando, T. & Tokuda, M. (2001). Implication of malignancy and prognosis of p27(kip1), Cyclin E, and Cdk2 expression in epithelial ovarian tumors. *Gynecol Oncol*, **83,** 56-63.

Sullivan, M. & Morgan, D.O. (2007). Finishing mitosis, one step at a time. *Nat Rev Mol Cell Biol*, **8,** 894-903.

Symington, L.S. & Gautier, J. (2011). Double-strand break end resection and repair pathway choice. *Annu Rev Genet*, **45,** 247-71.

Takata, M., Sasaki, M.S., Sonoda, E., Morrison, C., Hashimoto, M., Utsumi, H., Yamaguchi-Iwai, Y., Shinohara, A. & Takeda, S. (1998). Homologous recombination and non-homologous end-joining pathways of DNA double-strand break repair have overlapping roles in the maintenance of chromosomal integrity in vertebrate cells. *Embo J*, **17,** 5497-508.

Tang, L., Li, G., Tron, V.A., Trotter, M.J. & Ho, V.C. (1999). Expression of cell cycle regulators in human cutaneous malignant melanoma. *Melanoma Res*, **9,** 148-54.

Taylor, W.R. & Stark, G.R. (2001). Regulation of the G2/M transition by p53. *Oncogene*, **20,** 1803-15.

Terasima, T. & Tolmach, L.J. (1963). Variations in several responses of HeLa cells to x-irradiation during the division cycle. *Biophys J*, **3,** 11-33.

Tetsu, O. & McCormick, F. (2003). Proliferation of cancer cells despite CDK2 inhibition. *Cancer Cell*, **3,** 233-45.

Thun, M.J., DeLancey, J.O., Center, M.M., Jemal, A. & Ward, E.M. (2009). The global burden of cancer: priorities for prevention. *Carcinogenesis*, **31,** 100-10.

Tibbetts, R.S., Brumbaugh, K.M., Williams, J.M., Sarkaria, J.N., Cliby, W.A., Shieh, S.Y., Taya, Y., Prives, C. & Abraham, R.T. (1999). A role for ATR in the DNA damage-induced phosphorylation of p53. *Genes Dev*, **13,** 152-7.

Toyoshima, H. & Hunter, T. (1994). p27, a novel inhibitor of G1 cyclin-Cdk protein kinase activity, is related to p21. *Cell*, **78,** 67-74.

Trimarchi, J.M. & Lees, J.A. (2002). Sibling rivalry in the E2F family. *Nat Rev Mol Cell Biol*, **3,** 11-20.

Tsihlias, J., Kapusta, L. & Slingerland, J. (1999). The prognostic significance of altered cyclin-dependent kinase inhibitors in human cancer. *Annu Rev Med*, **50,** 401-23.

Ubersax, J.A. & Ferrell, J.E., Jr. (2007). Mechanisms of specificity in protein phosphorylation. *Nat Rev Mol Cell Biol*, **8,** 530-41.

Vakifahmetoglu, H., Olsson, M. & Zhivotovsky, B. (2008). Death through a tragedy: mitotic catastrophe. *Cell Death Differ*, **15,** 1153-62.

Valentin, J. (2005). Low-dose extrapolation of radiation-related cancer risk. *Ann ICRP*, **35,** 1-140.

Vermeulen, K., Van Bockstaele, D.R. & Berneman, Z.N. (2003). The cell cycle: a review of regulation, deregulation and therapeutic targets in cancer. *Cell Prolif*, **36,** 131-49.

Vidal, A.E., Boiteux, S., Hickson, I.D. & Radicella, J.P. (2001). XRCC1 coordinates the initial and late stages of DNA abasic site repair through protein-protein interactions. *Embo J*, **20,** 6530-9.

Vogelstein, B. & Kinzler, K.W. (2004). Cancer genes and the pathways they control. *Nat Med*, **10,** 789-99.

Vokes, E.E., Weichselbaum, R.R., Lippman, S.M. & Hong, W.K. (1993). Head and neck cancer. *N Engl J Med*, **328,** 184-94.

von Sonntag, C. (1987). *Chemical Basis of Radiation Biology*. Taylor and Francis, London.

Wachsberger, P., Burd, R. & Dicker, A.P. (2003). Tumor response to ionizing radiation combined with antiangiogenesis or vascular targeting agents: exploring mechanisms of interaction. *Clin Cancer Res*, **9,** 1957-71.

Wallenfang, M.R. & Seydoux, G. (2002). cdk-7 Is required for mRNA transcription and cell cycle progression in Caenorhabditis elegans embryos. *Proc Natl Acad Sci U S A*, **99,** 5527-32.

Ward, J.F. (1981). Some biochemical consequences of the spatial distribution of ionizing radiation-produced free radicals. *Radiat Res*, **86,** 185-95.

Ward, J.F. (1988). DNA damage produced by ionizing radiation in mammalian cells: identities, mechanisms of formation, and reparability. *Prog Nucleic Acid Res Mol Biol*, **35,** 95-125.

Ward, J.F. (1995). Radiation mutagenesis: the initial DNA lesions responsible. *Radiat Res*, **142,** 362-8.

Watanabe, M. & Horikawa, M. (1980). Analyses of differential sensitivities of synchronized HeLa S3 cells to radiations and chemical carcinogens during the cell cycle. Par V. Radiation- and chemical carcinogen-induced mutagenesis. *Mutat Res*, **71,** 219-31.

Weinberg, R.A. (1995). The retinoblastoma protein and cell cycle control. *Cell*, **81,** 323-30.

Weinert, T.A., Kiser, G.L. & Hartwell, L.H. (1994). Mitotic checkpoint genes in budding yeast and the dependence of mitosis on DNA replication and repair. *Genes Dev*, **8,** 652-65.

Weitzman, M.D., Wang, J.Y.J., Editors-in-Chief: William, J.L. & Lane, M.D. (2013). Cell Cycle: DNA Damage Checkpoints. In *Encyclopedia of Biological Chemistry* pp. 410-416. Academic Press: Waltham.

West, S.C. (2003). Molecular views of recombination proteins and their control. *Nat Rev Mol Cell Biol*, **4,** 435-45.

Wilken, R., Veena, M.S., Wang, M.B. & Srivatsan, E.S. (2011). Curcumin: A review of anti-cancer properties and therapeutic activity in head and neck squamous cell carcinoma. *Mol Cancer*, **10,** 12.

Wimmer, U., Ferrari, E., Hunziker, P. & Hubscher, U. (2008). Control of DNA polymerase lambda stability by phosphorylation and ubiquitination during the cell cycle. *EMBO Rep*, **9,** 1027-33.

Wohlbold, L. & Fisher, R.P. (2009). Behind the wheel and under the hood: functions of cyclin-dependent kinases in response to DNA damage. *DNA Repair (Amst)*, **8,** 1018-24.

Wohlbold, L., Merrick, K.A., De, S., Amat, R., Kim, J.H., Larochelle, S., Allen, J.J., Zhang, C., Shokat, K.M., Petrini, J.H. & Fisher, R.P. (2012). Chemical genetics reveals a specific requirement for cdk2 activity in the DNA damage response and identifies nbs1 as a cdk2 substrate in human cells. *PLoS Genet*, **8,** e1002935.

Wolfel, T., Hauer, M., Schneider, J., Serrano, M., Wolfel, C., Klehmann-Hieb, E., De Plaen, E., Hankeln, T., Meyer zum Buschenfelde, K.H. & Beach, D. (1995). A p16INK4a-insensitive CDK4 mutant targeted by cytolytic T lymphocytes in a human melanoma. *Science*, **269,** 1281-4.

Wyman, C. & Kanaar, R. (2004). Homologous recombination: down to the wire. *Curr Biol*, **14,** R629-31.

Xing, J., Spitz, M.R., Lu, C., Zhao, H., Yang, H., Wang, W., Stewart, D.J. & Wu, X. (2007). Deficient G2-M and S checkpoints are associated with increased lung cancer risk: a case-control analysis. *Cancer Epidemiol Biomarkers Prev*, **16,** 1517-22.

Xu, R., Boudreau, A. & Bissell, M.J. (2009). Tissue architecture and function: dynamic reciprocity via extra- and intra-cellular matrices. *Cancer Metastasis Rev*, **28,** 167-76.

Yamamoto, H., Monden, T., Miyoshi, H., Izawa, H., Ikeda, K., Tsujie, M., Ohnishi, T., Sekimoto, M., Tomita, N. & Monden, M. (1998). Cdk2/cdc2 expression in colon

carcinogenesis and effects of cdk2/cdc2 inhibitor in colon cancer cells. *Int J Oncol*, **13,** 233-9.

Yata, K. & Esashi, F. (2009). Dual role of CDKs in DNA repair: to be, or not to be. *DNA Repair (Amst)*, **8,** 6-18.

Yu, D.S. & Cortez, D. (2011). A role for CDK9-cyclin K in maintaining genome integrity. *Cell Cycle*, **10,** 28-32.

Yu, D.S., Zhao, R., Hsu, E.L., Cayer, J., Ye, F., Guo, Y., Shyr, Y. & Cortez, D. (2010). Cyclin-dependent kinase 9-cyclin K functions in the replication stress response. *EMBO Rep*, **11,** 876-82.

Zhang, C., Lundgren, K., Yan, Z., Arango, M.E., Price, S., Huber, A., Higgins, J., Troche, G., Skaptason, J., Koudriakova, T., Nonomiya, J., Yang, M., O'Connor, P., Bender, S., Los, G., Lewis, C. & Jessen, B. (2008). Pharmacologic properties of AG-012986, a pan-cyclin-dependent kinase inhibitor with antitumor efficacy. *Mol Cancer Ther*, **7,** 818-28.

Zhao, H., Watkins, J.L. & Piwnica-Worms, H. (2002). Disruption of the checkpoint kinase 1/cell division cycle 25A pathway abrogates ionizing radiation-induced S and G2 checkpoints. *Proc Natl Acad Sci U S A*, **99,** 14795-800.

Zhou, M., Halanski, M.A., Radonovich, M.F., Kashanchi, F., Peng, J., Price, D.H. & Brady, J.N. (2000). Tat modifies the activity of CDK9 to phosphorylate serine 5 of the RNA polymerase II carboxyl-terminal domain during human immunodeficiency virus type 1 transcription. *Mol Cell Biol*, **20,** 5077-86.

Zhu, C., Mills, K.D., Ferguson, D.O., Lee, C., Manis, J., Fleming, J., Gao, Y., Morton, C.C. & Alt, F.W. (2002). Unrepaired DNA breaks in p53-deficient cells lead to oncogenic gene amplification subsequent to translocations. *Cell*, **109,** 811-21.

Zhu, Y., Pe'ery, T., Peng, J., Ramanathan, Y., Marshall, N., Marshall, T., Amendt, B., Mathews, M.B. & Price, D.H. (1997). Transcription elongation factor P-TEFb is required for HIV-1 tat transactivation in vitro. *Genes Dev*, **11,** 2622-32.

Zschenker, O., Streichert, T., Hehlgans, S. & Cordes, N. (2012). Genome-wide gene expression analysis in cancer cells reveals 3D growth to affect ECM and processes associated with cell adhesion but not DNA repair. *PLoS One*, **7,** e34279.

Acknowledgment

First of all, I would like to return all the efforts and success to Allah who gave and always gives me the power to perform my work.

My special appreciation to my supervisor Prof. Dr. Nils Cordes for providing me the opportunity to obtain my PhD under his supervision, and for his patience, support and professional guidance. I had learned very much from him.

I would like to express my deep gratitude to Prof. Dr. Herwig Gutzeit for accepting me as one of his students and his sincere support and supervision.

Continuous gratitude and great thanks to Dr. Katja Storch for her effective help and advice during my study and for her great efforts in reviewing the manuscript.

My special thanks to Dr. Anne Vehlow for her fruitful assistance and discussions to finish the manuscript.

I am very thankful to Inga Lange and Claudia Förster for their help and guidance in the lab. Special thanks to Claudia Förster for helping me to finish the results.

My acknowledgment is sincerely extended to Prof. Dr. Eiman Aleem for helping to finish the German Egyptian Research Long-term Scholarship (GERLS) application and for her kind support and guidance.

I would like to thank all my colleagues in the Cellular and Molecular Radiobiology group for their daily support and motivation during my study.

Special thanks from my heart to my parents for their continuous support and encouragement and to my wife "Nahla", who there is no substitute for her love and support.

At the end, I would like to appreciate the financial support of my study from the Egyptian Ministry of Higher Education and Scientific Research (MHESR) and the German Academic Exchange Service (DAAD).

Dresden, den 07.05.2013

Ahmed Soffar

Erklärung

Hiermit versichere ich, dass ich die vorliegende Arbeit ohne unzulässige Hilfe Dritter und ohne Benutzung anderer als der angegebenen Hilfsmittel angefertigt habe; die aus fremden Quellen direkt oder indirekt übernommenen Gedanken sind als solche kenntlich gemacht. Die Arbeit wurde bisher weder im Inland noch im Ausland in gleicher oder ähnlicher Form einer anderen Prüfungsbehörde vorgelegt.

Die Arbeit wurde in der Gruppe "Molecular and Cellular Radiobiology" am OncoRay-National Center for Radiation Research in Oncology, Medizinische Fakultät Carl Gustav Carus, Technische Universität Dresden unter der wissenschaftlichen Leitung von Herrn Prof. Dr. Nils Cordes angefertigt.

Es fand kein frühres Promotionsverfahren statt.
Die Promotionsordnung wird anerkannt.

Dresden, den 07.05.2013

_____

Ahmed Soffar